Sideroflexins enable mitochondrial transport of polar neutral amino acids

by

Samuel Block

B.S. Biochemistry
University of Wisconsin-Madison

Submitted to the Department of Biology in Partial Fulfillment of the Requirements for the Degree of

DOCTOR OF PHILOSOPHY

at the

MASSACHUSETTS INSTITUTE OF TECHNOLOGY

February 2025

Authored by: Samuel Block
Department of Biology
October 31st, 2024

Certified by: Matthew G. Vander Heiden
Director, Koch Institute for Integrative Cancer Research
Lester Wolfe Professor of Molecular Biology
Thesis Supervisor

Accepted by: Mary Gehring
Professor of Biology
Member, Whitehead Institute
Director, Biology Graduate Committee

Sideroflexins enable mitochondrial transport of polar neutral amino acids

by

Samuel Block

Submitted to the Department of Biology on 10/31/2024 in Partial Fulfillment of the Requirements for the Degree of Doctor of Philosophy in Biochemistry

Abstract

Mitochondria contribute to compartmentalized metabolism in eukaryotic cells, facilitating diverse enzymatic reactions that support cell function. However, this compartmentalization of metabolism necessitates regulated transport of metabolites across the inner mitochondrial membrane. While many proteins enabling mitochondrial membrane transport of metabolites are known, how some metabolites are transported is not known, and several mitochondrial amino acid transporters are largely uncharacterized. The goal of this dissertation is to better understand which proteins in the mitochondrial inner membrane regulate amino acid transport, particularly for substrates that lack known transporters, and how these proteins regulate associated metabolic pathways.

Using CRISPR-Cas9-mediated candidate transporter knockouts coupled with assessment of metabolite transport via a mitochondrial swelling assay, we identified SFXN1 as a gene that mediates mitochondrial membrane permeability to polar neutral amino acids, including proline, glycine, taurine, hypotuarine, beta-alanine, and gamma-aminobutyric acid (GABA). SFXN2 and SFXN3 partially complemented loss of SFXN1 to enable glycine transport, while SFXN2 and SFXN5 partially complemented loss of SFXN1 to enable GABA transport. Altogether, this work suggests that sideroflexins regulate the delivery of polar neutral amino acids across the inner mitochondrial membrane, many of which lack known carriers, and contributes to a better understanding of how mitochondrial amino acid transport regulates cellular metabolism.

Thesis Supervisor: Matthew G. Vander Heiden, MD/PhD
Title: Director, Koch Institute for Integrative Cancer Research
Lester Wolfe Professor of Molecular Biology

Biographical Note

Samuel Block

EDUCATION

2018-2025	Massachusetts Institute of Technology Ph.D. Biochemistry
2013-2017	University of Wisconsin-Madison B.S. Biochemistry

RESEARCH EXPERIENCE

2019-2025	Massachusetts Institute of Technology, Ph.D. Candidate Laboratory of Dr. Matthew G. Vander Heiden
2015-2017	University of Wisconsin-Madison, Undergraduate Research Assistant Laboratory of Dr. Anjon Audhya

HONORS AND AWARDS

2016	Biochemistry Undergraduate Summer Research Award, University of Wisconsin-Madison
2013-2017	Arndt Family Scholarship

TEACHING EXPERIENCE

2021	Teaching Assistant, Cell Biology (7.06), Massachusetts Institute of Technology
2020	Teaching Assistant, Biochemistry (7.05), Massachusetts Institute of Technology

PRESENTATIONS

2023	Unlocking Transporters for Drug Discovery Conference, RESOLUTE, poster
2022	Cancer Metabolism Conference, EACR, poster
2017	Annual Meeting, ASBMB, poster

PUBLICATIONS

Block, S., Chi, F., Rosen, P. C., Pineda, S. S., Darnell, A. M., Abbott, K. L., Pena, I. A., Heiman, M., Yilmaz, Ö. H., Kory, N., & Vander Heiden, M. G. Sideroflexins enable mitochondrial transport of polar neutral amino acids. [Manuscript in preparation]

Pena, I. A., Shi, J. S., Chang, S. M., Yang, J., **Block, S.**, Adelmann, C. H., Keys, H. R., Ge, P., Bathla, S., Withan, I., Sienski, G., Nairn, A., Sabatini, D. M., Lewis, C. A., Kory, N., Vander Heiden, M. G., & Heiman, M. SLC25A38 is Required for Mitochondrial Pyridoxal 5'-Phosphate (PLP) accumulation. [Manuscript under revision]

Do, B. T., Hsu, P. P., Vermeulen, S. Y., Wang, Z., Hirz, T., Abbott, K. L., Aziz, N., Replogle, J. M., Bjelosevic, S., Paolino, J., Nelson, S. A., **Block, S.**, Darnell, A. M., Ferreira, R., Zhang, H., Milosevic, J., Schmidt, D. R., Chidley, C., Harris, I. S., Weissman, J. S., Pikman, Y., Stegmaier, K., Cheloufi, S., Su, X. A., Sykes, D. B., Vander Heiden, M. G. (2024). Nucleotide depletion promotes cell fate transitions by inducing DNA replication stress. *Developmental Cell*, S1534-5807(24)00327-7.

Moretton, A., Kourtis, S., Gañez Zapater, A., Calabrò, C., Espinar Calvo, M. L., Fontaine, F., Darai, E., Abad Cortel, E., **Block, S.**, Pascual-Reguant, L., Pardo-Lorente, N., Ghose, R., Vander Heiden, M. G., Janic, A., Müller, A. C., Loizou, J. I., & Sdelci, S. (2023). A metabolic map of the DNA damage response identifies PRDX1 in the control of nuclear ROS scavenging and aspartate availability. *Molecular Systems Biology*, *19*(7), e11267.

Kasberg, W., Luong, P., Hanna, M. G., Minushkin, K., Tsao, A., Shankar, R., **Block, S.**, & Audhya, A. (2023). The Sar1 GTPase is dispensable for COPII-dependent cargo export from the ER. *Cell Reports*, *42*(6), 112635.

Hicks, K. G., Cluntun, A. A., Schubert, H. L., Hackett, S. R., Berg, J. A., Leonard, P. G., Ajalla Aleixo, M. A., Zhou, Y., Bott, A. J., Salvatore, S. R., Chang, F., Blevins, A., Barta, P., Tilley, S., Leifer, A., Guzman, A., Arok, A., Fogarty, S., Winter, J. M., Ahn, H.-C., Allen, K. N., **Block, S.**, Cardoso, I. A., Ding, J., Dreveny, I., Gasper, W. C., Ho, Q., Matsuura, A., Palladino, M. J., Prajapati, S., Sun, P., Tittmann, K., Tolan, D. R., Unterlass, J., VanDemark, A. P., Vander Heiden, M. G., Webb, B. A., Yun, C.-H., Zhao, P., Wang, B., Schopfer, F. J., Hill, C. P., Nonato, M. C., Muller, F. L., Cox, J. E., Rutter, J. (2023). Protein-metabolite interactomics of carbohydrate metabolism reveal regulation of lactate dehydrogenase. *Science (New York, N.Y.)*, *379*(6636), 996–1003.

Lynch, A. M., Zhu, Y., Lucas, B. G., Winkelman, J. D., Bai, K., Martin, S. C. T., **Block, S.**, Slabodnick, M. M., Audhya, A., Goldstein, B., Pettitt, J., Gardel, M. L., & Hardin, J. (2022). TES-1/Tes and ZYX-1/Zyxin protect junctional actin networks under tension during epidermal morphogenesis in the C. elegans embryo. *Current Biology: CB*, *32*(23), 5189-5199.e6.

Block, S., Schuh, A. L., & Audhya, A. (2019). Biochemical Approaches to Studying Caenorhabditis elegans ESCRT Functions In Vitro. *Methods in Molecular Biology (Clifton, N.J.)*, *1998*, 189–202.

Wan, J., **Block, S.**, Scribano, C. M., Thiry, R., Esbona, K., Audhya, A., & Weaver, B. A. (2019). Mad1 destabilizes p53 by preventing PML from sequestering MDM2. *Nature Communications*, *10*(1), 1540.

Slosarek, E. L., Schuh, A. L., Pustova, I., Johnson, A., Bird, J., Johnson, M., Frankel, E. B., Bhattacharya, N., Hanna, M. G., Burke, J. E., Ruhl, D. A., Quinney, K., **Block, S.**, Peotter, J. L., Chapman, E. R., Sheets, M. D., Butcher, S. E., Stagg, S. M., & Audhya, A. (2018). Pathogenic TFG Mutations Underlying Hereditary Spastic Paraplegia Impair Secretory Protein Trafficking and Axon Fasciculation. *Cell Reports*, *24*(9), 2248–2260.

Hanna, M. G., **Block, S.**, Frankel, E. B., Hou, F., Johnson, A., Yuan, L., Knight, G., Moresco, J. J., Yates, J. R., Ashton, R., Schekman, R., Tong, Y., & Audhya, A. (2017). TFG facilitates outer coat disassembly on COPII transport carriers to promote tethering and fusion with ER-Golgi intermediate compartments. *Proceedings of the National Academy of Sciences of the United States of America*, *114*(37), E7707–E7716.

Acknowledgments

I would like to thank everyone who supported me through the process of obtaining my PhD. In particular, I would like to thank my advisor Matt Vander Heiden for his scientific and worldly advice, and for granting me the freedom to pursue the questions that interested me the most, regardless of where they led. Thank you to all members of the Vander Heiden Lab for your insight and for creating an environment that made this work possible. I would also like to thank my committee members Mike Hemann and Joey Davis for providing critical insight that challenged me to become a better scientist. Finally, I would like to thank the Kory, Heiman, and Yilmaz labs for their collaborative efforts that helped broaden the scope of my project and scientific thinking.

Table of Contents

Chapter 1: Mechanisms of mitochondrial transport

Authors: Samuel Block[1,2], Matthew G. Vander Heiden[1,2,3]

Author Affiliation:

[1]Koch Institute for Integrative Cancer Research, Massachusetts Institute of Technology, Cambridge, MA 02139, USA
[2]Department of Biology, Massachusetts Institute of Technology, Cambridge, MA 02139, USA
[3]Dana-Farber Cancer Institute, Boston, MA 02115, USA

Introduction

Mitochondria are membrane bound endosymbiotic organelles found in eukaryotic cells[1], often called the powerhouse of the cell[2] due to their key role in ATP production through oxidative phosphorylation[3,4]. Mitochondria also have additional metabolic functions including the synthesis and degradation of many fatty, amino, and nucleic acids[5] and play critical roles in various cellular and organismal processes such as thermogenesis[6], apoptosis[7], nitrogen detoxification[8], neurotransmitter regulation[9], and redox[10] and ion homeostasis[11]. Because all of these functions depend on interconnected metabolic pathways that involve reactions in the mitochondria and other cellular compartments, mitochondria require the ability to exchange small molecules with the cytosol, and this exchange involves transport across mitochondrial membranes.

While the outer mitochondrial membrane is permeable to many small solutes due to large pores formed by the voltage-dependent ion channels (VDAC)[12], the inner membrane contains designated transporters for nucleotides, amino acids, fatty acids, carboxylates, cofactors, and inorganic ions[13], and these substrates must traverse the inner mitochondrial membrane to carry out a variety of metabolic needs[14]. While many transporters have been identified for most of these substrates, the mitochondrial amino acid transporters remain poorly characterized, and the mechanism by which many amino acids pass the inner mitochondrial membrane is unknown. In this thesis, I will discuss the mechanisms of mitochondrial transport and provide evidence that sideroflexins enable mitochondrial transport of polar neutral amino acids.

Discovery of mitochondria

Structures that were likely mitochondria were first documented in the mid-1800s, and in 1888 it was discovered that granules isolated from insect cells swelled in water[15], although it is unclear if these were bona fide mitochondria[16]. The first clear depiction of mitochondria was provided by Richard Altmann in 1890[16,17]. Using an acid-fuchsin staining technique, Altmann observed ubiquitous structures representing filaments in various cell types and called them "bioplasts"[16–18]. While research detailing these organelles' endosymbiotic origin and metabolic functions was yet to come[1], Altmann hypothesized that these bioplasts represented autonomous microorganisms that carried out basic metabolic functions[16,18]. Around a decade later, Carl Benda also observed these structures using an alternative staining method and described them as *mitochondria*[19], which combines the Greek words mitos, meaning "thread," and chondros, meaning "granule," since these structures were found either in a thread or granule-like state[16,18].

Experiments that demonstrated mitochondria carry out metabolic reactions shortly followed their initial discovery. In 1899, Leonor Michaelis discovered that mitochondria could be selectively stained by the dye Janus green[20], which produces a blue-green color when oxidized[18]. At this time, respiration, the biochemical process that oxidizes fuel to produce energy, was known to occur within cells but the subcellular location remained a mystery[21]. In 1910, Otto Warburg discovered that membranes were vital for respiration[18,22], and in 1912, noticing that the fixation conditions used to observe mitochondria were redox-sensitive, Benjamin Kingsbury hypothesized that mitochondria were responsible for cellular respiration[16,23]. In the following decades,

many seminal biochemical studies began to elucidate the mechanisms underlying what is now known as oxidative phosphorylation. The idea of the respiratory chain emerged in the 1930s, fueled by the earlier discovery of cytochromes by David Keilin[21,24] and studies of oxidative metabolism by Otto Warburg[16], and the reactions of the Krebs cycle were published by Hans Krebs in 1937[25]. Still, definitive proof that mitochondria were responsible for carrying out these processes was lacking due to the inability of researchers at the time to isolate functional mitochondria from other cellular components[16]. This changed due to the development and optimization of fractionation techniques by Albert Claude[16]. Using differential centrifugation to isolate mitochondria from other cellular components, studies by Claude and colleagues demonstrated that mitochondria were the site of various oxidase activities[16,26]. Finally, in 1949 Eugene Kennedy and Albert Lehninger demonstrated that the citric acid cycle intermediates identified by Hans Krebs decades earlier were oxidized in isolated mitochondria, and these reactions were coupled to the NADH-dependent phosphorylation of ADP to produce ATP[3,16].

Using the fractionation techniques referenced above, various groups outlined the enzyme activities of mitochondria and identified many of the proteins involved in oxidative phosphorylation[16]. Still, the mechanism by which mitochondria produced ATP from ADP and inorganic phosphate remained elusive[16]. Glycolysis Produces ATP via reactions that are directly coupled to glucose oxidation, which involve high-energy chemical intermediates[16,27]. However, efforts to identify the mitochondrial equivalent of these high-energy chemical intermediates proved fruitless[16,21]. The theoretical breakthrough that described the ATP-generating mechanism behind oxidative

phosphorylation was published by Peter Mitchell in 1961[4,16]. In this publication, Mitchell outlined the "chemiosmotic hypothesis," which states that the energy obtained from the oxidation of fuels could be converted into a proton gradient across a membrane, and that this membrane may contain an enzyme capable of translocating these protons, which could harness the associated energy to form ATP[4,16]. Despite initial skepticism, subsequent biochemical studies using chloroplasts[28,29], isolated mitochondria[30], and artificial membranes[31] helped validate Mitchell's chemiosmotic coupling mechanism of oxidative phosphorylation[16], which is now widely accepted[21,32]. In this process, the oxidation of fuels transfers electrons to various coenzymes that then pass the electrons to the respiratory chain found within the inner mitochondrial membrane[32]. The mitochondrial respiratory chain is composed of a series of electron donors and acceptors[33], the last of which is O_2, which is reduced to H_2O[32]. As the electrons are passed along the respiratory chain through progressively lower free energy states, energy is released to pump protons across the inner mitochondrial membrane into the intermembrane space[32,34,35]. This creates an electrochemical proton gradient, which favors the movement of protons back across the inner mitochondria membrane toward the matrix[32]. The translocation of these protons back across the inner mitochondrial membrane is coupled to ATP production by ATP synthase[36], enabling energy capture from the oxidation of fuels[32]. Altogether, this understanding of energy transduction represents the combined efforts of decades of mitochondrial research[16,18,21] and serves as the foundation for contemporary mitochondrial metabolic studies.

Early studies of mitochondrial transport

It is now well appreciated that mitochondria require regulated transport of metabolites and inorganic ions to carry out oxidative phosphorylation[37]. For example, pyruvate produced from glycolysis needs to enter the mitochondrial matrix in order to be further oxidized in the Krebs cycle[38,39], ADP and inorganic phosphate must be imported from the cytosol to create ATP, which then needs to exit the mitochondria to provide energy for reactions elsewhere in the cell[40], and iron must be imported for the production of iron-sulfur clusters and heme which are used by several Krebs cycle enzymes and respiratory complexes[41]. After Albert Claude's groundbreaking fractionation technique was developed, researchers could study mitochondrial transport properties for the first time[16]. Another milestone that increased interest in mitochondrial transport was the publication of detailed images of mitochondria by George Palade[42] and Fritiof Sjostrand[43] using electron microscopy on fixed tissue sections[21]. These images showed that mitochondria were double membraned organelles[42,43], supporting contemporary studies on isolated mitochondria demonstrating that substrates needed to penetrate membranes in order to be processed by matrix-localized enzymes[16].

Most of these early transport studies took advantage of the osmotic properties of mitochondria, which swell when suspended in isosmotic solutions of penetrating solutes[16,44]. This swelling leads to decreased light scattering, so transport could be monitored using spectrophotometry[16,44]. Furthermore, by including ionophores, respiratory inhibitors, and other substrates in these assays, the energetic requirements and exchange properties of transport could be determined[16,44]. Employing these strategies and other techniques, such as monitoring downstream metabolic alterations

of specific substrates, it was found that calcium, phosphate, fatty acids, and many other substrates, such as nucleotides and amino acids, are all transported into mitochondria[16,44]. Interestingly, the carrier properties for many of these substrates were established long before their molecular identity was obtained[16,44]. For example, using isolated mitochondria, it was found that aspartate uptake required the presence of glutamate[44,45], and calcium uptake was dependent upon the energetic state of the mitochondria used[16,46,47], which we now know is due to the aspartate glutamate carriers (SLC25A12 and SLC25A13)[48] and the mitochondrial calcium uniporter (MCU)[49,50,51]. These initial transport studies paved the way for future endeavors that led to the identification and characterization of the mitochondrial carriers known today[14,16].

VDAC and the outer mitochondrial membrane

Studies using liposomes have demonstrated that in the absence of carriers, solutes can diffuse across lipid bilayers[52,53], and that the diffusion rate increases with decreasing solute size and increasing hydrophobicity[54]. However, for many solutes, diffusion rates across artificial membranes are slower than those observed across the membranes of isolated mitochondria[55,56], indicating that transport proteins are responsible for their translocation[56]. While the outer mitochondrial membrane in theory represents a barrier that must be overcome, most small solutes can cross this membrane due to the high abundance of relatively large and unselective pores formed by voltage-dependent anion channels (VDACs)[12,57]. Humans possess four VDAC isoforms; the most abundant and well-studied isoform is VDAC1[57]. Structural studies determined that VDAC1 contains a pore with a diameter of approximately 3nm[58,59], which likely explains why the outer mitochondrial membrane is permeable to most small solutes. VDAC1 can exist in high

(open) and low (closed) conductance states, with the open state favored at voltages ±40 mV[57]. At voltages outside this range, the channel favors a closed state and becomes more cation-selective[57]. While the physiological significance of this low conductance state induced by these voltages is uncertain, the closed state may be promoted by metabolite or protein binding[60]. In addition to small molecules, VDAC1 may also support the diffusion of pro-apoptotic proteins through oligomerization[59], and VDAC2 may promote apoptosis through its interaction with Bcl-2-associated X protein (BAX)[61].

SLC25 carriers

Since VDAC is absent from the inner mitochondrial membrane[12], solutes must pass through this barrier via designated carrier proteins[14]. Most of these carriers belong to the solute carrier 25 family (SLC25), which contains 53 members[37]. The mitochondrial genome encodes only 13 proteins, all of which are subunits of respiratory chain complexes[62]. Therefore, all SLC25 and other mitochondrial transporters are translated via cytosolic ribosomes and inserted into mitochondrial membranes[63]. Transporters in general can catalyze either active transport or passive transport[64] (Figure 1). Active transport involves transporting substrates against an electrochemical gradient by coupling transport to another energetically favorable process, which includes ATP hydrolysis (primary active transport) and the favorable transport of another substrate down its electrochemical gradient (secondary active transport)[64]. In contrast, passive transporters move substrates across lipid bilayers down their electrochemical gradient, a process known as facilitated diffusion, which does not pose an energetic cost[64]. Aquaporins also facilitate the diffusion of water across lipid bilayers[64], a process known as osmosis which in mitochondria is mediated by APQ8[65].

Figure 1

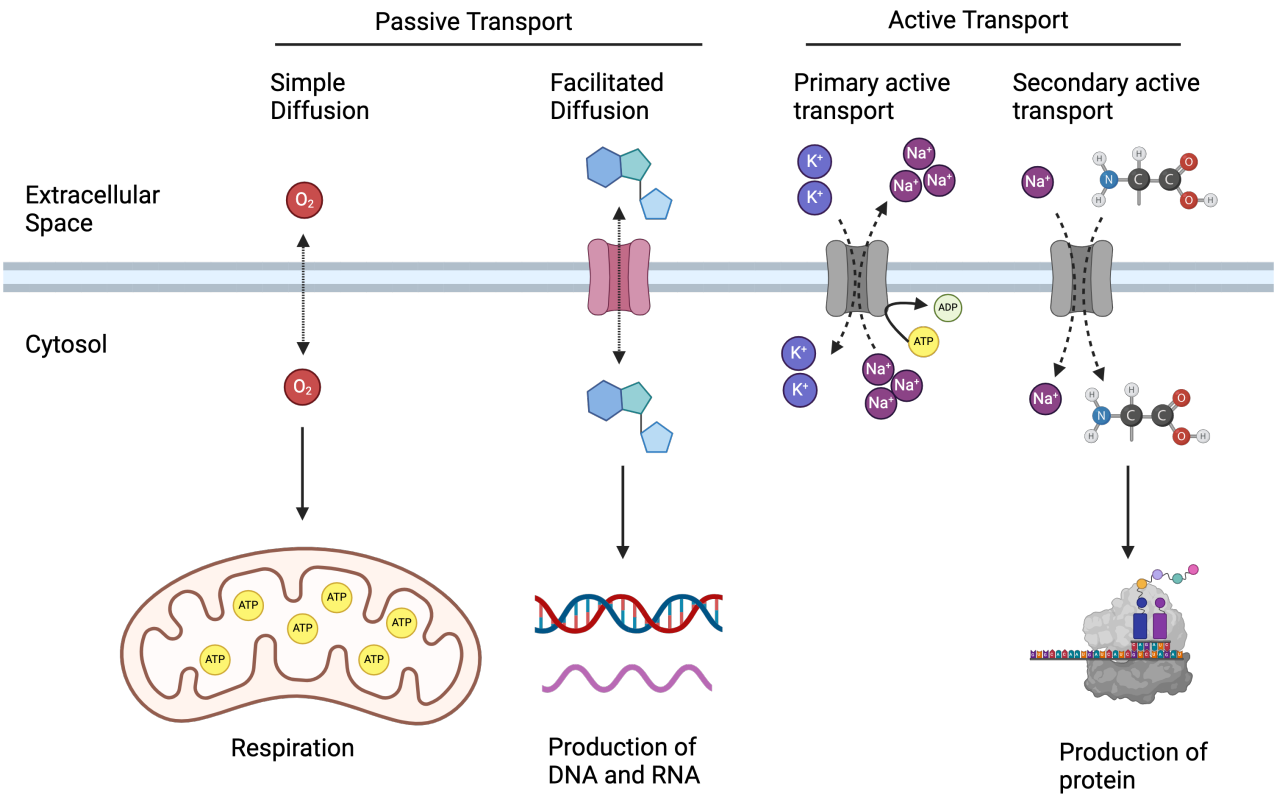
Passive Transport
Active Transport
Simple Diffusion
Facilitated Diffusion
Primary active transport
Secondary active transport
Extracellular Space
Cytosol
O_2
O_2
ATP
ADP
Na^+
K^+
Respiration
Production of DNA and RNA
Production of protein

Fig. 1. Mechanisms of membrane transport. Small lipophilic molecules can cross lipid bilayers directly, while larger hydrophilic molecules require transport proteins[64]. Transport can occur without the input of energy (passive transport), but molecules moving against their electrochemical gradient need transporters that utilize either chemical energy (primary active transport) or energy provided through other electrochemical gradients (secondary active transport)[64]. While plasma membrane transporters are shown, mitochondrial transporters also utilize these mechanisms. This schematic was generated using BioRender

The vast majority of the SLC25 carriers are secondary active transporters that catalyze exchange reactions between the mitochondrial matrix and intermembrane space, and all SLC25 members contain six transmembrane helices that form a tripartite structure[13]. The most abundant carrier in this family is the ADP/ATP exchanger, which in humans has four isoforms (SLC25A4, SLC25A5, SLC25A6, and SLC25A31)[13]. This exchange reaction ensures that ATP generated through respiration is exported from mitochondria to support energy-requiring cellular processes elsewhere, and also imports ADP to enable ATP synthesis within the matrix[13]. The charge imbalance that results from this exchange reaction makes this carrier electrogenic[66], and the negative inside membrane potential in the mitochondrial matrix favors ATP import and ADP export[67]. Other electrogenic carriers in the SLC25 family include the aspartate/glutamate carriers aralar (SCL25A12) and citrin (SLC25A13), which catalyze the exchange of glutamate and a proton for aspartate[13,68,69]. Together with the oxoglutarate carrier (SLC25A11), which exchanges malate for alpha-ketoglutarate[70], citrin and aralar catalyze exchange reactions vital to the malate-aspartate shuttle, which transfers redox equivalents between the mitochondrial matrix and intermembrane space[48]. This process ensures that reducing equivalents generated through glycolysis in the cytosol are transferred to the mitochondrial matrix, eventually generating mitochondrial NADH to fuel respiration[71]. It also supports the movement of the resulting oxidizing equivalents back to the cytosol, regenerating cytosolic NAD+ to support further glycolytic flux[71], and supports proliferation by providing cytosolic aspartate[72,73] (Figure 2). Other notable exchangers include the ornithine carriers (SLC25A2 and SLC25A15), which catalyze the exchange of citrulline and a proton for ornithine[13,74,75]. This reaction is vital to support the urea cycle since nitrogen in the form of carbamoyl phosphate within the

Figure 2

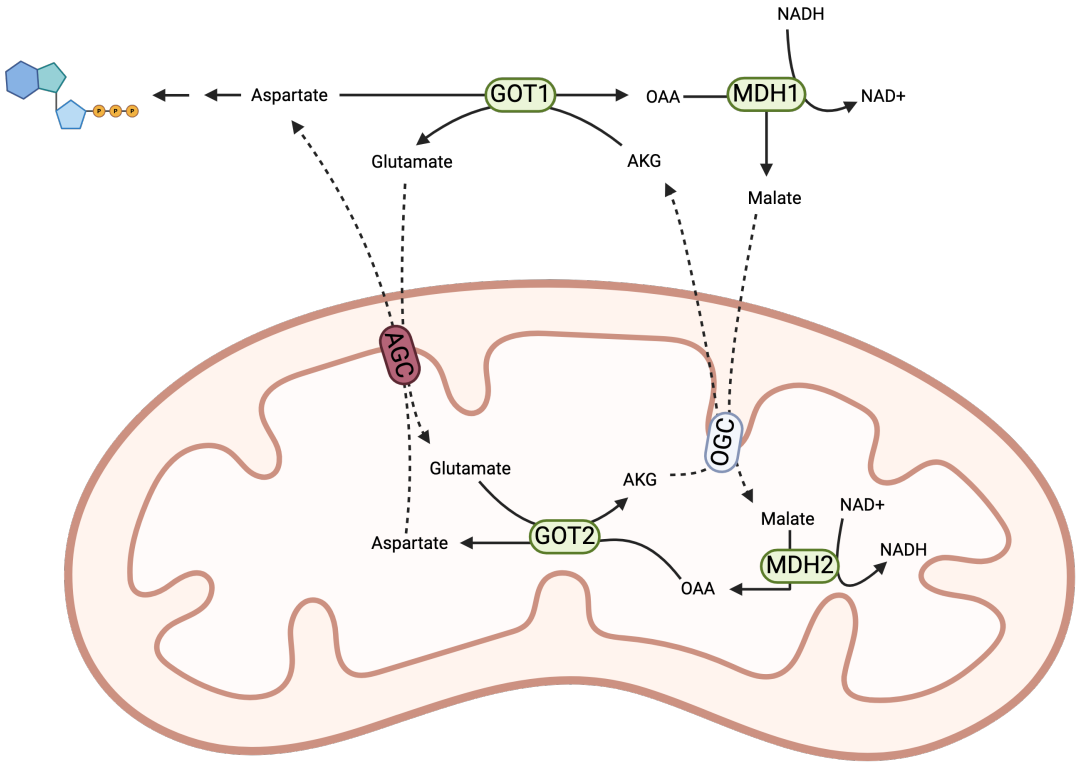
NADH
Aspartate
GOT1
OAA
MDH1
NAD+
Glutamate
AKG
Malate
AGC
OGC
Glutamate
AKG
Malate
NAD+
Aspartate
GOT2
MDH2
NADH
OAA

Fig.2. Mitochondrial transport is required for the malate-aspartate shuttle.

The aspartate/glutamate carriers (AGC, slc25a12 and slc25a13) and the oxoglutarate carrier (OGC, slc25a11) perform exchange reactions in the inner mitochondrial membrane that are required for the malate-aspartate shuttle[48]. This shuttle provides reducing equivalents for mitochondrial respiration[48], as well as cytosolic aspartate for nucleotide synthesis[72,73]. This schematic was generated using BioRender.

mitochondrial matrix must be transferred to ornithine to form citrulline, which is then exported to the cytosol to eventually produce urea[8,48]. In addition to carboxylates and amino acids, SLC25 carriers exchange fatty acids[13]. The carnitine-acylcarnitine carrier (SLC25A20) catalyzes the exchange of acylcarnitine for carnitine[76,77], which facilitates the carnitine shuttle[78]. For example, fatty acids conjugated to carnitine can be delivered to the mitochondrial matrix, where they can be broken down via β-oxidation to produce energy, most notably during fasting or periods of high energy demand such as exercise[78]. The carnitine liberated in the matrix from this process can then be exported through SLC25A20 for recycling[78].

Although most SLC25 family members catalyze exchange reactions, there are notable exceptions[13]. Uncoupling protein, also known as UCP1 (SLC25A7), operates as a uniporter and transports protons down their electrochemical gradient from the intermembrane space to the mitochondrial matrix[79], which uncouples the proton gradient from ATP synthesis[6]. UCP1 is highly expressed in brown fat[80], and dissipation of the proton gradient generated through mitochondrial respiration creates heat, which can maintain body temperature in response to cold exposure[6]. In tissues other than brown fat, the ADP/ATP exchanger contributes to uncoupling and thermogenesis[6]. The phosphate carrier (SLC25A3) catalyzes the symport of phosphate and a proton into the mitochondrial matrix[13,81]. Since the inner mitochondrial membrane contains a negative inside membrane potential, importing a proton supplies the energy required to transport the negatively charged phosphate against its electrical gradient[82]. The phosphate can then be conjugated to ADP to form ATP by ATP synthase[82]. The phosphate carrier, as well as the ADP/ATP exchanger, also binds cardiolipin, a lipid

enriched within the inner mitochondrial membrane, and binding promotes carrier activity[13,83]. In addition to phosphate, SLC25A3 may also import copper, which is required for cytochrome c oxidase biogenesis[84]. Other SLC25 family members that do not catalyze exchange reactions are the mitoferrins (SLC25A28 and SLC25A37), which import iron into the mitochondrial matrix needed for heme iron-sulfur cluster synthesis[41], and the glycine carrier (SLC25A38)[85]. Mitochondrial glycine import supports two vital metabolic pathways[85,86]. The first step in heme biosynthesis involves the conversion of glycine to 5-aminolevulinic acid by ALA synthase, a matrix localized enzyme[86,87]. The glycine cleavage system is also located within the mitochondrial matrix, and breakdown of glycine produces reducing power in the form of NADH[88] and one-carbon units that can be used for biosynthetic reactions[89].

While most SLC25 family members are solute carriers, some have evolved alternative functions and lack known transport activity. Mitochondrial carrier homologs 1 and 2 (MTCH1 or SLC25A49, and MTCH2 or SLC25A50) are two SLC25 family members that localize to the outer mitochondrial membrane, and MTCH2 has been shown to mediate the insertion of tail-anchored, signal-anchored, and multipass proteins[90]. These proteins lack characteristic sequence motifs found in canonical SCL25 family members, which may explain why they have evolved alternative functions other than solute transport[90]. Importantly, SLC25A34, SLC25A35, SLC25A43, SCL25A45, SLC25A47, SCL25A48, and SLC25A53 are orphan transporters that lack any known substrate[14]. However, Loss of SLC25A47 reduces mitochondrial NAD+ uptake, suggesting this protein may be an NAD+ transporter[91].

MPC

There are other carrier families outside of the SLC25 family that mediate solute transport across the inner mitochondrial membrane[14]. The mitochondrial pyruvate carrier (MPC1 and MPC2) facilitates the import of pyruvate, likely along with a proton, into the mitochondrial matrix[38,39,92]. This critical transport reaction ensures that pyruvate produced from glucose oxidation in the cytosol can be transferred to the mitochondrial matrix for further oxidation to acetyl-CoA, which can enter the Krebs cycle and fuel oxidative phosphorylation[93]. Decreased activity of the MPC leads to enhanced pyruvate reduction to lactate in the cytosol by lactate dehydrogenase (LDH), which regenerates NAD+ from NADH and enables the continuation of glycolytic flux[93]. This preferential reduction of pyruvate in the cytosol vs. oxidation within the mitochondria is a hallmark of the Warburg effect, also known as aerobic glycolysis, and is a phenotype exhibited by rapidly proliferating cells to support anabolic reactions, such as intestinal and skin epithelial cells, as well as many cancers[94].

MCU

The mitochondrial calcium uniporter (MCU) mediates the import of calcium from the intermembrane space into the mitochondrial matrix[49,50], a process driven by the negative inside mitochondrial membrane potential[47]. MCU acts in a complex along with MICU1, EMRE, and MCUb[95]. MICU1 contains a calcium-sensing domain, and through its shared interaction with the transmembrane protein EMRE, regulates MCU activity in response to fluctuations in cytosolic calcium levels[95,96]. MICU2 and MICU3 are paralogs that also form heterodimers with MICU1, which can also form a heterodimer with its alternative splice variant MICU1.1[95]. These proteins act as gatekeepers to MCU activity,

and calcium binding results in an increase in MCU calcium uniport activity[95]. MCUb is a dominant negative variant of MCU that can also modulate its activity depending on its expression levels by forming hetero-oligomers with MCU[95,97]. MCUR1 is another protein that interacts with the MCU, and loss of MCUR1 impairs mitochondrial calcium uptake, although this may also be due to its alternative role as a cytochrome c oxidase assembly factor[95,98]. By facilitating mitochondrial calcium uptake, the MCU allows mitochondria to act as a buffer to changes in cytosolic calcium and to regulate calcium-dependent signaling[95,99]. Furthermore, mitochondrial calcium uptake has been shown to increase the activity of the mitochondrial enzymes alpha-ketoglutarate dehydrogenase, isocitrate dehydrogenase, glycerol phosphate dehydrogenase, and pyruvate dehydrogenase[95,100]. Finally, mitochondrial calcium overload through the MCU complex leads to the opening of the mitochondrial permeability transition pore (mPTP), resulting in increased permeability of the inner mitochondrial membrane, mitochondrial swelling, and eventually rupture of the outer membrane, which leads to cytochrome c release to the cytosol, caspase activation, and cell death[95,101].

ABCB transporters

The ATP-binding cassette (ABC) transporter family members ABCB6, ABCB7, ABCB8, and ABCB10 localize to mitochondria[14,102]. While members of this transporter family are active transporters that couple the hydrolysis of ATP to the movement of substrates against their concentration gradient[103], the only strictly mitochondrial member with reported transport activity is ABCB10[104]. Mitochondrial metabolism generates significant reactive oxygen species (ROS), and various antioxidants are required to prevent ROS-induced cellular damage[32]. The antioxidant bilirubin is synthesized in the

cytosol and can enter the mitochondrial matrix to neutralize ROS, forming biliverdin in the process, which is exported through ABCB10 to promote cytosolic bilirubin regeneration[104]. In support of this function, loss of ABCB10 leads to intramitochondrial biliverdin accumulation[104]. The yeast orthologue of ABCB7 has been characterized as an iron-sulfur cluster transporter which promotes the activity of iron-sulfur cluster utilizing enzymes in other cellular compartments[14,105], and iron-sulfur clusters have been shown to stimulate human ABCB7 activity[106]. Furthermore, reduced levels of ABCB7 lead to decreased levels of cytosolic iron-sulfur clusters[107], and ABCB7 can complement the defect in the maturation of cytosolic iron-sulfur cluster proteins observed in yeast lacking the ABCB7 orthologue Atm1p[108]. Another ABCB family member that may not have strict mitochondrial localization is the porphyrin transporter ABCB6, which in addition to the outer mitochondrial membrane localizes to the plasma membrane and lysosome[14]. At the outer mitochondrial membrane, this protein may mediate the import of heme and other porphyrins into the intermembrane space[14,109]. While not involved as a direct transporter, ABCB8 localizes to the inner mitochondrial membrane and binds to the potassium channel CCDC51, where it mediates the channel's sensitivity to ATP and regulates mitochondrial volume[110].

Sideroflexins

The sideroflexin (SLC56) family contains 5 members consisting of SFXN1, SFXN2, SFXN3, SFXN4, and SFXN5[111]. A frameshift in SFXN1 was identified in *flexed-tail* mice, which have skeletal abnormalities and anemia associated with abnormal mitochondrial iron deposits[112]. However, later studies also identified intronic mutations that lead to splicing defects in Smad5 that may inhibit BMP4 in *flexed-tail* mice, which could

explain the anemia observed in this mouse model[111,113]. Still, various studies have provided evidence that sideroflexins regulate mitochondrial iron homeostasis, although the underlying mechanism remains unclear[111]. Loss of SFXN1 was also shown to be synthetic lethal with loss of the cytosolic serine producing enzyme SHMT1 in cells grown in media lacking serine, leading to the hypothesis that SFXN1 may be a mitochondrial serine transporter[114]. Indeed, loss of SFXN1 significantly reduced mitochondrial serine uptake, and SFXN1 reconstituted into proteoliposomes demonstrates serine transport activity, which can be inhibited by several other related amino acids[114]. In proliferating cells, serine is transported into mitochondria and converted into glycine through SHMT2[115]. This reaction also converts THF into 5,10-meTHF, which can supply one-carbon units for biosynthetic reactions such as nucleotide synthesis[116], and loss of SFXN1 phenocopies loss of SHMT2's effects on this biosynthetic pathway[114]. SFXN1 shares significant sequence homology with the other sideroflexins, most of all with SFXN3, and loss of SFXN1 and SFXN3 also leads to glycine auxotrophy[114]. This phenotype is rescued by SFXN2 and SFXN5, but not SFXN4, and SFXN4 also demonstrates evolutionary divergence from the other sideroflexin paralogs, indicating it may have an alternative function other than serine transport[114]. Consistent with this idea, loss of SFXN4 leads to downregulation of complex I subunits and inhibition of respiration, potentially through interactions with the MICA complex, and therefore may act as a chaperone as opposed to a solute transporter[117]. Sideroflexins have also been shown to regulate other mitochondrial metabolic pathways. Loss of SFXN4 inhibits iron-sulfur cluster formation and leads to mitochondrial iron accumulation[118], and loss of SFXN1 was shown to inhibit the formation of complex III[119]. Furthermore, loss of SFXN1 also protects cells against inducers of ferroptosis, leading to mitochondrial

accumulation of taurine and hypotaruine[120]. Whether these effects are due to loss of SFXN1's transport activity or another alternative function remains undetermined. SFXN1 may also act in a complex with other proteins such as SERAC1, and loss of SERAC1 reduces SFXN1 protein levels and mitochondrial DNA content, potentially through reduced mitochondrial serine uptake and impaired nucleotide biosynthesis[121].

Other mitochondrial transporters

Several other mitochondrial carriers outside of the aforementioned families also localize to mitochondria[102]. SLC11A2 localizes to endosomes[122] and the outer mitochondrial membrane[123], and acts as a symporter mediating the uptake of divalent metal cations with a proton[124], which supports mitochondrial iron uptake[125] through early endosome-mitochondria interactions[126]. SLC22A4 localizes to the plasma membrane[128,129] and to the mitochondria[127], and mediates the uptake of the antioxidant ergothioneine[128]. When localized to mitochondria, expression of SLC22A4 has been shown to increase mitochondrial carnitine uptake, indicating there may be alternative carnitine transport mechanisms other than the carnitine shuttle system[127]. Interestingly, mitochondria lacking SLC22A4 can still import ergothioneine, suggesting there may also be alternative transporters for this molecule[129]. SLC30A9 may localize to the endoplasmic reticulum[130] and mitochondria[131], where it acts as a proton-coupled zinc antiporter and is required for optimal mitochondrial zinc export[131] and oxidative phosphorylation[132]. A variant of the plasma membrane neutral amino acid transporter SLC1A5 also localizes to mitochondria and is required for mitochondrial glutamine uptake, which may contribute to Krebs cycle anaplerosis by providing substrate to mitochondrial glutaminase[133]. Other mitochondrial transporters include Translocator protein (TSPO),

which localizes to the outer mitochondrial membrane and transports cholesterol to promote steroid biosynthesis[134], and PRELID3A and PRELID3B, which promote phosphatidic acid transport to the inner mitochondrial membrane for cardiolipin synthesis[135]. ATP7B (Wilson's disease protein) is a P-type ATPase that transports copper[136]. Variants of this protein have been shown to localize to both the Golgi[137] and mitochondria[138], and loss of ATP7B has been shown to induce cardiolipin fragmentation due to mitochondrial copper overload[139]. Other ion transporters include GHITM and SLC8B1, which are calcium antiporters that localize to mitochondria and mediate calcium efflux[140,141].

Diseases associated with mitochondrial carriers

Mitochondria assist in vital cellular processes in all organs. Aside from producing ATP[3] and performing biosynthetic reactions needed for cell growth[5], mitochondria also promote nitrogen detoxification through the urea cycle[8], assist in neurotransmitter production and regulation[9], regulate cellular ion homeostasis[11], and respond to various stimuli to promote regulated cell death[7], and mitochondrial carriers are required for all of these processes[13]. The SLC25 carrier family represents the largest solute transporter family in humans, and mutations in roughly one-third of these carriers have been identified that lead to disease, and in most cases these mutations lead to reductions or complete loss of transport activity, often with lethal consequences[142]. Most of the mutations are rare, although there are more common exceptions that lead to milder forms of disease, typically involving impairments in the urea cycle[142]. More than 600 patients have been identified that have loss of function mutations in the aspartate/glutamate carrier SLC25A13, which leads to both adult and neonatal-onset

citrullinemia type II due to the requirement of mitochondrial aspartate export for the urea cycle[142,143]. Additionally, over 90 patients have also been identified with mutations in the ornithine carrier SLC25A15 that result in hyperornithinemia, hyperammonemia, and homocitrullinuria (HHH) syndrome[142,144].

Mutations in other mitochondrial carrier families have also been identified that lead to disease. Mutations in ABCB7 lead to anemia and ataxia[145], and mutations in SFXN4 lead to anemia associated with mitochondrial dysfunction[146]. Mutations in ATP7B reduce its copper transport activity and lead to Wilson's disease, which is associated with abnormal copper accumulation, particularly in the liver and brain, which results in a wide range of symptoms including ataxia and tremors, and can eventually result in liver failure[147].

Many mitochondrial carriers have been implicated in cancer since tumors require mitochondrial metabolism to support cancer cell proliferation[148]. The citrate/malate exchanger SLC25A1 is overexpressed in lung cancer and promotes cancer resistance to therapy[148,149], and the dicarboxylate exchanger SLC25A10 has been shown to promote cancer progression through inhibition of ROS generation[148,150]. Mitochondrial export of aspartate is essential for cell proliferation[72,151], and loss of the aspartate/glutamate exchanger SLC25A12 has been found to inhibit liver cancer cell growth, where it is upregulated through epigenetic mechanisms[148,152]. Some mitochondrial transporters may also function as tumor suppressors. Loss of SFXN1 enhances liver tumor growth in mice fed a high-fat diet, potentially through inhibition of ROS, although the mechanism underlying this phenomenon is poorly understood[120,153]. Downregulation of the MPC in a variety of tumors also leads to enhanced growth and cancer progression, likely by

promoting the Warbug effect[93], and loss of SLC25A43 may promote the growth of HER2-positive breast cancer[148,154].

Recent insights

Considerable progress has been made in recent years towards characterizing mitochondrial transporters that lack known substrates. SLC25A39 and its paralog SLC25A40 were identified as likely mitochondrial glutathione transporters[155,156]. Loss of SLC25A39 led to decreased mitochondrial glutathione and impaired cellular prolifreration[155,156]. Interestingly, loss of mitochondrial glutathione through SLC25A39 depletion led to impaired iron-sulfur cluster biogenesis and erythropoiesis, and cellular growth in these conditions was insensitive to redox perturbations, indicating the primary function for mitochondrial glutathione is to support iron-sulfur cluster synthesis through glutaredoxins[155]. It was also found that SLC25A39 protein levels respond to cellular glutathione levels through a feedback mechanism involving the mitochondrial protease AFG3L2, indicating that mechanisms have evolved to regulate mitochondrial transporter availability in response to fluctuations in metabolite levels[157]. SLC25A51 and SLC25A52 were also recently identified as mitochondrial NAD+ transporters, and loss of mitochondrial NAD+ import led to decreased mitochondrial NAD+ and NADH levels and impaired respiration[158–160], while overexpression of SLC25A51 was found to promote progression of acute myeloid leukemia (AML) and was associated with poor prognosis[161]. SLC25A44 was recently identified as a mitochondrial branched-chain amino acid transporter required for the import of leucine and valine in brown fat[162]. Loss of SLC25A44 impaired thermogenesis and temperature regulation in response to cold exposure and fever, indicating that mitochondrial branched-chain

amino acid oxidation is required for optimal response to these stress conditions[162,163]. Another mitochondrial carrier that was recently characterized is the choline transporter SLC25A48[164]. Loss of SLC25A48 impairs mitochondrial choline import, which is required for betaine synthesis, an important intermediate in one-carbon metabolism that also acts as an osmolyte[164]. Mitochondrial choline import through SLC25A48 in brown fat also regulates thermogenesis by supporting purine nucleotide synthesis, and loss of SLC25A48 leads to reduced cold tolerance[165].

Unknown mechanisms of mitochondrial transport

The transporters that many metabolites use to cross this bilayer have yet to be identified. In particular, nearly half of the amino acids lack a known mitochondrial carrier, and many of these amino acids participate in crucial matrix-associated metabolic pathways. For example, the first step in iron-sulfur cluster biosynthesis involves the desulfuration of cysteine by the iron-sulfur cluster (ISC) assembly complex located within the mitochondrial matrix[166]. This leads to the production of iron-sulfur clusters, which are required for numerous electron transfer reactions including those of the Krebs cycle and respiratory chain[166]. Since mitochondria lack any known enzymes that produce cysteine within the matrix, cysteine import is likely utilized for mitochondrial iron-sulfur cluster biogenesis, yet its carrier has yet to be discovered, although glutathione catabolism can support iron-sulfur cluster synthesis when cells are deprived of cysteine[167].

Another amino acid without an assigned mitochondrial transporter is proline. Proline degradation occurs at the inner mitochondrial membrane through the action of the proline dehydrogenases[168,169], and inhibition of this metabolic pathway has been shown

to impair the formation of cancer metastases[170]. As a conditionally essential amino acid, proline can also be synthesized via the matrix enzymes PYCR1 and PYCR2[169,171,172]. While a third cytosolic enzyme (PYCR3) is capable of producing proline, recent studies have shown mitochondrial proline synthesis is required to maintain cellular proline levels to support proliferation when environmental levels are limiting[168,173,174]. Proline synthesis can be utilized by rapidly proliferating cells when electron acceptors are limiting since the synthesis of proline regenerates NAD+ from NADH, which supports glycolytic flux and biosynthetic metabolism, and mitochondrial export of proline likely facilitates its continued synthesis[175,176]. In support of this, cells grown in hypoxic conditions upregulate proline synthesis through PYCR1, which is then exported into the extracellular space[175]. Many aspects of mitochondrial proline metabolism are rewired in cancer to support redox balance and proliferation in tumor cells, as well as aid the production of collagen and desmoplasia by cancer-associated fibroblasts, which can inhibit drug delivery and promote hypoxic environments that favor cancer progression[168,175,177]. Despite the fundamental importance of mitochondrial proline transport in these processes, the carrier involved remains unknown.

In addition to cysteine and proline, the mitochondrial carriers for methionine, alanine, threonine, asparagine, phenylalanine, tyrosine, and tryptophan are still unidentified. Since inhibition of mitochondrial protein synthesis impairs cellular respiration[178], it is likely that all of these amino acids must be transported into the mitochondrial matrix to support this process. However, another possible source of matrix amino acids could be those obtained from the proteolysis of nuclear-encoded mitochondrial proteins, which are synthesized via cytosolic ribosomes[48]. Future studies are needed to identify the

mitochondrial transporters for these amino acids and determine the relative contribution of transporter-mediated import to the mitochondrial matrix amino acid pool.

In addition to the proteinogenic amino acids, non-canonical amino acids must also pass the inner mitochondrial membrane to support metabolic processes. The amino sulfonic acid taurine is the most abundant free amino acid in human tissues (with the exception of the liver, where it is second to aspartate)[179], and it was recently discovered that taurine levels decrease with aging, and that lifespan can be improved through taurine supplementation[180]. Exactly how taurine regulates the physiological changes associated with aging is unclear since taurine is required for multiple biological processes[179–181]. While taurine can be obtained from dietary sources, it is predominantly synthesized in the liver, where it is used to produce bile salts that aid in the digestion of dietary fat[179]. Throughout the human body, taurine acts as an osmolyte and antioxidant and is required for a range of processes including neuronal development, immune maturation, and insulin secretion[179]. At the subcellular level, taurine is found in high concentrations in mitochondria, where it reduces oxidative stress and acts as a pH buffer[179,181]. In the matrix, taurine is also conjugated to mitochondrial tRNAs and is required for the optimal production of mitochondrial proteins that support cellular respiration[182–184]. In cells, taurine is synthesized through the transulfuration and cysteinesulfinic acid pathways in the cytosol[179], and since mitochondria lack defined taurine-producing enzymes, it is likely that taurine import through an unknown inner membrane carrier is required for its mitochondrial functions.

Another non-proteinogenic amino acid that must pass the inner mitochondrial membrane is gamma-aminobutyric acid (GABA). Beginning with early work demonstrating GABA inhibits the firing of crayfish neurons[185], GABA is now appreciated to be the primary inhibitory neurotransmitter in humans[9,186]. While it is most abundant in the brain, GABA is also found in lower concentrations in other tissues, such as the pancreas[187], where it regulates hormone secretion by pancreatic beta cells[188]. GABA can also be produced from the gut microbiome[189], and supplementation with GABA-producing probiotics has been shown to alleviate tremors and improve depressive symptoms[190]. In the brain, GABA is predominantly synthesized in GABAergic neurons from the excitatory amino acid glutamate through glutamate decarboxylases[9], although some neurons and glial cells may utilize an alternative synthesis pathway utilizing putrescine for GABA production[191,192]. Once synthesized, GABA loaded into presynaptic vesicles is released after neuronal depolarization and subsequently binds to GABA receptors expressed by postsynaptic neurons, leading to hyperpolarization and decreased responsiveness[9,186]. GABA levels at the synapse are regulated by surrounding astrocytes, which convert GABA back to glutamine, which can then be utilized by GABAergic neurons to resynthesize glutamate and GABA[9]. This recycling pathway, known as the glutamate/GABA-glutamine cycle, is an essential regulator of neurotransmitter pools within neurons and at synapses[9,186]. In astrocytes, GABA is degraded through the GABA transaminase ABAT, which localizes to the mitochondrial matrix, and inhibition of GABA degradation leads to increased synaptic GABA levels[9,169,193]. Increased synaptic GABA has been shown to dampen excitotoxicity, and inhibitors of ABAT are used clinically in the treatment of epilepsy[193]. Through ABAT, GABA is converted to succinic semialdehyde and eventually to alpha-ketoglutarate,

allowing GABA to also fuel Krebs cycle anaplerosis to promote proliferation, and some cancers that metastasize to the brain may utilize this pathway for growth[9,194]. Interestingly, in some tissues like the liver, ABAT may produce GABA[195]. Higher liver expression of ABAT is found in humans with obesity, and inhibition of GABA production in this tissue through ABAT inhibition has been shown to improve insulin sensitivity and promote weight loss in obese mice, likely by inhibiting GABA binding to receptors located in surrounding nerve cells[195]. Despite the requirement for mitochondrial GABA transport in all of these processes, no inner membrane carrier has been identified in humans.

Conclusions

Numerous small molecules must pass the inner mitochondrial membrane to carry out metabolic functions, many of which are amino acids that lack known transporters. In chapter 2 of this thesis, I will discuss the known mitochondrial amino acid transporters and present results that suggest the sideroflexins are regulators of mitochondrial permeability to a wide range of polar neutral amino acids.

References

(1) Sagan, L. On the Origin of Mitosing Cells. *J. Theor. Biol.* **1967**, *14* (3), 255–274. https://doi.org/10.1016/0022-5193(67)90079-3.

(2) Siekevitz, P. Powerhouse of the Cell. *Sci. Am.* **1957**, *197* (1), 131–144.

(3) Kennedy, E. P.; Lehninger, A. L. Oxidation of Fatty Acids and Tricarboxylic Acid Cycle Intermediates by Isolated Rat Liver Mitochondria. *J. Biol. Chem.* **1949**, *179* (2), 957–972.

(4) Mitchell, P. Coupling of Phosphorylation to Electron and Hydrogen Transfer by a Chemi-Osmotic Type of Mechanism. *Nature* **1961**, *191* (4784), 144–148. https://doi.org/10.1038/191144a0.

(5) Ahn, C. S.; Metallo, C. M. Mitochondria as Biosynthetic Factories for Cancer Proliferation. *Cancer Metab.* **2015**, *3*, 1. https://doi.org/10.1186/s40170-015-0128-2.

(6) Bertholet, A. M.; Kirichok, Y. Mitochondrial H+ Leak and Thermogenesis. *Annu. Rev. Physiol.* **2022**, *84* (Volume 84, 2022), 381–407. https://doi.org/10.1146/annurev-physiol-021119-034405.

(7) Czabotar, P. E.; Garcia-Saez, A. J. Mechanisms of BCL-2 Family Proteins in Mitochondrial Apoptosis. *Nat. Rev. Mol. Cell Biol.* **2023**, *24* (10), 732–748. https://doi.org/10.1038/s41580-023-00629-4.

(8) Morris, S. M. Regulation of Enzymes of the Urea Cycle and Arginine Metabolism. *Annu. Rev. Nutr.* **2002**, *22*, 87–105. https://doi.org/10.1146/annurev.nutr.22.110801.140547.

(9) Andersen, J. V.; Schousboe, A. Milestone Review: Metabolic Dynamics of Glutamate and GABA Mediated Neurotransmission — The Essential Roles of Astrocytes. *J. Neurochem.* **2023**, *166* (2), 109–137. https://doi.org/10.1111/jnc.15811.

(10) Jacobs, L. J. H. C.; Riemer, J. Maintenance of Small Molecule Redox Homeostasis in Mitochondria. *FEBS Lett.* **2023**, *597* (2), 205–223. https://doi.org/10.1002/1873-3468.14485.

(11) Szabo, I.; Szewczyk, A. Mitochondrial Ion Channels. *Annu. Rev. Biophys.* **2023**, *52* (Volume 52, 2023), 229–254. https://doi.org/10.1146/annurev-biophys-092622-094853.

(12) Colombini, M. A Candidate for the Permeability Pathway of the Outer Mitochondrial Membrane. *Nature* **1979**, *279* (5714), 643–645. https://doi.org/10.1038/279643a0.

(13) Ruprecht, J. J.; Kunji, E. R. S. The SLC25 Mitochondrial Carrier Family: Structure and Mechanism. *Trends Biochem. Sci.* **2020**, *45* (3), 244–258. https://doi.org/10.1016/j.tibs.2019.11.001.

(14) Cunningham, C. N.; Rutter, J. 20,000 Picometers under the OMM: Diving into the Vastness of Mitochondrial Metabolite Transport. *EMBO Rep.* **2020**, *21* (5), e50071. https://doi.org/10.15252/embr.202050071.

(15) Logan, D. C. Mitochondrial Dynamics. *New Phytol.* **2003**, *160* (3), 463–478. https://doi.org/10.1046/j.1469-8137.2003.00918.x.

(16) Ernster, L.; Schatz, G. Mitochondria: A Historical Review. *J. Cell Biol.* **1981**, *91* (3), 227s–255s. https://doi.org/10.1083/jcb.91.3.227s.

(17) Altmann, R. *Die Elementarorganismen Und Ihre Beziehungen Zu Den Zellen*; Veit, 1890.

(18) Bechtel, W. *Discovering Cell Mechanisms: The Creation of Modern Cell Biology*; Cambridge University Press, 2006.

(19) Benda, C. Ueber Die Spermatogenese Der Vertebraten Und Höherer Evertebraten, II. Theil: Die Histiogenese Der Spermien. *Arch. Für Physiol.* **1898**, 393–398.

(20) Michaelis, L. Die vitale Färbung, eine Darstellungsmethode der Zellgranula. *Arch. Für Mikrosk. Anat.* **1899**, *55* (1), 558–575. https://doi.org/10.1007/BF02977747.

(21) Pagliarini, D. J.; Rutter, J. Hallmarks of a New Era in Mitochondrial Biochemistry. *Genes Dev.* **2013**, *27* (24), 2615–2627. https://doi.org/10.1101/gad.229724.113.

(22) Kohler, R. E. The Background to Otto Warburg's Conception of the Atmungsferment. *J. Hist. Biol.* **1973**, *6* (2), 171–192. https://doi.org/10.1007/BF00127607.

(23) Kingsbury, B. F. Cytoplasmic Fixation. *Anat. Rec.* **1912**, *6* (2), 39–52. https://doi.org/10.1002/ar.1090060202.

(24) On Cytochrome, a Respiratory Pigment, Common to Animals, Yeast, and Higher Plants. *Proc. R. Soc. Lond. Ser. B Contain. Pap. Biol. Character* **1925**, *98* (690), 312–339. https://doi.org/10.1098/rspb.1925.0039.

(25) Krebs, H. A.; Johnson, W. A. Metabolism of Ketonic Acids in Animal Tissues. *Biochem. J.* **1937**, *31* (4), 645–660.

(26) Hogeboom, G. H.; Claude, A.; Hotch-Kiss, R. D. The Distribution of Cytochrome Oxidase and Succinoxidase in the Cytoplasm of the Mammalian Liver Cell. *J. Biol. Chem.* **1946**, *165* (2), 615–629.

(27) Chandel, N. S. Glycolysis. *Cold Spring Harb. Perspect. Biol.* **2021**, *13* (5), a040535. https://doi.org/10.1101/cshperspect.a040535.

(28) Jagendorf, A. T. Acid-Base Transitions and Phosphorylation by Chloroplasts. *Fed. Proc.* **1967**, *26* (5), 1361–1369.

(29) Jagendorf, A. T.; Uribe, E. ATP Formation Caused by Acid-Base Transition of Spinach Chloroplasts. *Proc. Natl. Acad. Sci.* **1966**, *55* (1), 170–177. https://doi.org/10.1073/pnas.55.1.170.

(30) Chappell, J. B.; Crofts, A. R. Gramicidin and Ion Transport in Isolated Liver Mitochondria. *Biochem. J.* **1965**, *95* (2), 393–402.

(31) Racker, E.; Kandrach, A. Reconstitution of the Third Site of Oxidative Phosphorylation. *J. Biol. Chem.* **1971**, *246* (22), 7069–7071. https://doi.org/10.1016/S0021-9258(19)45951-6.

(32) Nolfi-Donegan, D.; Braganza, A.; Shiva, S. Mitochondrial Electron Transport Chain: Oxidative Phosphorylation, Oxidant Production, and Methods of Measurement. *Redox Biol.* **2020**, *37*, 101674. https://doi.org/10.1016/j.redox.2020.101674.

(33) Slater, E. C. Keilin, Cytochrome, and the Respiratory Chain. *J. Biol. Chem.* **2003**, *278* (19), 16455–16461. https://doi.org/10.1074/jbc.X200011200.

(34) Ramsay, R. R. Electron Carriers and Energy Conservation in Mitochondrial Respiration. *ChemTexts* **2019**, *5* (2), 9. https://doi.org/10.1007/s40828-019-0085-4.

(35) Schultz, B. E.; Chan, S. I. Structures and Proton-Pumping Strategies of Mitochondrial Respiratory Enzymes. *Annu. Rev. Biophys. Biomol. Struct.* **2001**, *30*, 23–65. https://doi.org/10.1146/annurev.biophys.30.1.23.

(36) Jonckheere, A. I.; Smeitink, J. A. M.; Rodenburg, R. J. T. Mitochondrial ATP Synthase: Architecture, Function and Pathology. *J. Inherit. Metab. Dis.* **2012**, *35* (2), 211–225. https://doi.org/10.1007/s10545-011-9382-9.

(37) Kunji, E. R. S.; King, M. S.; Ruprecht, J. J.; Thangaratnarajah, C. The SLC25 Carrier Family: Important Transport Proteins in Mitochondrial Physiology and Pathology. *Physiology* **2020**, *35* (5), 302–327. https://doi.org/10.1152/physiol.00009.2020.

(38) Bricker, D. K.; Taylor, E. B.; Schell, J. C.; Orsak, T.; Boutron, A.; Chen, Y.-C.; Cox, J. E.; Cardon, C. M.; Van Vranken, J. G.; Dephoure, N.; Redin, C.; Boudina, S.; Gygi, S. P.; Brivet, M.; Thummel, C. S.; Rutter, J. A Mitochondrial Pyruvate Carrier Required for Pyruvate Uptake in Yeast, Drosophila, and Humans. *Science* **2012**, *337* (6090), 96–100. https://doi.org/10.1126/science.1218099.

(39) Herzig, S.; Raemy, E.; Montessuit, S.; Veuthey, J.-L.; Zamboni, N.; Westermann, B.; Kunji, E. R. S.; Martinou, J.-C. Identification and Functional Expression of the Mitochondrial Pyruvate Carrier. *Science* **2012**, *337* (6090), 93–96. https://doi.org/10.1126/science.1218530.

(40) Stubbs, M. Inhibitors of the Adenine Nucleotide Translocase. *Pharmacol. Ther.* **1979**, *7* (2), 329–350. https://doi.org/10.1016/0163-7258(79)90035-4.

(41) Dietz, J. V.; Fox, J. L.; Khalimonchuk, O. Down the Iron Path: Mitochondrial Iron Homeostasis and Beyond. *Cells* **2021**, *10* (9), 2198. https://doi.org/10.3390/cells10092198.

(42) Palade, G. E. An Electron Microscope Study of the Mitochondrial Structure. *J. Histochem. Cytochem. Off. J. Histochem. Soc.* **1953**, *1* (4), 188–211. https://doi.org/10.1177/1.4.188.

(43) Sjostrand, F. S. Electron Microscopy of Mitochondria and Cytoplasmic Double Membranes. *Nature* **1953**, *171* (4340), 30–32. https://doi.org/10.1038/171030a0.

(44) LaNoue, K. F.; Schoolwerth, A. C. Metabolite Transport in Mitochondria. *Annu. Rev. Biochem.* **1979**, *48* (1), 871–922. https://doi.org/10.1146/annurev.bi.48.070179.004255.

(45) Azzi, A.; Chappell, J. B.; Robinson, B. H. Penetration of the Mitochondrial Membrane by Glutamate and Aspartate. *Biochem. Biophys. Res. Commun.* **1967**, *29* (1), 148–152. https://doi.org/10.1016/0006-291x(67)90556-6.

(46) Vasington, F. D.; Murphy, J. V. Ca++ Uptake by Rat Kidney Mitochondria and Its Dependence on Respiration and Phosphorylation. *J. Biol. Chem.* **1962**, *237* (8), 2670–2677. https://doi.org/10.1016/S0021-9258(19)73805-8.

(47) Deluca, H. F.; Engstrom, G. W. Calcium Uptake by Rat Kidney Mitochondria. *Proc. Natl. Acad. Sci. U. S. A.* **1961**, *47* (11), 1744–1750. https://doi.org/10.1073/pnas.47.11.1744.

(48) Monné, M.; Vozza, A.; Lasorsa, F. M.; Porcelli, V.; Palmieri, F. Mitochondrial Carriers for Aspartate, Glutamate and Other Amino Acids: A Review. *Int. J. Mol. Sci.* **2019**, *20* (18), 4456. https://doi.org/10.3390/ijms20184456.

(49) Baughman, J. M.; Perocchi, F.; Girgis, H. S.; Plovanich, M.; Belcher-Timme, C. A.; Sancak, Y.; Bao, X. R.; Strittmatter, L.; Goldberger, O.; Bogorad, R. L.; Koteliansky, V.; Mootha, V. K. Integrative Genomics Identifies MCU as an Essential Component of the Mitochondrial Calcium Uniporter. *Nature* **2011**, *476* (7360), 341–345. https://doi.org/10.1038/nature10234.

(50) De Stefani, D.; Raffaello, A.; Teardo, E.; Szabò, I.; Rizzuto, R. A Forty-Kilodalton Protein of the Inner Membrane Is the Mitochondrial Calcium Uniporter. *Nature* **2011**, *476* (7360), 336–340. https://doi.org/10.1038/nature10230.

(51) Marchi, S.; Pinton, P. The Mitochondrial Calcium Uniporter Complex: Molecular Components, Structure and Physiopathological Implications. *J. Physiol.* **2014**, *592* (Pt 5), 829–839. https://doi.org/10.1113/jphysiol.2013.268235.

(52) Chakrabarti, A. C. Permeability of Membranes to Amino Acids and Modified Amino Acids: Mechanisms Involved in Translocation. *Amino Acids* **1994**, *6* (3), 213–229. https://doi.org/10.1007/BF00813743.

(53) Deamer, D. W.; Bramhall, J. Permeability of Lipid Bilayers to Water and Ionic Solutes. *Chem. Phys. Lipids* **1986**, *40* (2–4), 167–188. https://doi.org/10.1016/0009-3084(86)90069-1.

(54) Yang, N. J.; Hinner, M. J. Getting Across the Cell Membrane: An Overview for Small Molecules, Peptides, and Proteins. *Methods Mol. Biol. Clifton NJ* **2015**, *1266*, 29–53. https://doi.org/10.1007/978-1-4939-2272-7_3.

(55) Halling, P. J.; Brand, M. D.; Chappell, J. B. Permeability of Mitochondria to Neutral Amino Acids. *FEBS Lett.* **1973**, *34* (2), 169–171. https://doi.org/10.1016/0014-5793(73)80785-9.

(56) Cybulski, R. L.; Fisher, R. R. Mitochondrial Neutral Amino Acid Transport: Evidence for a Carrier Mediated Mechanism. *Biochemistry* **1977**, *16* (23), 5116–5120. https://doi.org/10.1021/bi00642a026.

(57) Camara, A. K. S.; Zhou, Y.; Wen, P.-C.; Tajkhorshid, E.; Kwok, W.-M. Mitochondrial VDAC1: A Key Gatekeeper as Potential Therapeutic Target. *Front. Physiol.* **2017**, *8*. https://doi.org/10.3389/fphys.2017.00460.

(58) Bayrhuber, M.; Meins, T.; Habeck, M.; Becker, S.; Giller, K.; Villinger, S.; Vonrhein, C.; Griesinger, C.; Zweckstetter, M.; Zeth, K. Structure of the Human Voltage-Dependent Anion Channel. *Proc. Natl. Acad. Sci. U. S. A.* **2008**, *105* (40), 15370–15375. https://doi.org/10.1073/pnas.0808115105.

(59) Shoshan-Barmatz, V.; Shteinfer-Kuzmine, A.; Verma, A. VDAC1 at the Intersection of Cell Metabolism, Apoptosis, and Diseases. *Biomolecules* **2020**, *10* (11), 1485. https://doi.org/10.3390/biom10111485.

(60) Varughese, J. T.; Buchanan, S. K.; Pitt, A. S. The Role of Voltage-Dependent Anion Channel in Mitochondrial Dysfunction and Human Disease. *Cells* **2021**, *10* (7), 1737. https://doi.org/10.3390/cells10071737.

(61) Chin, H. S.; Li, M. X.; Tan, I. K. L.; Ninnis, R. L.; Reljic, B.; Scicluna, K.; Dagley, L. F.; Sandow, J. J.; Kelly, G. L.; Samson, A. L.; Chappaz, S.; Khaw, S. L.; Chang, C.; Morokoff, A.; Brinkmann, K.; Webb, A.; Hockings, C.; Hall, C. M.; Kueh, A. J.; Ryan, M. T.; Kluck, R. M.; Bouillet, P.; Herold, M. J.; Gray, D. H. D.; Huang, D. C. S.; van Delft, M. F.; Dewson, G. VDAC2 Enables BAX to Mediate Apoptosis and Limit Tumor Development. *Nat. Commun.* **2018**, *9* (1), 4976. https://doi.org/10.1038/s41467-018-07309-4.

(62) Shokolenko, I.; Alexeyev, M. Mitochondrial DNA: Consensuses and Controversies. *DNA* **2022**, *2* (2), 131–148. https://doi.org/10.3390/dna2020010.

(63) Haastrup, M. O.; Vikramdeo, K. S.; Singh, S.; Singh, A. P.; Dasgupta, S. The Journey of Mitochondrial Protein Import and the Roadmap to Follow. *Int. J. Mol. Sci.* **2023**, *24* (3), 2479. https://doi.org/10.3390/ijms24032479.

(64) Stillwell, W. Chapter 19 - Membrane Transport. In *An Introduction to Biological Membranes (Second Edition)*; Stillwell, W., Ed.; Elsevier, 2016; pp 423–451. https://doi.org/10.1016/B978-0-444-63772-7.00019-1.

(65) Calamita, G.; Ferri, D.; Gena, P.; Liquori, G. E.; Cavalier, A.; Thomas, D.; Svelto, M. The Inner Mitochondrial Membrane Has Aquaporin-8 Water Channels and Is

Highly Permeable to Water. *J. Biol. Chem.* **2005**, *280* (17), 17149–17153. https://doi.org/10.1074/jbc.C400595200.

(66) Villiers, C.; Michejda, J. W.; Block, M.; Lauquin, G. J.; Vignais, P. V. The Electrogenic Nature of ADP/ATP Transport in inside-out Submitochondrial Particles. *Biochim. Biophys. Acta* **1979**, *546* (1), 157–170. https://doi.org/10.1016/0005-2728(79)90177-4.

(67) Gropp, T.; Brustovetsky, N.; Klingenberg, M.; Müller, V.; Fendler, K.; Bamberg, E. Kinetics of Electrogenic Transport by the ADP/ATP Carrier. *Biophys. J.* **1999**, *77* (2), 714–726.

(68) LaNoue, K. F.; Meijer, A. J.; Brouwer, A. Evidence for Electrogenic Aspartate Transport in Rat Liver Mitochondria. *Arch. Biochem. Biophys.* **1974**, *161* (2), 544–550. https://doi.org/10.1016/0003-9861(74)90337-3.

(69) Palmieri, L.; Pardo, B.; Lasorsa, F. M.; del Arco, A.; Kobayashi, K.; Iijima, M.; Runswick, M. J.; Walker, J. E.; Saheki, T.; Satrústegui, J.; Palmieri, F. Citrin and Aralar1 Are Ca2+-Stimulated Aspartate/Glutamate Transporters in Mitochondria. *EMBO J.* **2001**, *20* (18), 5060–5069. https://doi.org/10.1093/emboj/20.18.5060.

(70) Fiermonte, G.; Walker, J. E.; Palmieri, F. Abundant Bacterial Expression and Reconstitution of an Intrinsic Membrane-Transport Protein from Bovine Mitochondria. *Biochem. J.* **1993**, *294 (Pt 1)* (Pt 1), 293–299. https://doi.org/10.1042/bj2940293.

(71) Borst, P. The Malate–Aspartate Shuttle (Borst Cycle): How It Started and Developed into a Major Metabolic Pathway. *Iubmb Life* **2020**, *72* (11), 2241–2259. https://doi.org/10.1002/iub.2367.

(72) Sullivan, L. B.; Gui, D. Y.; Hosios, A. M.; Bush, L. N.; Freinkman, E.; Vander Heiden, M. G. Supporting Aspartate Biosynthesis Is an Essential Function of Respiration in Proliferating Cells. *Cell* **2015**, *162* (3), 552–563. https://doi.org/10.1016/j.cell.2015.07.017.

(73) Birsoy, K.; Wang, T.; Chen, W.; Freinkman, E.; Abu-Remaileh, M.; Sabatini, D. M. An Essential Role of the Mitochondrial Electron Transport Chain in Cell Proliferation Is to Enable Aspartate Synthesis. *Cell* **2015**, *162* (3), 540–551. https://doi.org/10.1016/j.cell.2015.07.016.

(74) Indiveri, C.; Tonazzi, A.; Palmieri, F. Identification and Purification of the Ornithine/Citrulline Carrier from Rat Liver Mitochondira. *Eur. J. Biochem.* **1992**, *207* (2), 449–454. https://doi.org/10.1111/j.1432-1033.1992.tb17070.x.

(75) Indiveri, C.; Tonazzi, A.; Stipani, I.; Palmieri, F. The Purified and Reconstituted Ornithine/Citrulline Carrier from Rat Liver Mitochondria: Electrical Nature and Coupling of the Exchange Reaction with H+ Translocation. *Biochem. J.* **1997**, *327* (Pt 2), 349–355.

(76) Indiveri, C.; Iacobazzi, V.; Giangregorio, N.; Palmieri, F. Bacterial Overexpression, Purification, and Reconstitution of the Carnitine/Acylcarnitine Carrier from Rat Liver Mitochondria. *Biochem. Biophys. Res. Commun.* **1998**, *249* (3), 589–594. https://doi.org/10.1006/bbrc.1998.9197.

(77) Giangregorio, N.; Tonazzi, A.; Console, L.; Indiveri, C.; Palmieri, F. Site-Directed Mutagenesis of Charged Amino Acids of the Human Mitochondrial Carnitine/Acylcarnitine Carrier: Insight into the Molecular Mechanism of Transport. *Biochim. Biophys. Acta* **2010**, *1797* (6–7), 839–845. https://doi.org/10.1016/j.bbabio.2010.03.017.

(78) Knottnerus, S. J. G.; Bleeker, J. C.; Wüst, R. C. I.; Ferdinandusse, S.; IJlst, L.; Wijburg, F. A.; Wanders, R. J. A.; Visser, G.; Houtkooper, R. H. Disorders of Mitochondrial Long-Chain Fatty Acid Oxidation and the Carnitine Shuttle. *Rev. Endocr. Metab. Disord.* **2018**, *19* (1), 93–106. https://doi.org/10.1007/s11154-018-9448-1.

(79) Klingenberg, M.; Winkler, E. The Reconstituted Isolated Uncoupling Protein Is a Membrane Potential Driven H+ Translocator. *EMBO J.* **1985**, *4* (12), 3087–3092.

(80) Ricquier, D.; Kader, J. C. Mitochondrial Protein Alteration in Active Brown Fat: A Soidum Dodecyl Sulfate-Polyacrylamide Gel Electrophoretic Study. *Biochem. Biophys. Res. Commun.* **1976**, *73* (3), 577–583. https://doi.org/10.1016/0006-291x(76)90849-4.

(81) Fiermonte, G.; Dolce, V.; Palmieri, F. Expression in Escherichia Coli, Functional Characterization, and Tissue Distribution of Isoforms A and B of the Phosphate Carrier from Bovine Mitochondria. *J. Biol. Chem.* **1998**, *273* (35), 22782–22787. https://doi.org/10.1074/jbc.273.35.22782.

(82) Krämer, R. Structural and Functional Aspects of the Phosphate Carrier from Mitochondria. *Kidney Int.* **1996**, *49* (4), 947–952. https://doi.org/10.1038/ki.1996.133.

(83) Kadenbach, B.; Mende, P.; Kolbe, H. V.; Stipani, I.; Palmieri, F. The Mitochondrial Phosphate Carrier Has an Essential Requirement for Cardiolipin. *FEBS Lett.* **1982**, *139* (1), 109–112. https://doi.org/10.1016/0014-5793(82)80498-5.

(84) Boulet, A.; Vest, K. E.; Maynard, M. K.; Gammon, M. G.; Russell, A. C.; Mathews, A. T.; Cole, S. E.; Zhu, X.; Phillips, C. B.; Kwong, J. Q.; Dodani, S. C.; Leary, S. C.; Cobine, P. A. The Mammalian Phosphate Carrier SLC25A3 Is a Mitochondrial

Copper Transporter Required for Cytochrome c Oxidase Biogenesis. *J. Biol. Chem.* **2018**, *293* (6), 1887–1896. https://doi.org/10.1074/jbc.RA117.000265.

(85) Lunetti, P.; Damiano, F.; De Benedetto, G.; Siculella, L.; Pennetta, A.; Muto, L.; Paradies, E.; Marobbio, C. M. T.; Dolce, V.; Capobianco, L. Characterization of Human and Yeast Mitochondrial Glycine Carriers with Implications for Heme Biosynthesis and Anemia. *J. Biol. Chem.* **2016**, *291* (38), 19746–19759. https://doi.org/10.1074/jbc.M116.736876.

(86) Gibson, K. D.; Laver, W. G.; Neuberger, A. Initial Stages in the Biosynthesis of Porphyrins. 2. The Formation of δ-Aminolaevulic Acid from Glycine and Succinyl-Coenzyme A by Particles from Chicken Erythrocytes. *Biochem. J.* **1958**, *70* (1), 71–81.

(87) Munakata, H.; Sun, J.-Y.; Yoshida, K.; Nakatani, T.; Honda, E.; Hayakawa, S.; Furuyama, K.; Hayashi, N. Role of the Heme Regulatory Motif in the Heme-Mediated Inhibition of Mitochondrial Import of 5-Aminolevulinate Synthase. *J. Biochem. (Tokyo)* **2004**, *136* (2), 233–238. https://doi.org/10.1093/jb/mvh112.

(88) Kikuchi, G.; Motokawa, Y.; Yoshida, T.; Hiraga, K. Glycine Cleavage System: Reaction Mechanism, Physiological Significance, and Hyperglycinemia. *Proc. Jpn. Acad. Ser. B Phys. Biol. Sci.* **2008**, *84* (7), 246–263. https://doi.org/10.2183/pjab.84.246.

(89) Mukha, D.; Fokra, M.; Feldman, A.; Sarvin, B.; Sarvin, N.; Nevo-Dinur, K.; Besser, E.; Hallo, E.; Aizenshtein, E.; Schug, Z. T.; Shlomi, T. Glycine Decarboxylase Maintains Mitochondrial Protein Lipoylation to Support Tumor Growth. *Cell Metab.* **2022**, *34* (5), 775-782.e9. https://doi.org/10.1016/j.cmet.2022.04.006.

(90) Guna, A.; Stevens, T. A.; Inglis, A. J.; Replogle, J. M.; Esantsi, T. K.; Muthukumar, G.; Shaffer, K. C. L.; Wang, M. L.; Pogson, A. N.; Jones, J. J.; Lomenick, B.; Chou, T.-F.; Weissman, J. S.; Voorhees, R. M. MTCH2 Is a Mitochondrial Outer Membrane Protein Insertase. *Science* **2022**, *378* (6617), 317–322. https://doi.org/10.1126/science.add1856.

(91) Cheng, L.; Deepak, R. N. V. K.; Wang, G.; Meng, Z.; Tao, L.; Xie, M.; Chi, W.; Zhang, Y.; Yang, M.; Liao, Y.; Chen, R.; Liang, Y.; Zhang, J.; Huang, Y.; Wang, W.; Guo, Z.; Wang, Y.; Lin, J. D.; Fan, H.; Chen, L. Hepatic Mitochondrial NAD+ Transporter SLC25A47 Activates AMPKα Mediating Lipid Metabolism and Tumorigenesis. *Hepatol. Baltim. Md* **2023**, *78* (6), 1828–1842. https://doi.org/10.1097/HEP.0000000000000314.

(92) Nagampalli, R. S. K.; Quesñay, J. E. N.; Adamoski, D.; Islam, Z.; Birch, J.; Sebinelli, H. G.; Girard, R. M. B. M.; Ascenção, C. F. R.; Fala, A. M.; Pauletti, B. A.; Consonni, S. R.; de Oliveira, J. F.; Silva, A. C. T.; Franchini, K. G.; Leme, A. F. P.; Silber, A. M.; Ciancaglini, P.; Moraes, I.; Dias, S. M. G.; Ambrosio, A. L. B. Human Mitochondrial Pyruvate Carrier 2 as an Autonomous Membrane Transporter. *Sci. Rep.* **2018**, *8* (1), 3510. https://doi.org/10.1038/s41598-018-21740-z.

(93) Ruiz-Iglesias, A.; Mañes, S. The Importance of Mitochondrial Pyruvate Carrier in Cancer Cell Metabolism and Tumorigenesis. *Cancers* **2021**, *13* (7), 1488. https://doi.org/10.3390/cancers13071488.

(94) Vander Heiden, M. G.; Cantley, L. C.; Thompson, C. B. Understanding the Warburg Effect: The Metabolic Requirements of Cell Proliferation. *Science* **2009**, *324* (5930), 1029–1033. https://doi.org/10.1126/science.1160809.

(95) D'Angelo, D.; Vecellio Reane, D.; Raffaello, A. Neither Too Much nor Too Little: Mitochondrial Calcium Concentration as a Balance between Physiological and Pathological Conditions. *Front. Mol. Biosci.* **2023**, *10*. https://doi.org/10.3389/fmolb.2023.1336416.

(96) Van Keuren, A. M.; Tsai, C.-W.; Balderas, E.; Rodriguez, M. X.; Chaudhuri, D.; Tsai, M.-F. Mechanisms of EMRE-Dependent MCU Opening in the Mitochondrial Calcium Uniporter Complex. *Cell Rep.* **2020**, *33* (10), 108486. https://doi.org/10.1016/j.celrep.2020.108486.

(97) Raffaello, A.; De Stefani, D.; Sabbadin, D.; Teardo, E.; Merli, G.; Picard, A.; Checchetto, V.; Moro, S.; Szabò, I.; Rizzuto, R. The Mitochondrial Calcium Uniporter Is a Multimer That Can Include a Dominant-Negative Pore-Forming Subunit. *EMBO J.* **2013**, *32* (17), 2362–2376. https://doi.org/10.1038/emboj.2013.157.

(98) Paupe, V.; Prudent, J.; Dassa, E. P.; Rendon, O. Z.; Shoubridge, E. A. CCDC90A (MCUR1) Is a Cytochrome c Oxidase Assembly Factor and Not a Regulator of the Mitochondrial Calcium Uniporter. *Cell Metab.* **2015**, *21* (1), 109–116. https://doi.org/10.1016/j.cmet.2014.12.004.

(99) Groten, C. J.; MacVicar, B. A. Mitochondrial Ca2+ Uptake by the MCU Facilitates Pyramidal Neuron Excitability and Metabolism during Action Potential Firing. *Commun. Biol.* **2022**, *5* (1), 900. https://doi.org/10.1038/s42003-022-03848-1.

(100) Denton, R. M. Regulation of Mitochondrial Dehydrogenases by Calcium Ions. *Biochim. Biophys. Acta* **2009**, *1787* (11), 1309–1316. https://doi.org/10.1016/j.bbabio.2009.01.005.

(101) Bauer, T. M.; Murphy, E. Role of Mitochondrial Calcium and the Permeability Transition Pore in Regulating Cell Death. *Circ. Res.* **2020**, *126* (2), 280–293. https://doi.org/10.1161/CIRCRESAHA.119.316306.

(102) Morgenstern, M.; Peikert, C. D.; Lübbert, P.; Suppanz, I.; Klemm, C.; Alka, O.; Steiert, C.; Naumenko, N.; Schendzielorz, A.; Melchionda, L.; Mühlhäuser, W. W. D.; Knapp, B.; Busch, J. D.; Stiller, S. B.; Dannenmaier, S.; Lindau, C.; Licheva, M.; Eickhorst, C.; Galbusera, R.; Zerbes, R. M.; Ryan, M. T.; Kraft, C.; Kozjak-Pavlovic, V.; Drepper, F.; Dennerlein, S.; Oeljeklaus, S.; Pfanner, N.; Wiedemann, N.; Warscheid, B. Quantitative High-Confidence Human Mitochondrial Proteome and Its Dynamics in Cellular Context. *Cell Metab.* **2021**, *33* (12), 2464-2483.e18. https://doi.org/10.1016/j.cmet.2021.11.001.

(103) Moore, J. M.; Bell, E. L.; Hughes, R. O.; Garfield, A. S. ABC Transporters: Human Disease and Pharmacotherapeutic Potential. *Trends Mol. Med.* **2023**, *29* (2), 152–172. https://doi.org/10.1016/j.molmed.2022.11.001.

(104) Shum, M.; Shintre, C. A.; Althoff, T.; Gutierrez, V.; Segawa, M.; Saxberg, A. D.; Martinez, M.; Adamson, R.; Young, M. R.; Faust, B.; Gharakhanian, R.; Su, S.; Chella Krishnan, K.; Mahdaviani, K.; Veliova, M.; Wolf, D. M.; Ngo, J.; Nocito, L.; Stiles, L.; Abramson, J.; Lusis, A. J.; Hevener, A. L.; Zoghbi, M. E.; Carpenter, E. P.; Liesa, M. ABCB10 Exports Mitochondrial Biliverdin, Driving Metabolic Maladaptation in Obesity. *Sci. Transl. Med.* **2021**, *13* (594), eabd1869. https://doi.org/10.1126/scitranslmed.abd1869.

(105) Schaedler, T. A.; Thornton, J. D.; Kruse, I.; Schwarzländer, M.; Meyer, A. J.; van Veen, H. W.; Balk, J. A Conserved Mitochondrial ATP-Binding Cassette Transporter Exports Glutathione Polysulfide for Cytosolic Metal Cofactor

Assembly. *J. Biol. Chem.* **2014**, *289* (34), 23264–23274. https://doi.org/10.1074/jbc.M114.553438.

(106) Pearson, S. A.; Cowan, J. A. Evolution of the Human Mitochondrial ABCB7 [2Fe–2S](GS)4 Cluster Exporter and the Molecular Mechanism of an E433K Disease-Causing Mutation. *Arch. Biochem. Biophys.* **2021**, *697*, 108661. https://doi.org/10.1016/j.abb.2020.108661.

(107) Pondarré, C.; Antiochos, B. B.; Campagna, D. R.; Clarke, S. L.; Greer, E. L.; Deck, K. M.; McDonald, A.; Han, A.-P.; Medlock, A.; Kutok, J. L.; Anderson, S. A.; Eisenstein, R. S.; Fleming, M. D. The Mitochondrial ATP-Binding Cassette Transporter Abcb7 Is Essential in Mice and Participates in Cytosolic Iron-Sulfur Cluster Biogenesis. *Hum. Mol. Genet.* **2006**, *15* (6), 953–964. https://doi.org/10.1093/hmg/ddl012.

(108) Bekri, S.; Kispal, G.; Lange, H.; Fitzsimons, E.; Tolmie, J.; Lill, R.; Bishop, D. F. Human ABC7 Transporter: Gene Structure and Mutation Causing X-Linked Sideroblastic Anemia with Ataxia with Disruption of Cytosolic Iron-Sulfur Protein Maturation. *Blood* **2000**, *96* (9), 3256–3264.

(109) Krishnamurthy, P. C.; Du, G.; Fukuda, Y.; Sun, D.; Sampath, J.; Mercer, K. E.; Wang, J.; Sosa-Pineda, B.; Murti, K. G.; Schuetz, J. D. Identification of a Mammalian Mitochondrial Porphyrin Transporter. *Nature* **2006**, *443* (7111), 586–589. https://doi.org/10.1038/nature05125.

(110) Paggio, A.; Checchetto, V.; Campo, A.; Menabò, R.; Di Marco, G.; Di Lisa, F.; Szabo, I.; Rizzuto, R.; De Stefani, D. Identification of an ATP-Sensitive Potassium Channel in Mitochondria. *Nature* **2019**, *572* (7771), 609–613. https://doi.org/10.1038/s41586-019-1498-3.

(111) Tifoun, N.; De las Heras, J. M.; Guillaume, A.; Bouleau, S.; Mignotte, B.; Le Floch, N. Insights into the Roles of the Sideroflexins/SLC56 Family in Iron Homeostasis and Iron-Sulfur Biogenesis. *Biomedicines* **2021**, *9* (2), 103. https://doi.org/10.3390/biomedicines9020103.

(112) Fleming, M. D.; Campagna, D. R.; Haslett, J. N.; Trenor, C. C.; Andrews, N. C. A Mutation in a Mitochondrial Transmembrane Protein Is Responsible for the Pleiotropic Hematological and Skeletal Phenotype of Flexed-Tail (f/f) Mice. *Genes Dev*. **2001**, *15* (6), 652–657. https://doi.org/10.1101/gad.873001.

(113) Lenox, L. E.; Perry, J. M.; Paulson, R. F. BMP4 and Madh5 Regulate the Erythroid Response to Acute Anemia. *Blood* **2005**, *105* (7), 2741–2748. https://doi.org/10.1182/blood-2004-02-0703.

(114) Kory, N.; Wyant, G. A.; Prakash, G.; Uit de Bos, J.; Bottanelli, F.; Pacold, M. E.; Chan, S. H.; Lewis, C. A.; Wang, T.; Keys, H. R.; Guo, Y. E.; Sabatini, D. M. SFXN1 Is a Mitochondrial Serine Transporter Required for One-Carbon Metabolism. *Science* **2018**, *362* (6416), eaat9528. https://doi.org/10.1126/science.aat9528.

(115) Lewis, C. A.; Parker, S. J.; Fiske, B. P.; McCloskey, D.; Gui, D. Y.; Green, C. R.; Vokes, N. I.; Feist, A. M.; Vander Heiden, M. G.; Metallo, C. M. Tracing Compartmentalized NADPH Metabolism in the Cytosol and Mitochondria of Mammalian Cells. *Mol. Cell* **2014**, *55* (2), 253–263. https://doi.org/10.1016/j.molcel.2014.05.008.

(116) García-Cañaveras, J. C.; Lancho, O.; Ducker, G. S.; Ghergurovich, J. M.; Xu, X.; da Silva-Diz, V.; Minuzzo, S.; Indraccolo, S.; Kim, H.; Herranz, D.; Rabinowitz, J. D. SHMT Inhibition Is Effective and Synergizes with Methotrexate in T-Cell Acute

Lymphoblastic Leukemia. *Leukemia* **2021**, *35* (2), 377–388. https://doi.org/10.1038/s41375-020-0845-6.

(117) Jackson, T. D.; Crameri, J. J.; Muellner-Wong, L.; Frazier, A. E.; Palmer, C. S.; Formosa, L. E.; Hock, D. H.; Fujihara, K. M.; Stait, T.; Sharpe, A. J.; Thorburn, D. R.; Ryan, M. T.; Stroud, D. A.; Stojanovski, D. Sideroflexin 4 Is a Complex I Assembly Factor That Interacts with the MCIA Complex and Is Required for the Assembly of the ND2 Module. *Proc. Natl. Acad. Sci. U. S. A.* **2022**, *119* (13), e2115566119. https://doi.org/10.1073/pnas.2115566119.

(118) Paul, B. T.; Tesfay, L.; Winkler, C. R.; Torti, F. M.; Torti, S. V. Sideroflexin 4 Affects Fe-S Cluster Biogenesis, Iron Metabolism, Mitochondrial Respiration and Heme Biosynthetic Enzymes. *Sci. Rep.* **2019**, *9* (1), 19634. https://doi.org/10.1038/s41598-019-55907-z.

(119) Acoba, M. G.; Alpergin, E. S. S.; Renuse, S.; Fernández-del-Río, L.; Lu, Y.-W.; Khalimonchuk, O.; Clarke, C. F.; Pandey, A.; Wolfgang, M. J.; Claypool, S. M. The Mitochondrial Carrier SFXN1 Is Critical for Complex III Integrity and Cellular Metabolism. *Cell Rep.* **2021**, *34* (11), 108869. https://doi.org/10.1016/j.celrep.2021.108869.

(120) Soula, M.; Weber, R. A.; Zilka, O.; Alwaseem, H.; La, K.; Yen, F.; Molina, H.; Garcia-Bermudez, J.; Pratt, D. A.; Birsoy, K. Metabolic Determinants of Cancer Cell Sensitivity to Canonical Ferroptosis Inducers. *Nat. Chem. Biol.* **2020**, *16* (12), 1351–1360. https://doi.org/10.1038/s41589-020-0613-y.

(121) Fang, H.; Xie, A.; Du, M.; Li, X.; Yang, K.; Fu, Y.; Yuan, X.; Fan, R.; Yu, W.; Zhou, Z.; Sang, T.; Nie, K.; Li, J.; Zhao, Q.; Chen, Z.; Yang, Y.; Hong, C.; Lyu, J. SERAC1 Is a Component of the Mitochondrial Serine Transporter Complex Required for

the Maintenance of Mitochondrial DNA. *Sci. Transl. Med.* **2022**, *14* (634), eabl6992. https://doi.org/10.1126/scitranslmed.abl6992.

(122) Tabuchi, M.; Tanaka, N.; Nishida-Kitayama, J.; Ohno, H.; Kishi, F. Alternative Splicing Regulates the Subcellular Localization of Divalent Metal Transporter 1 Isoforms. *Mol. Biol. Cell* **2002**, *13* (12), 4371–4387. https://doi.org/10.1091/mbc.e02-03-0165.

(123) Wolff, N. A.; Ghio, A. J.; Garrick, L. M.; Garrick, M. D.; Zhao, L.; Fenton, R. A.; Thévenod, F. Evidence for Mitochondrial Localization of Divalent Metal Transporter 1 (DMT1). *FASEB J. Off. Publ. Fed. Am. Soc. Exp. Biol.* **2014**, *28* (5), 2134–2145. https://doi.org/10.1096/fj.13-240564.

(124) Illing, A. C.; Shawki, A.; Cunningham, C. L.; Mackenzie, B. Substrate Profile and Metal-Ion Selectivity of Human Divalent Metal-Ion Transporter-1. *J. Biol. Chem.* **2012**, *287* (36), 30485–30496. https://doi.org/10.1074/jbc.M112.364208.

(125) Wolff, N. A.; Garrick, M. D.; Zhao, L.; Garrick, L. M.; Ghio, A. J.; Thévenod, F. A Role for Divalent Metal Transporter (DMT1) in Mitochondrial Uptake of Iron and Manganese. *Sci. Rep.* **2018**, *8*, 211. https://doi.org/10.1038/s41598-017-18584-4.

(126) Barra, J.; Crosbourne, I.; Roberge, C. L.; Bossardi-Ramos, R.; Warren, J. S. A.; Matteson, K.; Wang, L.; Jourd'heuil, F.; Borisov, S. M.; Bresnahan, E.; Bravo-Cordero, J. J.; Dmitriev, R. I.; Jourd'heuil, D.; Adam, A. P.; Lamar, J. M.; Corr, D. T.; Barroso, M. M. DMT1-Dependent Endosome-Mitochondria Interactions Regulate Mitochondrial Iron Translocation and Metastatic Outgrowth. *Oncogene* **2024**, *43* (9), 650–667. https://doi.org/10.1038/s41388-023-02933-x.

(127) Lamhonwah, A.-M.; Tein, I. Novel Localization of OCTN1, an Organic Cation/Carnitine Transporter, to Mammalian Mitochondria. *Biochem. Biophys.*

Res. Commun. **2006**, *345* (4), 1315–1325. https://doi.org/10.1016/j.bbrc.2006.05.026.

(128) Gründemann, D.; Harlfinger, S.; Golz, S.; Geerts, A.; Lazar, A.; Berkels, R.; Jung, N.; Rubbert, A.; Schömig, E. Discovery of the Ergothioneine Transporter. *Proc. Natl. Acad. Sci. U. S. A.* **2005**, *102* (14), 5256–5261. https://doi.org/10.1073/pnas.0408624102.

(129) Fong, Z. W.; Tang, R. M. Y.; Cheah, I. K.-M.; Leow, D. M. K.; Chen, L.; Halliwell, B. Ergothioneine and Mitochondria: An Important Protective Mechanism? *Biochem. Biophys. Res. Commun.* **2024**, *726*, 150269. https://doi.org/10.1016/j.bbrc.2024.150269.

(130) Perez, Y.; Shorer, Z.; Liani-Leibson, K.; Chabosseau, P.; Kadir, R.; Volodarsky, M.; Halperin, D.; Barber-Zucker, S.; Shalev, H.; Schreiber, R.; Gradstein, L.; Gurevich, E.; Zarivach, R.; Rutter, G. A.; Landau, D.; Birk, O. S. SLC30A9 Mutation Affecting Intracellular Zinc Homeostasis Causes a Novel Cerebro-Renal Syndrome. *Brain J. Neurol.* **2017**, *140* (4), 928–939. https://doi.org/10.1093/brain/awx013.

(131) Kowalczyk, A.; Gbadamosi, O.; Kolor, K.; Sosa, J.; Andrzejczuk, L.; Gibson, G.; St Croix, C.; Chikina, M.; Aizenman, E.; Clark, N.; Kiselyov, K. Evolutionary Rate Covariation Identifies SLC30A9 (ZnT9) as a Mitochondrial Zinc Transporter. *Biochem. J.* **2021**, *478* (17), 3205–3220. https://doi.org/10.1042/BCJ20210342.

(132) Rensvold, J. W.; Shishkova, E.; Sverchkov, Y.; Miller, I. J.; Cetinkaya, A.; Pyle, A.; Manicki, M.; Brademan, D. R.; Alanay, Y.; Raiman, J.; Jochem, A.; Hutchins, P. D.; Peters, S. R.; Linke, V.; Overmyer, K. A.; Salome, A. Z.; Hebert, A. S.; Vincent, C. E.; Kwiecien, N. W.; Rush, M. J. P.; Westphall, M. S.; Craven, M.; Akarsu, N. A.;

Taylor, R. W.; Coon, J. J.; Pagliarini, D. J. Defining Mitochondrial Protein Functions through Deep Multiomic Profiling. *Nature* **2022**, *606* (7913), 382–388. https://doi.org/10.1038/s41586-022-04765-3.

(133) Yoo, H. C.; Park, S. J.; Nam, M.; Kang, J.; Kim, K.; Yeo, J. H.; Kim, J.-K.; Heo, Y.; Lee, H. S.; Lee, M. Y.; Lee, C. W.; Kang, J. S.; Kim, Y.-H.; Lee, J.; Choi, J.; Hwang, G.-S.; Bang, S.; Han, J. M. A Variant of SLC1A5 Is a Mitochondrial Glutamine Transporter for Metabolic Reprogramming in Cancer Cells. *Cell Metab.* **2020**, *31* (2), 267-283.e12. https://doi.org/10.1016/j.cmet.2019.11.020.

(134) Rone, M. B.; Midzak, A. S.; Issop, L.; Rammouz, G.; Jagannathan, S.; Fan, J.; Ye, X.; Blonder, J.; Veenstra, T.; Papadopoulos, V. Identification of a Dynamic Mitochondrial Protein Complex Driving Cholesterol Import, Trafficking, and Metabolism to Steroid Hormones. *Mol. Endocrinol.* **2012**, *26* (11), 1868–1882. https://doi.org/10.1210/me.2012-1159.

(135) Miliara, X.; Garnett, J. A.; Tatsuta, T.; Abid Ali, F.; Baldie, H.; Pérez-Dorado, I.; Simpson, P.; Yague, E.; Langer, T.; Matthews, S. Structural Insight into the TRIAP1/PRELI-like Domain Family of Mitochondrial Phospholipid Transfer Complexes. *EMBO Rep.* **2015**, *16* (7), 824–835. https://doi.org/10.15252/embr.201540229.

(136) Huster, D.; Kühne, A.; Bhattacharjee, A.; Raines, L.; Jantsch, V.; Noe, J.; Schirrmeister, W.; Sommerer, I.; Sabri, O.; Berr, F.; Mössner, J.; Stieger, B.; Caca, K.; Lutsenko, S. Diverse Functional Properties of Wilson Disease ATP7B Variants. *Gastroenterology* **2012**, *142* (4), 947-956.e5. https://doi.org/10.1053/j.gastro.2011.12.048.

(137) Yang, X. L.; Miura, N.; Kawarada, Y.; Terada, K.; Petrukhin, K.; Gilliam, T.; Sugiyama, T. Two Forms of Wilson Disease Protein Produced by Alternative Splicing Are Localized in Distinct Cellular Compartments. *Biochem. J.* **1997**, *326 (Pt 3)* (Pt 3), 897–902. https://doi.org/10.1042/bj3260897.

(138) Lutsenko, S.; Cooper, M. J. Localization of the Wilson's Disease Protein Product to Mitochondria. *Proc. Natl. Acad. Sci. U. S. A.* **1998**, *95* (11), 6004–6009. https://doi.org/10.1073/pnas.95.11.6004.

(139) Yurkova, I. L.; Arnhold, J.; Fitzl, G.; Huster, D. Fragmentation of Mitochondrial Cardiolipin by Copper Ions in the Atp7b-/- Mouse Model of Wilson's Disease. *Chem. Phys. Lipids* **2011**, *164* (5), 393–400. https://doi.org/10.1016/j.chemphyslip.2011.05.006.

(140) Austin, S.; Mekis, R.; Mohammed, S. E. M.; Scalise, M.; Wang, W.-A.; Galluccio, M.; Pfeiffer, C.; Borovec, T.; Parapatics, K.; Vitko, D.; Dinhopl, N.; Demaurex, N.; Bennett, K. L.; Indiveri, C.; Nowikovsky, K. TMBIM5 Is the Ca2+ /H+ Antiporter of Mammalian Mitochondria. *EMBO Rep.* **2022**, *23* (12), e54978. https://doi.org/10.15252/embr.202254978.

(141) De Marchi, U.; Santo-Domingo, J.; Castelbou, C.; Sekler, I.; Wiederkehr, A.; Demaurex, N. NCLX Protein, but Not LETM1, Mediates Mitochondrial Ca2+ Extrusion, Thereby Limiting Ca2+-Induced NAD(P)H Production and Modulating Matrix Redox State. *J. Biol. Chem.* **2014**, *289* (29), 20377–20385. https://doi.org/10.1074/jbc.M113.540898.

(142) Palmieri, F.; Scarcia, P.; Monné, M. Diseases Caused by Mutations in Mitochondrial Carrier Genes SLC25: A Review. *Biomolecules* **2020**, *10* (4), 655. https://doi.org/10.3390/biom10040655.

(143) Saheki, T.; Kobayashi, K. Mitochondrial Aspartate Glutamate Carrier (Citrin) Deficiency as the Cause of Adult-Onset Type II Citrullinemia (CTLN2) and Idiopathic Neonatal Hepatitis (NICCD). *J. Hum. Genet.* **2002**, *47* (7), 333–341. https://doi.org/10.1007/s100380200046.

(144) Camacho, J. A.; Obie, C.; Biery, B.; Goodman, B. K.; Hu, C. A.; Almashanu, S.; Steel, G.; Casey, R.; Lambert, M.; Mitchell, G. A.; Valle, D. Hyperornithinaemia-Hyperammonaemia-Homocitrullinuria Syndrome Is Caused by Mutations in a Gene Encoding a Mitochondrial Ornithine Transporter. *Nat. Genet.* **1999**, *22* (2), 151–158. https://doi.org/10.1038/9658.

(145) Pondarre, C.; Campagna, D. R.; Antiochos, B.; Sikorski, L.; Mulhern, H.; Fleming, M. D. Abcb7, the Gene Responsible for X-Linked Sideroblastic Anemia with Ataxia, Is Essential for Hematopoiesis. *Blood* **2007**, *109* (8), 3567–3569. https://doi.org/10.1182/blood-2006-04-015768.

(146) Hildick-Smith, G. J.; Cooney, J. D.; Garone, C.; Kremer, L. S.; Haack, T. B.; Thon, J. N.; Miyata, N.; Lieber, D. S.; Calvo, S. E.; Akman, H. O.; Yien, Y. Y.; Huston, N. C.; Branco, D. S.; Shah, D. I.; Freedman, M. L.; Koehler, C. M.; Italiano, J. E.; Merkenschlager, A.; Beblo, S.; Strom, T. M.; Meitinger, T.; Freisinger, P.; Donati, M. A.; Prokisch, H.; Mootha, V. K.; DiMauro, S.; Paw, B. H. Macrocytic Anemia and Mitochondriopathy Resulting from a Defect in Sideroflexin 4. *Am. J. Hum. Genet.* **2013**, *93* (5), 906–914. https://doi.org/10.1016/j.ajhg.2013.09.011.

(147) Członkowska, A.; Litwin, T.; Dusek, P.; Ferenci, P.; Lutsenko, S.; Medici, V.; Rybakowski, J. K.; Weiss, K. H.; Schilsky, M. L. Wilson Disease. *Nat. Rev. Dis. Primer* **2018**, *4* (1), 21. https://doi.org/10.1038/s41572-018-0018-3.

(148) Rochette, L.; Meloux, A.; Zeller, M.; Malka, G.; Cottin, Y.; Vergely, C. Mitochondrial SLC25 Carriers: Novel Targets for Cancer Therapy. *Mol. Basel Switz.* **2020**, *25* (10), 2417. https://doi.org/10.3390/molecules25102417.

(149) Fernandez, H. R.; Gadre, S. M.; Tan, M.; Graham, G. T.; Mosaoa, R.; Ongkeko, M. S.; Kim, K. A.; Riggins, R. B.; Parasido, E.; Petrini, I.; Pacini, S.; Cheema, A.; Varghese, R.; Ressom, H. W.; Zhang, Y.; Albanese, C.; Üren, A.; Paige, M.; Giaccone, G.; Avantaggiati, M. L. The Mitochondrial Citrate Carrier, SLC25A1, Drives Stemness and Therapy Resistance in Non-Small Cell Lung Cancer. *Cell Death Differ.* **2018**, *25* (7), 1239–1258. https://doi.org/10.1038/s41418-018-0101-z.

(150) Zhou, X.; Paredes, J. A.; Krishnan, S.; Curbo, S.; Karlsson, A. The Mitochondrial Carrier SLC25A10 Regulates Cancer Cell Growth. *Oncotarget* **2015**, *6* (11), 9271–9283.

(151) Alkan, H. F.; Walter, K. E.; Luengo, A.; Madreiter-Sokolowski, C. T.; Stryeck, S.; Lau, A. N.; Al-Zoughbi, W.; Lewis, C. A.; Thomas, C. J.; Hoefler, G.; Graier, W. F.; Madl, T.; Vander Heiden, M. G.; Bogner-Strauss, J. G. Cytosolic Aspartate Availability Determines Cell Survival When Glutamine Is Limiting. *Cell Metab.* **2018**, *28* (5), 706-720.e6. https://doi.org/10.1016/j.cmet.2018.07.021.

(152) Infantino, V.; Dituri, F.; Convertini, P.; Santarsiero, A.; Palmieri, F.; Todisco, S.; Mancarella, S.; Giannelli, G.; Iacobazzi, V. Epigenetic Upregulation and Functional Role of the Mitochondrial Aspartate/Glutamate Carrier Isoform 1 in Hepatocellular Carcinoma. *Biochim. Biophys. Acta Mol. Basis Dis.* **2019**, *1865* (1), 38–47. https://doi.org/10.1016/j.bbadis.2018.10.018.

(153) Yagi, K.; Shimada, S.; Akiyama, Y.; Hatano, M.; Asano, D.; Ishikawa, Y.; Ueda, H.; Watanabe, S.; Akahoshi, K.; Ono, H.; Tanabe, M.; Tanaka, S. Loss of SFXN1 Mitigates Lipotoxicity and Predicts Poor Outcome in Non-Viral Hepatocellular Carcinoma. *Sci. Rep.* **2023**, *13* (1), 9449. https://doi.org/10.1038/s41598-023-36660-w.

(154) Tina, E.; Lindqvist, B. M.; Gabrielson, M.; Lubovac, Z.; Wegman, P.; Wingren, S. The Mitochondrial Transporter SLC25A43 Is Frequently Deleted and May Influence Cell Proliferation in HER2-Positive Breast Tumors. *BMC Cancer* **2012**, *12*, 350. https://doi.org/10.1186/1471-2407-12-350.

(155) Wang, Y.; Yen, F. S.; Zhu, X. G.; Timson, R. C.; Weber, R.; Xing, C.; Liu, Y.; Allwein, B.; Luo, H.; Yeh, H.-W.; Heissel, S.; Unlu, G.; Gamazon, E. R.; Kharas, M. G.; Hite, R.; Birsoy, K. SLC25A39 Is Necessary for Mitochondrial Glutathione Import in Mammalian Cells. *Nature* **2021**, *599* (7883), 136–140. https://doi.org/10.1038/s41586-021-04025-w.

(156) Shi, X.; Reinstadler, B.; Shah, H.; To, T.-L.; Byrne, K.; Summer, L.; Calvo, S. E.; Goldberger, O.; Doench, J. G.; Mootha, V. K.; Shen, H. Combinatorial GxGxE CRISPR Screen Identifies SLC25A39 in Mitochondrial Glutathione Transport Linking Iron Homeostasis to OXPHOS. *Nat. Commun.* **2022**, *13* (1), 2483. https://doi.org/10.1038/s41467-022-30126-9.

(157) Liu, Y.; Liu, S.; Tomar, A.; Yen, F. S.; Unlu, G.; Ropek, N.; Weber, R. A.; Wang, Y.; Khan, A.; Gad, M.; Peng, J.; Terzi, E.; Alwaseem, H.; Pagano, A. E.; Heissel, S.; Molina, H.; Allwein, B.; Kenny, T. C.; Possemato, R. L.; Zhao, L.; Hite, R. K.; Vinogradova, E. V.; Mansy, S. S.; Birsoy, K. Autoregulatory Control of

Mitochondrial Glutathione Homeostasis. *Science* **2023**, *382* (6672), 820–828. https://doi.org/10.1126/science.adf4154.

(158) Kory, N.; Uit de Bos, J.; van der Rijt, S.; Jankovic, N.; Güra, M.; Arp, N.; Pena, I. A.; Prakash, G.; Chan, S. H.; Kunchok, T.; Lewis, C. A.; Sabatini, D. M. MCART1/SLC25A51 Is Required for Mitochondrial NAD Transport. *Sci. Adv.* **2020**, *6* (43), eabe5310. https://doi.org/10.1126/sciadv.abe5310.

(159) Girardi, E.; Agrimi, G.; Goldmann, U.; Fiume, G.; Lindinger, S.; Sedlyarov, V.; Srndic, I.; Gürtl, B.; Agerer, B.; Kartnig, F.; Scarcia, P.; Di Noia, M. A.; Liñeiro, E.; Rebsamen, M.; Wiedmer, T.; Bergthaler, A.; Palmieri, L.; Superti-Furga, G. Epistasis-Driven Identification of SLC25A51 as a Regulator of Human Mitochondrial NAD Import. *Nat. Commun.* **2020**, *11* (1), 6145. https://doi.org/10.1038/s41467-020-19871-x.

(160) Luongo, T. S.; Eller, J. M.; Lu, M.-J.; Niere, M.; Raith, F.; Perry, C.; Bornstein, M. R.; Oliphint, P.; Wang, L.; McReynolds, M. R.; Migaud, M. E.; Rabinowitz, J. D.; Johnson, F. B.; Johnsson, K.; Ziegler, M.; Cambronne, X. A.; Baur, J. A. SLC25A51 Is a Mammalian Mitochondrial NAD+ Transporter. *Nature* **2020**, *588* (7836), 174–179. https://doi.org/10.1038/s41586-020-2741-7.

(161) Lu, M.-J.; Busquets, J.; Impedovo, V.; Wilson, C. N.; Chan, H.-R.; Chang, Y.-T.; Matsui, W.; Tiziani, S.; Cambronne, X. A. SLC25A51 Decouples the Mitochondrial NAD+/NADH Ratio to Control Proliferation of AML Cells. *Cell Metab.* **2024**, *36* (4), 808-821.e6. https://doi.org/10.1016/j.cmet.2024.01.013.

(162) Yoneshiro, T.; Wang, Q.; Tajima, K.; Matsushita, M.; Maki, H.; Igarashi, K.; Dai, Z.; White, P. J.; McGarrah, R. W.; Ilkayeva, O. R.; Deleye, Y.; Oguri, Y.; Kuroda, M.; Ikeda, K.; Li, H.; Ueno, A.; Ohishi, M.; Ishikawa, T.; Kim, K.; Chen, Y.;

Sponton, C. H.; Pradhan, R. N.; Majd, H.; Greiner, V. J.; Yoneshiro, M.; Brown, Z.; Chondronikola, M.; Takahashi, H.; Goto, T.; Kawada, T.; Sidossis, L.; Szoka, F. C.; McManus, M. T.; Saito, M.; Soga, T.; Kajimura, S. BCAA Catabolism in Brown Fat Controls Energy Homeostasis through SLC25A44. *Nature* **2019**, *572* (7771), 614–619. https://doi.org/10.1038/s41586-019-1503-x.

(163) Yoneshiro, T.; Kataoka, N.; Walejko, J. M.; Ikeda, K.; Brown, Z.; Yoneshiro, M.; Crown, S. B.; Osawa, T.; Sakai, J.; McGarrah, R. W.; White, P. J.; Nakamura, K.; Kajimura, S. Metabolic Flexibility via Mitochondrial BCAA Carrier SLC25A44 Is Required for Optimal Fever. *eLife* **2021**, *10*, e66865. https://doi.org/10.7554/eLife.66865.

(164) Khan, A.; Unlu, G.; Lin, P.; Liu, Y.; Kilic, E.; Kenny, T. C.; Birsoy, K.; Gamazon, E. R. Metabolic Gene Function Discovery Platform GeneMAP Identifies SLC25A48 as Necessary for Mitochondrial Choline Import. *Nat. Genet.* **2024**, *56* (8), 1614–1623. https://doi.org/10.1038/s41588-024-01827-2.

(165) Verkerke, A. R. P.; Shi, X.; Li, M.; Higuchi, Y.; Yamamuro, T.; Katoh, D.; Nishida, H.; Auger, C.; Abe, I.; Gerszten, R. E.; Kajimura, S. SLC25A48 Controls Mitochondrial Choline Import and Metabolism. *Cell Metab.* **2024**, S1550-4131(24)00281-X. https://doi.org/10.1016/j.cmet.2024.07.010.

(166) Shi, R.; Hou, W.; Wang, Z.-Q.; Xu, X. Biogenesis of Iron-Sulfur Clusters and Their Role in DNA Metabolism. *Front. Cell Dev. Biol.* **2021**, *9*, 735678. https://doi.org/10.3389/fcell.2021.735678.

(167) Ward, N. P.; Yoon, S. J.; Flynn, T.; Sherwood, A. M.; Olley, M. A.; Madej, J.; DeNicola, G. M. Mitochondrial Respiratory Function Is Preserved under Cysteine

Starvation via Glutathione Catabolism in NSCLC. *Nat. Commun.* **2024**, *15* (1), 4244. https://doi.org/10.1038/s41467-024-48695-2.

(168) Burke, L.; Guterman, I.; Palacios Gallego, R.; Britton, R. G.; Burschowsky, D.; Tufarelli, C.; Rufini, A. The Janus-like Role of Proline Metabolism in Cancer. *Cell Death Discov.* **2020**, *6* (1), 1–17. https://doi.org/10.1038/s41420-020-00341-8.

(169) Rath, S.; Sharma, R.; Gupta, R.; Ast, T.; Chan, C.; Durham, T. J.; Goodman, R. P.; Grabarek, Z.; Haas, M. E.; Hung, W. H. W.; Joshi, P. R.; Jourdain, A. A.; Kim, S. H.; Kotrys, A. V.; Lam, S. S.; McCoy, J. G.; Meisel, J. D.; Miranda, M.; Panda, A.; Patgiri, A.; Rogers, R.; Sadre, S.; Shah, H.; Skinner, O. S.; To, T.-L.; Walker, M. A.; Wang, H.; Ward, P. S.; Wengrod, J.; Yuan, C.-C.; Calvo, S. E.; Mootha, V. K. MitoCarta3.0: An Updated Mitochondrial Proteome Now with Sub-Organelle Localization and Pathway Annotations. *Nucleic Acids Res.* **2021**, *49* (D1), D1541–D1547. https://doi.org/10.1093/nar/gkaa1011.

(170) Elia, I.; Broekaert, D.; Christen, S.; Boon, R.; Radaelli, E.; Orth, M. F.; Verfaillie, C.; Grünewald, T. G. P.; Fendt, S.-M. Proline Metabolism Supports Metastasis Formation and Could Be Inhibited to Selectively Target Metastasizing Cancer Cells. *Nat. Commun.* **2017**, *8* (1), 15267. https://doi.org/10.1038/ncomms15267.

(171) Rhee, H.-W.; Zou, P.; Udeshi, N. D.; Martell, J. D.; Mootha, V. K.; Carr, S. A.; Ting, A. Y. Proteomic Mapping of Mitochondria in Living Cells via Spatially-Restricted Enzymatic Tagging. *Science* **2013**, *339* (6125), 1328–1331. https://doi.org/10.1126/science.1230593.

(172) Phang, J. M. Perspectives, Past, Present and Future: The Proline Cycle/Proline-Collagen Regulatory Axis. *Amino Acids* **2021**, *53* (12), 1967–1975. https://doi.org/10.1007/s00726-021-03103-7.

(173) Tran, D. H.; Kesavan, R.; Rion, H.; Soflaee, M. H.; Solmonson, A.; Bezwada, D.; Vu, H. S.; Cai, F.; Phillips, J. A.; DeBerardinis, R. J.; Hoxhaj, G. Mitochondrial NADP+ Is Essential for Proline Biosynthesis during Cell Growth. *Nat. Metab.* **2021**, *3* (4), 571–585. https://doi.org/10.1038/s42255-021-00374-y.

(174) Zhu, J.; Schwörer, S.; Berisa, M.; Kyung, Y. J.; Ryu, K. W.; Yi, J.; Jiang, X.; Cross, J. R.; Thompson, C. B. Mitochondrial NADP(H) Generation Is Essential for Proline Biosynthesis. *Science* **2021**, *372* (6545), 968–972. https://doi.org/10.1126/science.abd5491.

(175) Westbrook, R. L.; Bridges, E.; Roberts, J.; Escribano-Gonzalez, C.; Eales, K. L.; Vettore, L. A.; Walker, P. D.; Vera-Siguenza, E.; Rana, H.; Cuozzo, F.; Eskla, K.-L.; Vellama, H.; Shaaban, A.; Nixon, C.; Luuk, H.; Lavery, G. G.; Hodson, D. J.; Harris, A. L.; Tennant, D. A. Proline Synthesis through PYCR1 Is Required to Support Cancer Cell Proliferation and Survival in Oxygen-Limiting Conditions. *Cell Rep.* **2022**, *38* (5), 110320. https://doi.org/10.1016/j.celrep.2022.110320.

(176) Schwörer, S.; Berisa, M.; Violante, S.; Qin, W.; Zhu, J.; Hendrickson, R. C.; Cross, J. R.; Thompson, C. B. Proline Biosynthesis Is a Vent for TGFβ-Induced Mitochondrial Redox Stress. *EMBO J.* **2020**, *39* (8), e103334. https://doi.org/10.15252/embj.2019103334.

(177) Kay, E. J.; Paterson, K.; Riera-Domingo, C.; Sumpton, D.; Däbritz, J. H. M.; Tardito, S.; Boldrini, C.; Hernandez-Fernaud, J. R.; Athineos, D.; Dhayade, S.; Stepanova, E.; Gjerga, E.; Neilson, L. J.; Lilla, S.; Hedley, A.; Koulouras, G.; McGregor, G.; Jamieson, C.; Johnson, R. M.; Park, M.; Kirschner, K.; Miller, C.; Kamphorst, J. J.; Loayza-Puch, F.; Saez-Rodriguez, J.; Mazzone, M.; Blyth, K.; Zagnoni, M.; Zanivan, S. Cancer-Associated Fibroblasts Require Proline Synthesis

by PYCR1 for the Deposition of pro-Tumorigenic Extracellular Matrix. *Nat. Metab.* **2022**, *4* (6), 693–710. https://doi.org/10.1038/s42255-022-00582-0.

(178) Pious, D. A.; Hawley, P. Effect of Antibiotics on Respiration in Human Cells. *Pediatr. Res.* **1972**, *6* (8), 687–692. https://doi.org/10.1203/00006450-197208000-00007.

(179) Duszka, K. Versatile Triad Alliance: Bile Acid, Taurine and Microbiota. *Cells* **2022**, *11* (15), 2337. https://doi.org/10.3390/cells11152337.

(180) Singh, P.; Gollapalli, K.; Mangiola, S.; Schranner, D.; Yusuf, M. A.; Chamoli, M.; Shi, S. L.; Lopes Bastos, B.; Nair, T.; Riermeier, A.; Vayndorf, E. M.; Wu, J. Z.; Nilakhe, A.; Nguyen, C. Q.; Muir, M.; Kiflezghi, M. G.; Foulger, A.; Junker, A.; Devine, J.; Sharan, K.; Chinta, S. J.; Rajput, S.; Rane, A.; Baumert, P.; Schönfelder, M.; Iavarone, F.; di Lorenzo, G.; Kumari, S.; Gupta, A.; Sarkar, R.; Khyriem, C.; Chawla, A. S.; Sharma, A.; Sarper, N.; Chattopadhyay, N.; Biswal, B. K.; Settembre, C.; Nagarajan, P.; Targoff, K. L.; Picard, M.; Gupta, S.; Velagapudi, V.; Papenfuss, A. T.; Kaya, A.; Ferreira, M. G.; Kennedy, B. K.; Andersen, J. K.; Lithgow, G. J.; Ali, A. M.; Mukhopadhyay, A.; Palotie, A.; Kastenmüller, G.; Kaeberlein, M.; Wackerhage, H.; Pal, B.; Yadav, V. K. Taurine Deficiency as a Driver of Aging. *Science* **2023**, *380* (6649), eabn9257. https://doi.org/10.1126/science.abn9257.

(181) Jong, C. J.; Sandal, P.; Schaffer, S. W. The Role of Taurine in Mitochondria Health: More Than Just an Antioxidant. *Molecules* **2021**, *26* (16), 4913. https://doi.org/10.3390/molecules26164913.

(182) Suzuki, T.; Suzuki, T.; Wada, T.; Saigo, K.; Watanabe, K. Taurine as a Constituent of Mitochondrial tRNAs: New Insights into the Functions of Taurine and Human

Mitochondrial Diseases. *EMBO J.* **2002**, *21* (23), 6581–6589. https://doi.org/10.1093/emboj/cdf656.

(183) Asano, K.; Suzuki, T.; Saito, A.; Wei, F.-Y.; Ikeuchi, Y.; Numata, T.; Tanaka, R.; Yamane, Y.; Yamamoto, T.; Goto, T.; Kishita, Y.; Murayama, K.; Ohtake, A.; Okazaki, Y.; Tomizawa, K.; Sakaguchi, Y.; Suzuki, T. Metabolic and Chemical Regulation of tRNA Modification Associated with Taurine Deficiency and Human Disease. *Nucleic Acids Res.* **2018**, *46* (4), 1565–1583. https://doi.org/10.1093/nar/gky068.

(184) Fakruddin, M.; Wei, F.-Y.; Suzuki, T.; Asano, K.; Kaieda, T.; Omori, A.; Izumi, R.; Fujimura, A.; Kaitsuka, T.; Miyata, K.; Araki, K.; Oike, Y.; Scorrano, L.; Suzuki, T.; Tomizawa, K. Defective Mitochondrial tRNA Taurine Modification Activates Global Proteostress and Leads to Mitochondrial Disease. *Cell Rep.* **2018**, *22* (2), 482–496. https://doi.org/10.1016/j.celrep.2017.12.051.

(185) Basemore, A. W.; Elliot, K. A.; Florey, E. Isolation of Factor I. *J. Neurochem.* **1957**, *1* (4), 334–339. https://doi.org/10.1111/j.1471-4159.1957.tb12090.x.

(186) Koh, W.; Kwak, H.; Cheong, E.; Lee, C. J. GABA Tone Regulation and Its Cognitive Functions in the Brain. *Nat. Rev. Neurosci.* **2023**, *24* (9), 523–539. https://doi.org/10.1038/s41583-023-00724-7.

(187) Erdö, S. L.; Wolff, J. R. Gamma-Aminobutyric Acid Outside the Mammalian Brain. *J. Neurochem.* **1990**, *54* (2), 363–372. https://doi.org/10.1111/j.1471-4159.1990.tb01882.x.

(188) Hagan, D. W.; Ferreira, S. M.; Santos, G. J.; Phelps, E. A. The Role of GABA in Islet Function. *Front. Endocrinol.* **2022**, *13*, 972115. https://doi.org/10.3389/fendo.2022.972115.

(189) Strandwitz, P.; Kim, K. H.; Terekhova, D.; Liu, J. K.; Sharma, A.; Levering, J.; McDonald, D.; Dietrich, D.; Ramadhar, T. R.; Lekbua, A.; Mroue, N.; Liston, C.; Stewart, E. J.; Dubin, M. J.; Zengler, K.; Knight, R.; Gilbert, J. A.; Clardy, J.; Lewis, K. GABA-Modulating Bacteria of the Human Gut Microbiota. *Nat. Microbiol.* **2019**, *4* (3), 396–403. https://doi.org/10.1038/s41564-018-0307-3.

(190) Zhong, H.-J.; Wang, S.-Q.; Zhang, R.-X.; Zhuang, Y.-P.; Li, L.; Yi, S.-Z.; Li, Y.; Wu, L.; Ding, Y.; Zhang, J.; Xie, X.; He, X.-X.; Wu, Q. Supplementation with High-GABA-Producing Lactobacillus Plantarum L5 Ameliorates Essential Tremor Triggered by Decreased Gut Bacteria-Derived GABA. *Transl. Neurodegener.* **2023**, *12* (1), 58. https://doi.org/10.1186/s40035-023-00391-9.

(191) Kim, J.-I.; Ganesan, S.; Luo, S. X.; Wu, Y.-W.; Park, E.; Huang, E. J.; Chen, L.; Ding, J. B. Aldehyde Dehydrogenase 1a1 Mediates a GABA Synthesis Pathway in Midbrain Dopaminergic Neurons. *Science* **2015**, *350* (6256), 102–106. https://doi.org/10.1126/science.aac4690.

(192) Yoon, B.-E.; Lee, C. J. GABA as a Rising Gliotransmitter. *Front. Neural Circuits* **2014**, *8*, 141. https://doi.org/10.3389/fncir.2014.00141.

(193) Ben-Menachem, E. Mechanism of Action of Vigabatrin: Correcting Misperceptions. *Acta Neurol. Scand.* **2011**, *124* (s192), 5–15. https://doi.org/10.1111/j.1600-0404.2011.01596.x.

(194) Neman, J.; Termini, J.; Wilczynski, S.; Vaidehi, N.; Choy, C.; Kowolik, C. M.; Li, H.; Hambrecht, A. C.; Roberts, E.; Jandial, R. Human Breast Cancer Metastases to the Brain Display GABAergic Properties in the Neural Niche. *Proc. Natl. Acad. Sci.* **2014**, *111* (3), 984–989. https://doi.org/10.1073/pnas.1322098111.

(195) Geisler, C. E.; Ghimire, S.; Bruggink, S. M.; Miller, K. E.; Weninger, S. N.; Kronenfeld, J. M.; Yoshino, J.; Klein, S.; Duca, F. A.; Renquist, B. J. A Critical Role of Hepatic GABA in the Metabolic Dysfunction and Hyperphagia of Obesity. *Cell Rep.* **2021**, *35* (13), 109301. https://doi.org/10.1016/j.celrep.2021.109301.

Chapter 2: Sideroflexins enable mitochondrial polar neutral amino acid transport

Authors: Samuel Block[1,2], Fangtao Chi[2], Paul C. Rosen[1], Alicia M. Darnell[1,2], Keene L. Abbott[1,2], Ömer H. Yilmaz[1,2], Nora Kory[3,4], Matthew G. Vander Heiden[1,2,4]

Affiliations:

[1]Department of Biology, MIT, Cambridge, MA, USA

[2]David H. Koch Institute for Integrative Cancer Research, MIT, Cambridge, MA, USA

[3]Department of Molecular Metabolism, Harvard T.H. Chan School of Public Health, Boston, MA, USA

[4]Dana-Farber Cancer Institute, Boston, MA, USA

Introduction

Most inner mitochondrial membrane transporters belong to the SLC25 protein family, which contains 53 members in humans[1,2]. These proteins, together with the sideroflexins (SFXN)[3,4], mitochondrial pyruvate carrier (MPC)[5–7], mitochondrial calcium uniporter (MCU)[8,9], ABCB transporters[10], and a few other individual transporters[11,12], are responsible for shuttling nucleotides, amino acids, fatty acids, carboxylates, cofactors and inorganic ions across the inner mitochondrial membrane[2]. Thus, mitochondrial transporters play crucial roles in metabolism and other biological processes.

Owing to redundancy in transport properties and challenges inherent in studying the functions of membrane proteins, the mechanism by which many amino acids that are central to human physiology cross the inner mitochondrial membrane remains unknown. To date, 11 mitochondrial amino acid transporters have been identified. SLC25A12 and SLC25A13 (AGC1 and AGC2) transport glutamate and aspartate[13,14], an exchange reaction required for the malate aspartate shuttle, and also export n-acetyl-aspartate for myelin synthesis[15]. SLC25A8 (UCP2) also transports aspartate in addition to other carboxylates[15,16]. SLC25A22 and SLC25A18 (GC1 and GC2) import glutamate into mitochondria for ammonia detoxification in hepatic tissue[17], or export it in pancreatic beta cells to facilitate insulin secretion[15,18]. SLC25A15 and SLC25A2 (ORC1 and ORC2) transport arginine, and exchange ornithine and citrulline as part of the urea cycle[19,20], and ORC2 also transports other basic amino acids, including histidine[15,20]. SLC25A29 imports arginine for nitric oxide production[15,21], and also lysine[15,21], which feeds into the matrix localized saccharopine pathway[15,22]. More recently identified

amino acid carriers include SLC25A38, which is required for mitochondrial glycine import[23] needed for heme synthesis in erythrocytes[24], and SLC25A44, which imports branched-chain amino acids (BCAA) for degradation and thermogenesis in brown adipose tissue[25,26]. Of note, members of other mitochondrial carrier families can also transport amino acids. SFXN1 mediates mitochondrial import of serine, a donor for mitochondrial one-carbon metabolism[4,27]. Finally, a variant of the plasma membrane carrier SLC1A5 and SLC25A15 have been ascribed functions in glutamine[28] and serine[29] transport, respectively. However, tissue and cell type specificity of many of these transport processes has not been elucidated.

Aside from being required for the synthesis of mitochondrial genome encoded proteins, which are critical for respiration[30], mitochondrial transport of amino acids affects many metabolic pathways that are often altered in disease. For example, mitochondrial proline export is upregulated in cancer-associated fibroblasts and is required for collagen synthesis, which promotes tumor growth and metastasis[31], while impaired mitochondrial proline import and degradation leads to synaptic dysfunction[32] and is associated with schizophrenia and hyperprolinemia[33]. Non-proteinogenic amino acids must also cross mitochondrial membranes, such as the inhibitory neurotransmitter GABA which is degraded within glial mitochondria[34]. However, the mitochondrial transporters for proline, methionine, alanine, cysteine, threonine, asparagine, phenylalanine, tyrosine, tryptophan, and many non-proteinogenic amino acids including GABA remain unknown. To address this, we used CRISPR-Cas9 gene editing to delete candidate transporters and assessed these effects on mitochondrial uptake of amino acids using a mitochondrial swelling assay. This approach identified SFXN1 as a

regulator of mitochondrial permeability to proline, and together with supporting metabolic studies suggest that sideroflexins enable transport of several polar neutral amino acids across mitochondrial membranes including glycine, threonine, taurine, hypotaurine, beta alanine, and GABA.

Results

A targeted swelling screen identifies SFXN1 as a regulator of mitochondrial proline permeability

Studies using mitochondria isolated from other organisms[35–38] have provided evidence for the existence of a mitochondrial proline transporter, but whether this extends to humans remains unknown. To determine if humans contain a mitochondrial proline transporter, we isolated mitochondria from HEK293T cells and measured the kinetics of proline uptake using mitochondrial swelling, a well-established transport assay used to assess the properties of many mitochondrial carriers[39–42] (Fig. 1A). Compared to sucrose, which does not penetrate the inner mitochondrial membrane, we observed robust swelling with proline (Extended Data Fig. 1A), including a preference for the physiological L isomer (Fig. 1B-C). These data suggest that the purified mitochondria have an intact inner membrane that contains a proline transporter, since both isomers would elicit equal responses if swelling occurred by diffusion, consistent with studies using mitochondria isolated from rat[35], yeast[37] and plants[36].

To screen for mitochondrial proline transporters, we used CRISPR-Cas9 gene editing[43] to individually delete 10 candidate transporters and compared how loss of each candidate affects mitochondrial proline swelling relative to non-targeting control (NTC)

(Fig. 1D). These transporters include SFXN1-5 and SLC25A38 which have been shown to transport other small neutral amino acids[4,23], as well as SLC25A16, SLC25A30, SLC25A35, and SLC25A53 which are uncharacterized putative mitochondrial transporters we found to be expressed in HEK293T cells by proteomics (Extended Data Fig. 1B). Of note, mitochondria isolated from cells expressing a guide targeting SFXN1 demonstrated reduced swelling with proline compared to NTC (Fig. 1D). To validate that loss of SFXN1 reduces proline swelling, we generated clonal knockout lines of SFXN1 in HEK293T and K562 cells (Extended Data Fig.1 C-D). Mitochondria isolated from these cells also showed reduced swelling with proline (Fig1. E, Extended Data Fig.1 E), which was rescued by re-expression of SFXN1 but not overexpression of SFXN2-5 (Fig1. F). To determine the amino acid specificity of this effect, we performed swelling with alanine, which unlike proline demonstrates minimal stereospecificity in mitochondria isolated from yeast[37], indicating alanine import occurs through a separate transporter. While conflicting results have been published using rat liver mitochondria[35,44], we found that alanine demonstrates minimal swelling stereospecificity using HEK293T mitochondria (Fig1. G), and loss of SFXN1 had no effect on L-alanine swelling (Fig1. H).

Figure 1

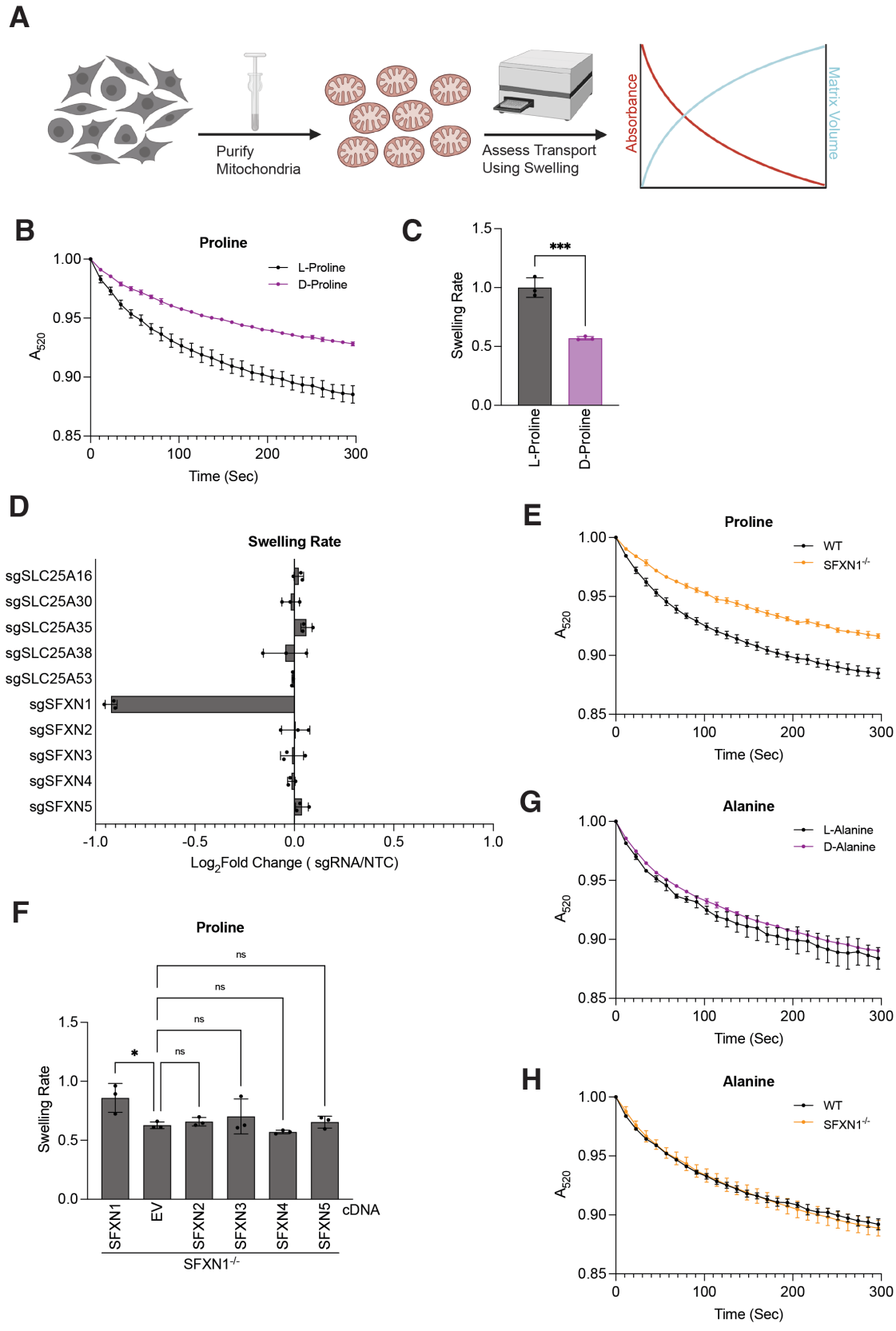
A
Purify
Mitochondria
Assess Transport
Using Swelling
Absorbance
Matrix Volume
B
Proline
L-Proline
D-Proline
A520
Time (Sec)
C
Swelling Rate
***
L-Proline
D-Proline
D
Swelling Rate
sgSLC25A16
sgSLC25A30
sgSLC25A35
sgSLC25A38
sgSLC25A53
sgSFXN1
sgSFXN2
sgSFXN3
sgSFXN4
sgSFXN5
Log2Fold Change (sgRNA/NTC)
E
Proline
WT
SFXN1-/-
A520
Time (Sec)
F
Proline
Swelling Rate
ns
*
SFXN1
EV
SFXN2
SFXN3
SFXN4
SFXN5
cDNA
SFXN1-/-
G
Alanine
L-Alanine
D-Alanine
A520
Time (Sec)
H
Alanine
WT
SFXN1-/-
A520
Time (Sec)

Fig. 1. Loss of SFXN1 reduces mitochondrial proline permeability. (A) Schematic of mitochondrial swelling experiment to study transport. **(B)** Swelling curves of HEK239T mitochondria treated with either L or D-proline; n=3 ± SD. **(C)** Swelling rates of HEK239T mitochondria treated with either L or D-proline. Values were normalized to L-proline; n=3 ± SD, unpaired t-test ***$p < 0.001$. **(D)** Results of swelling screen. Swelling rates of mitochondria treated with proline from target cell lines (sgRNA) were compared to a non-targeting control (NTC); n=3 ± SD. **(E)** Swelling curves of HEK239T mitochondria treated with proline from either wild type (WT) or SFXN1 knockout (SFXN1$^{-/-}$) cells; n=3 ± SD. **(F)** Proline swelling rates from SFXN1$^{-/-}$ mitochondria expressing other sideroflexins (SFXN1-5) or empty vector (EV); n=3 ± SD, one-way ANOVA followed by Dunnett's multiple comparisons test *$p < 0.05$, ns = not significant. (**G)** Swelling curves of HEK293T mitochondria treated with either L or D-alanine; n=3 ± SD. **(H)** Swelling curves of HEK293T mitochondria treated with L-alanine; n=3 ± SD.

Extended Data Figure 1

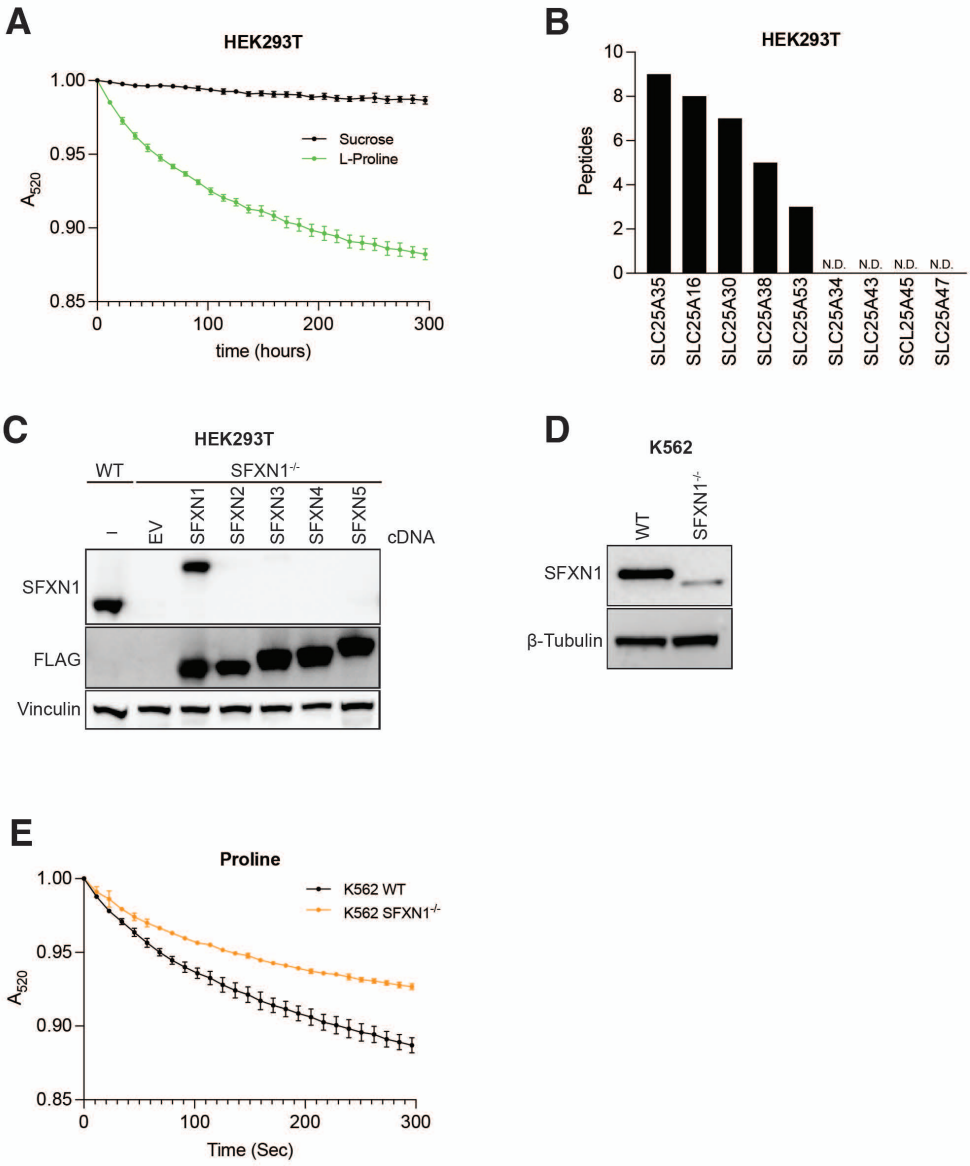

Extended Data Fig. 1. (A). Swelling curves of HEK293T mitochondria treated with either sucrose or L-proline; *n*=3 ± SD. **(B)** Peptide counts of uncharacterized SLC25 family members from HEK293T mitochondria determined by proteomics; *n*=3, N.D. is not detected. **(C)** Immunoblot of HEK293T cells. SFXN1-5 cDNA cells express the indicated sideroflexin isoform with an N-terminal 3x FLAG-tag. Vinculin was used as a loading control. **(D)** Immunoblot of K562 cells. β-Tubulin was used as a loading control. **(E)** Swelling curves of K562 mitochondria treated with L-proline; *n*=3 ± SD.

Loss of SFXN inhibits mitochondrial proline export

Proline can be synthesized in the cytosol through PYCR3 or within mitochondria through PYCR1/2[45], and glutamine is the predominant source of mitochondrial proline synthesis in cultured mammalian cells[46] (Fig2. A). To determine if the reduction in mitochondrial proline permeability we observe in SFXN1 knockout mitochondria is associated with impaired export of mitochondrially-synthesized proline from glutamine, we incubated HEK293T cells with $^{13}C_5$-L-glutamine and measured proline released into the media by liquid chromatography-mass spectrometry (LC-MS). For comparison, we also generated cells lacking various combinations of PYCR1-3 (Extended Data Fig2. A). Interestingly, loss of SFXN1 markedly reduced M+5 proline released into media, to levels similar to those found in PYCR1/2 double knockout cells (Fig2. B). To test whether loss of SFXN1 reduces labeled proline excretion due to lower labeling of upstream metabolites, independent of its effect on mitochondrial proline release, we assessed labeling of relevant metabolites from $^{13}C_5$-L-glutamine and found no difference in M+5 P5C in SFXN1 knockout cells, even in the absence of PYCR3 (Fig2. C). Surprisingly, loss of all PYCR enzymes was required to completely inhibit M+5 proline release, whereas loss of PYCR3 in cells lacking SFXN1 had minimal effect (Fig2. B) These data suggest that PYCR3 is capable of producing proline in the cytosol when PYCR1/2 are absent, and that other mitochondrial proline transporters may compensate for loss of SFXN1. In support of this, cells lacking PYCR1/2, SFXN1, or SFXN1/PYCR3 can still proliferate in the absence of proline, whereas PYCR1/2/3 triple knockouts are proline auxotrophs (Fig2. D). Furthermore, we performed a proliferation based CRISPR-Cas9 screen using cells lacking PYCR3 in the absence of proline and identified SLC25A21 as a major hit (Extended Data Fig2. B), although mitochondria isolated from

cells in which SLC25A21 was targeted using CRISPR-Cas9 showed little difference in proline swelling (Extended Data Fig2. C). Since recent studies reported that sideroflexins regulate the assembly of other mitochondrial proteins[47,48], it is conceivable that loss of SFXN1 indirectly reduces proline export by altering the levels of other mitochondrial transporters. To test this idea, we used quantitative proteomics to look for changes in protein levels in cells lacking SFXN1 and SFXN4, which has a known role in Complex I assembly[48]. While loss of SFXN4 significantly reduced the levels of Complex I proteins (Extended Data Fig2. D-E) as previously described[48], we were unable to detect any significant protein level changes in SFXN1 knockout cells (Extended Data Fig2. F).

Humans primarily obtain glutamine from de novo synthesis in muscle[49], while most dietary glutamine is broken down within enterocytes of the small intestine to produce energy and other substrates, such as proline[50]. To study the effects of loss of SFXN1 on mitochondrial proline metabolism in this context, we generated SFXN1 knockout intestinal organoids using Cre-*loxP* mice (Extended Data Fig2. G). When incubated with $^{13}C_5$-L-glutamine, organoids lacking SFXN1 released markedly less M+5 proline (Fig2. E).

Figure 2

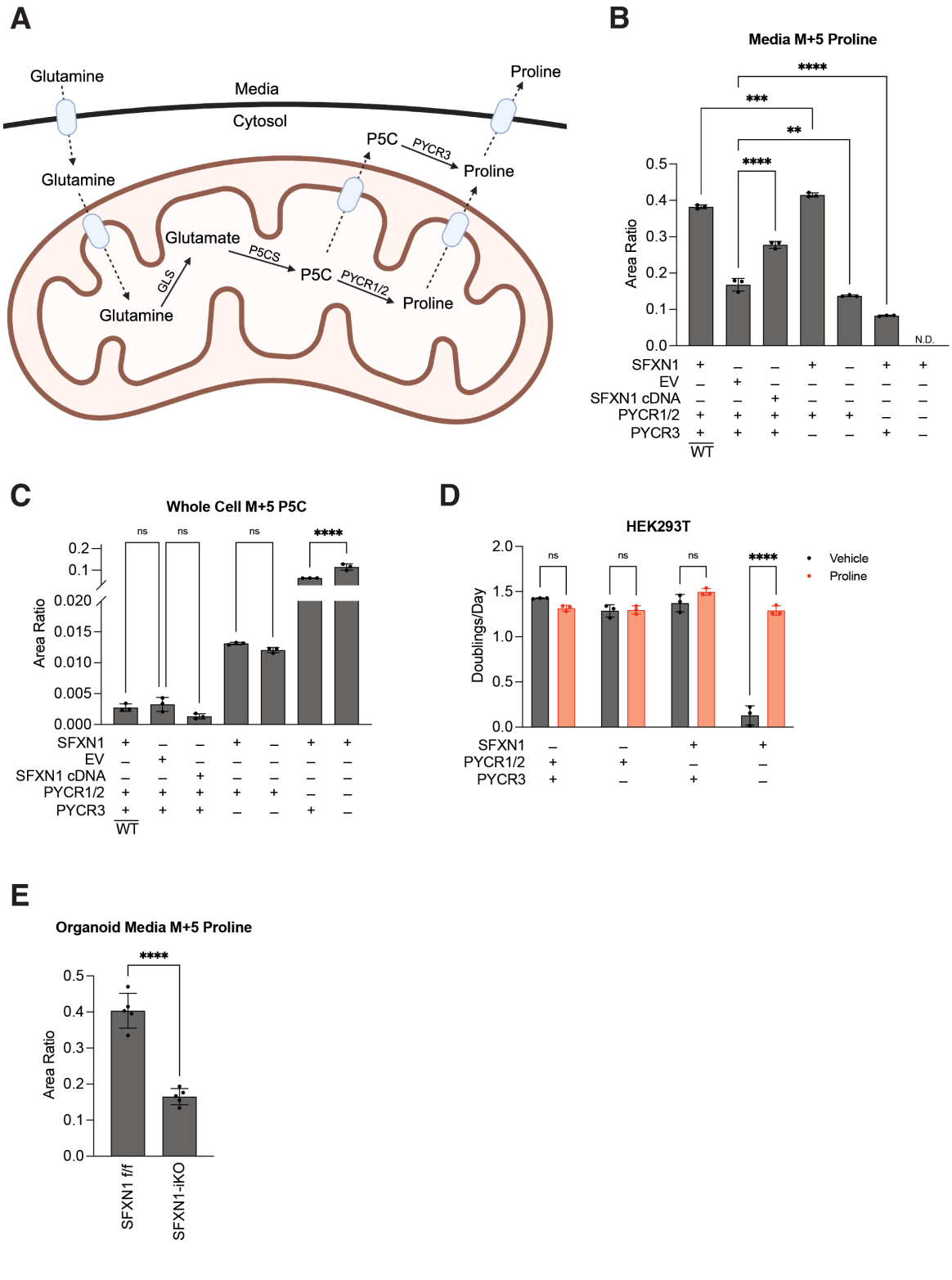
A
Glutamine
Media
Proline
Cytosol
P5C
PYCR3
Glutamine
Proline
Glutamate
P5CS
GLS
P5C
PYCR1/2
Glutamine
Proline
B
Media M+5 Proline
****
***
**
****
Area Ratio
0.5
0.4
0.3
0.2
0.1
0.0
N.D.
SFXN1 + – – + – + +
EV – + – – – – –
SFXN1 cDNA – – + – – – –
PYCR1/2 + + + + + – –
PYCR3 + + + – – + –
WT
C
Whole Cell M+5 P5C
ns ns ns ****
Area Ratio
0.2
0.1
0.020
0.015
0.010
0.005
0.000
SFXN1 + – – + – + +
EV – + – – – – –
SFXN1 cDNA – – + – – – –
PYCR1/2 + + + + + – –
PYCR3 + + + – – + –
WT
D
HEK293T
ns ns ns ****
Vehicle
Proline
Doublings/Day
2.0
1.5
1.0
0.5
0.0
SFXN1 – – + +
PYCR1/2 + + – –
PYCR3 + – + –
E
Organoid Media M+5 Proline
****
Area Ratio
0.5
0.4
0.3
0.2
0.1
0.0
SFXN1 f/f
SFXN1-iKO

Fig. 2. SFXN1 regulates mitochondrial proline export. (A) Schematic of glutamine tracing. **(B)** Relative media M+5 proline levels of HEK293T cells cultured in $^{13}C_5$-L-glutamine for 24 hours; n=3 ± SD, one-way ANOVA followed by Dunnett's multiple comparisons test $^{**}p < 0.01$, $^{****}p < 0.0001$. **(C)** Relative whole cell M+5 P5C levels from HEK239T cells cultured in $^{13}C_5$-L-glutamine for 8 hours; n=3 ± SD, one-way ANOVA followed by Šídák's multiple comparisons test $^{****}p < 0.0001$, ns is not significant. **(D)** Proliferation rates of HEK293T cells grown in vehicle or 1mM proline for 48 hours; n=3 ± SD, two-way ANOVA followed by Šídák's multiple comparisons test $^{****}p < 0.0001$. **(E)** Relative media M+5 proline levels from SFXN1 floxed (f/f) and SFXN1 knockout (-iKO) intestinal crypt organoids cultured in $^{13}C_5$-L-glutamine for 24 hours; n=3 ± SD, unpaired t-test $^{****}p < 0.0001$.

Extended Data Figure 2

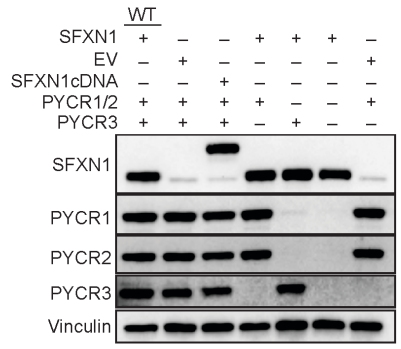

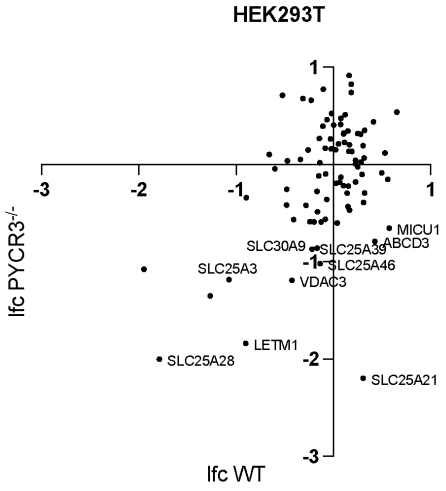

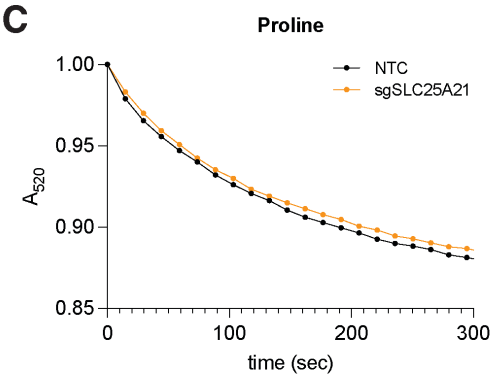

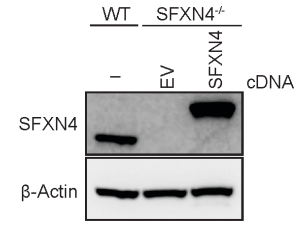

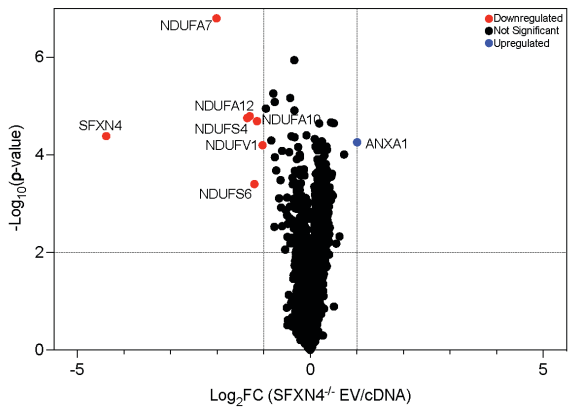

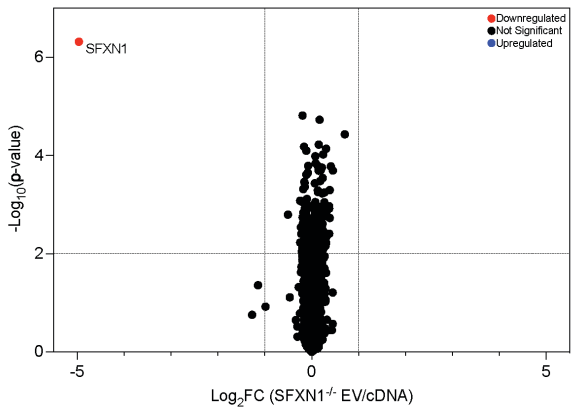

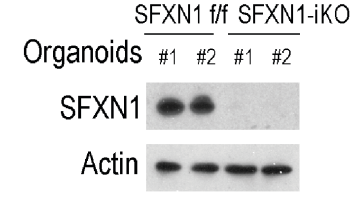

Extended Data Fig. 2. (A) Immunoblot of HEK293T cell lines depleted of SFXN1 and PYCR isoforms. Vinculin was used as a loading control. **(B)** CRISPR-Cas9 proliferation screen using HEK293T cells and a library targeting mitochondrial transporters. WT cells and a clonal PYCR3 knockout line ($PYCR3^{-/-}$) were grown in the absence of proline; lfc=$\log_2$ fold change. **(C)** Swelling curves of HEK293T mitochondria treated with proline; *n*=1. **(D)** Immunoblot of HEK293T cells. β-Actin was used as a loading control. **(E)** Quantitative proteomics comparing proteome levels of $SFXN4^{-/-}$ HEK293T cells expressing empty vector (EV) to SFXN4 (cDNA); *n*=3. **(F)** Quantitative proteomics comparing proteome levels of $SFXN1^{-/-}$ HEK293T cells expressing empty vector (EV) to SFXN1 (cDNA); *n*=3. **(G)** Immunoblot of SFXN1 floxed (f/f) and SFXN1 knockout (-iKO) intestinal crypt organoids. Actin was used as a loading control.

Polar neutral amino acids accumulate in SFXN1 KO mitochondria

SFXN1 has a known role in mitochondrial serine transport[4]. Given our findings that SFXN1 also appeared to be requried for mitochondrial proline transport, we hypothesized SFXN1 might be invovled in transporting other substrates across mitochondrial membranes. To explore this possibility, we immunopurified mitochondria[51] from SFXN1 knockout and control cells (Extended Data Fig3. A) and measured metabolites using LC-MS. Surprisingly, proline levels were similar in immunopurified mitochondria from control and SFXN1 knockout cells (Extended Data Fig3. B). We hypothesized that upstream metabolites involved in proline synthesis, such as glutamate, might show increased release from mitochodria when mitochondrial proline export is inhibited, particulary since glutamate can be exported from mitochondria through multiple known transporters[15]. In support of this, SFXN1 and PYCR1/2 knockout cells excreted increased amounts of M+5 glutamate produced from $^{13}C_5$-L-glutamine (Extended Data Fig3. C). Nevertheless, levels of several polar neutral amino acids were found to be elevated in SFXN1 knockout mitochondria, including hypotaurine, which is consistent with previous previous data[52], as well as elevated glycine and beta-alanine (Fig3. A).

The buildup of polar neutral amino acids such as hypotaurine, beta-alanine, and glycine in SFXN1 knockout mitochondria may reflect a role for SFXN1 in transport of this class of substrates. Indeed, mitochondria isolated from SFXN1 knockout cells showed evidence for decreased mitochondrial membrane permeability to these amino acids using swelling assays (Fig3. B-D), and this result extended to the other polar neutral

amino acids taurine and threonine (Fig3. E-F), which were also elevated in SFXN1 knockout immunopurified mitochondria (Fig1. A).

Since serine undergoes conversion to glycine predominantly within mitochondria[53], we were surprised that loss of a mitochondrial serine transporter resulted in elevated mitochondrial glycine. We hypothesized that compensation by other SFXN isoforms, such as SFXN2, which is expressed by HEK293Ts, might provide an alternative route for serine transport[4]. In line with this, loss of SFXN1 only mildly reduced mitochondrial serine swelling (Extended Data Fig3. D), while concomitant loss of SFXN2 led to a dramatic decrease (Extended Data Fig3. E-F).

To test whether SFXN1 was involved in mitochondrial glycine export, we cultured cells with $^{13}C_3$-L-serine, which like glutamine is net consumed[54] and can be converted into glycine by cytosolic SHMT1 or mitochondrial SHMT2[55] (Fig3. G), and measured glycine released into media by LC-MS. Loss of SFXN1 completely inhibited M+2 glycine secretion (Fig3. H), supporting previous data that showed glycine is primarily synthesized within mitochondria[53]. Interestingly, over-expression of SFXN2 and SFXN3 were also able to partially rescue M+2 glycine secretion in SFXN1 null cells (Fig3. H), while over-expression of SFXN4 and SFXN5 had no effect, which correlated with their ability to rescue mitochondrial swelling in response to glycine (Fig3. I). While it is possible that lower M+2 glycine secretion could be due to lower mitochondrial serine levels, we observed increased levels of serine in SFXN1 knockout immunopurified mitochondria (Extended Data Fig. G). Another explanation for these data could be that SFXN1 regulates SHMT2 activity independent of a role in direct serine/glycine transport. However, while the SHMT inhibitor SHIN2[56] completely blocked M+2 glycine

production from $^{13}C_3$-L-serine (Extended Data Fig3. H), it had no effect on mitochondrial serine or glycine swelling (Extended Data Fig3. I-J). Interestingly, targeting the mitochondrial glycine transporter SLC25A38[23] using CRISPR-Cas9 had no effect on mitochondrial glycine swelling (Extended Data Fig3. K-L).

Figure 3

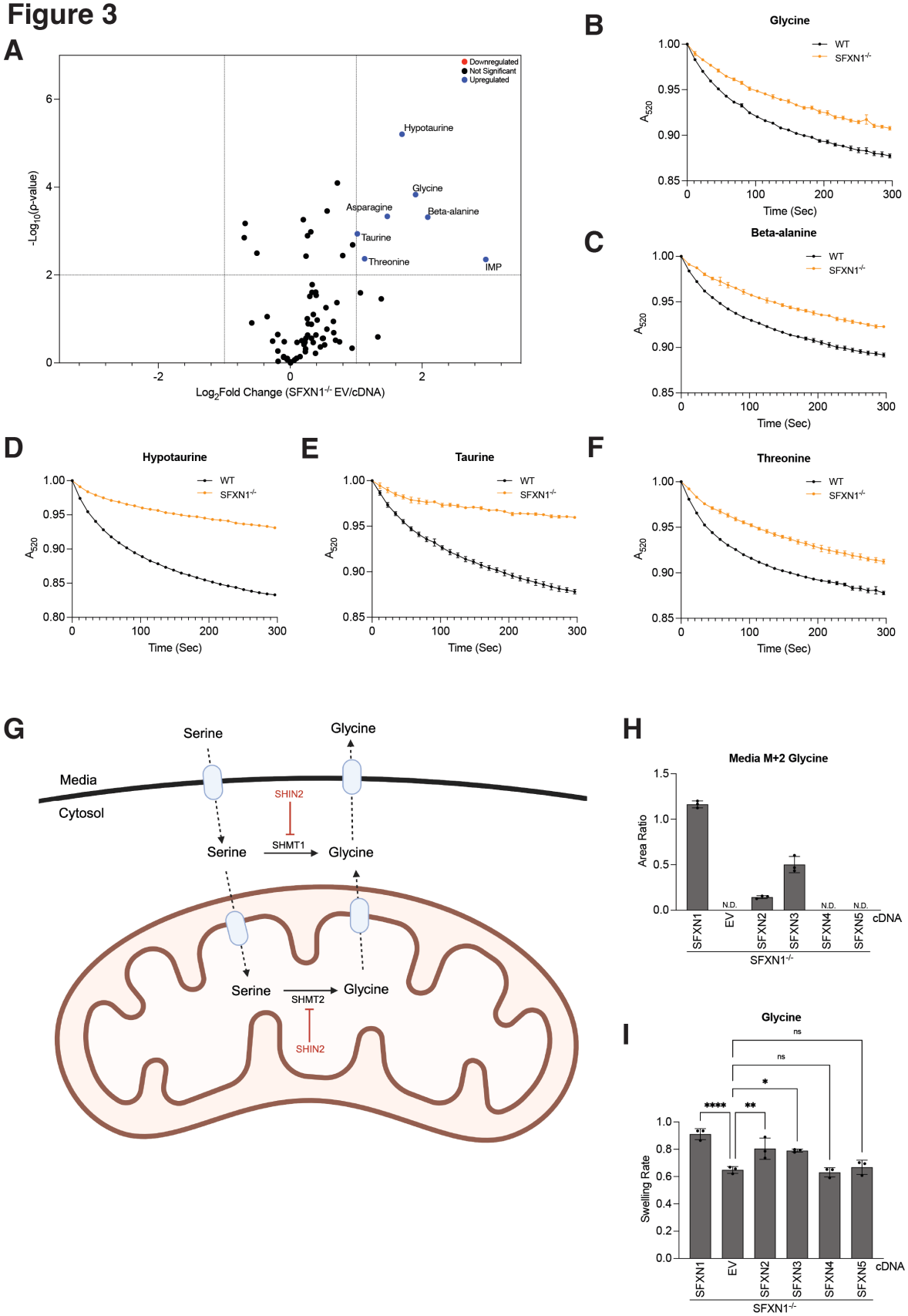
A
Downregulated
Not Significant
Upregulated
Hypotaurine
Glycine
Asparagine
Beta-alanine
Taurine
Threonine
IMP
-Log10(p-value)
Log2Fold Change (SFXN1-/- EV/cDNA)
B
Glycine
WT
SFXN1-/-
A520
Time (Sec)
C
Beta-alanine
D
Hypotaurine
E
Taurine
F
Threonine
G
Serine
Glycine
Media
Cytosol
SHIN2
SHMT1
SHMT2
H
Media M+2 Glycine
Area Ratio
N.D.
SFXN1
EV
SFXN2
SFXN3
SFXN4
SFXN5
cDNA
SFXN1-/-
I
Glycine
Swelling Rate
ns
*
**
****

Fig. 3. SFXN1 regulates mitochondrial permeability of many polar neutral amino acids. (A). Untargeted metabolomics of immunopurified mitochondria from SFXN1$^{-/-}$ HEK293T cells expressing empty vector (EV) compared to SFXN1 (cDNA); n=3, unpaired t-tests. **(B-F)** Swelling curves of HEK293T mitochondria treated with indicated amino acids. **(G)** Schematic of Serine tracing. **(H)** Relative media M+2 glycine levels of HEK293T cells cultured in $^{13}C_3$-L-Serine for 24 hours; n=3 ± SD, N.D. is not detected. **(I)** Swelling rates of HEK293T mitochondria treated with glycine; n=3 ± SD, one-way ANOVA followed by Dunnett's multiple comparisons test *$p < 0.05$, **$p < 0.01$, ****$p < 0.0001$, ns is not significant.

Extended Data Figure 3

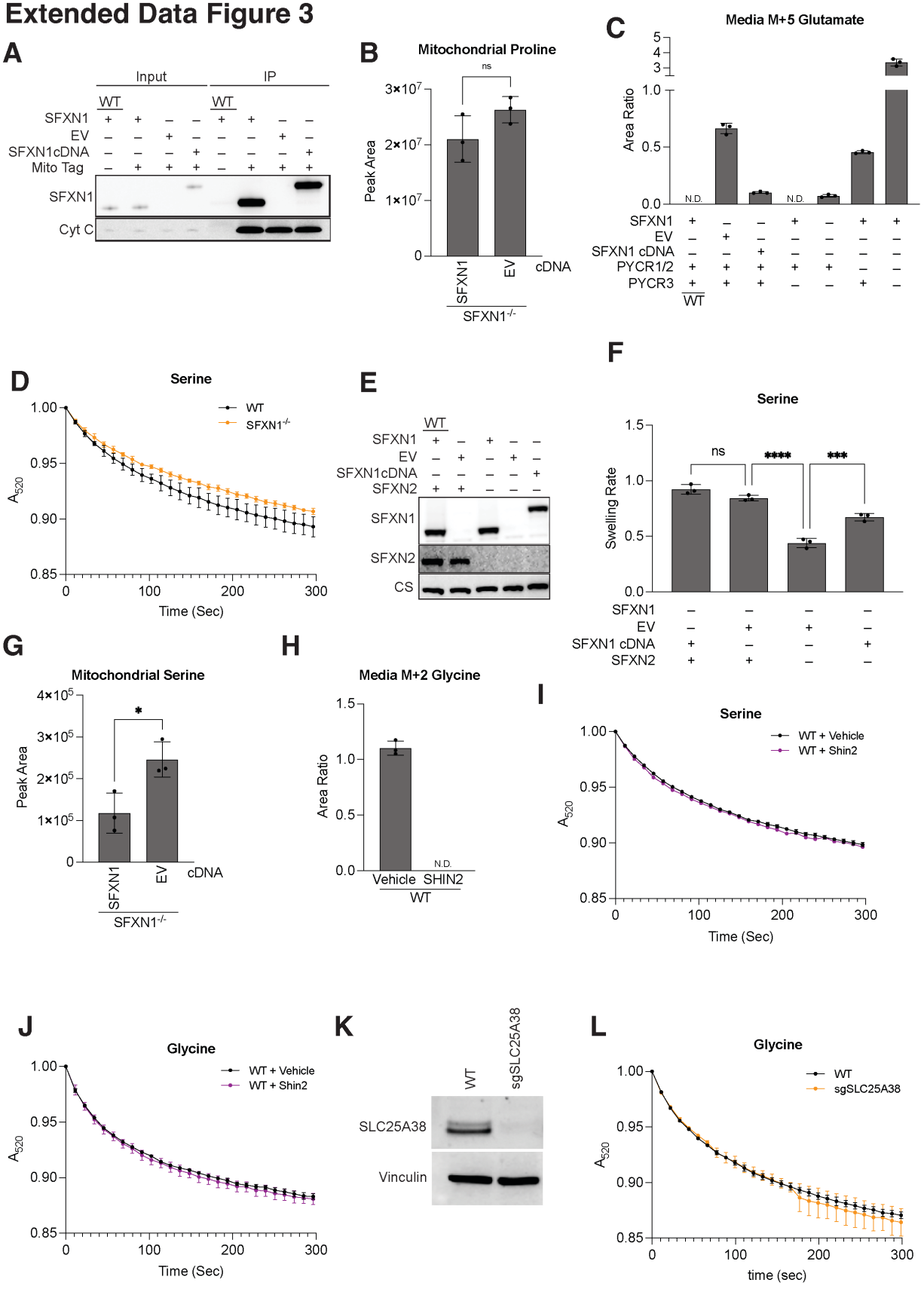

Extended Data Fig. 3. (A) Immunoblot of whole cell (WC) and immunoprecipitated mitochondria (IP) from HEK293T cells. Cyt C is cytochrome c. **(B)** Relative immunoprecipitated mitochondrial proline levels from HEK293T cells; n=3 ± SD, unpaired t-test, ns is not significant. **(C)** Relative media M+5 glutamate levels from HEK293T cells cultured in $^{13}C_5$-L-glutamine for 24 hours; n=3 ± SD, N.D. is not detected. **(D)** Swelling curves of HEK293T mitochondria treated with serine; n=3 ± SD. **(E)** Immunoblot of HEK293T cells. CS is citrate synthase and was used as a loading control. **(F)** Swelling rates of HEK293T mitochondria treated with serine; n=3 ± SD, one-way ANOVA followed by Šídák's multiple comparisons test ****$p < 0.0001$, ns is not significant. **(G)** Relative immunoprecipitated mitochondrial serine levels from HEK293T cells; n=3 ± SD, unpaired t-test *$p < 0.05$. **(H)** Relative media M+2 glycine levels from HEK239T cells cultured in $^{13}C_3$-L-serine supplemented either with vehicle (DMSO) or 5 μM (Rac)-SHIN2 for 24 hours; n=3 ± SD, N.D. is not detected. **(I-J)** Swelling curves of HEK293T mitochondria treated with serine and glycine. Mitochondria were pre-incubated with either vehicle (DMSO) or 5 μM (Rac)-SHIN2 for 30 minutes before swelling; n=3 ± SD. **(K)** Immunoblot of HEK293T cells. Vinculin was used as a loading control. **(L)** Swelling curves of HEK293T mitochondria treated with glycine; n=3 ± SD.

Loss of SFXN1 reduces mitochondrial GABA permeability

Solute carriers often transport multiple chemically similar substrates[57]. Most transporters for proline, glycine, taurine, and beta-alanine are members of the SLC6 family, which in humans contains 19 plasma membrane carriers divided among 3 classes: amino acid, monoamine, and GABA transporters[58]. Since the monoamines serotonin, dopamine, and noradrenaline are synthesized in the cytosol[59], and their degradation occurs on the cytosolic side of the outer mitochondrial membrane[60], it is unlikely mitochondrial transport of these neurotransmitters is relevant. In contrast, ABAT, the rate-limiting enzyme in GABA degradation localizes to the mitochondrial matrix[61]. Furthermore, the GABA and amino acid transporters within the SLC6 family demonstrate significant overlapping substrate promiscuity[58], and carrier dependent GABA transport into mitochondria has been described in rat brain[62], although the identity of the mammalian mitochondrial GABA transporter has not been reported. To test if SFXN1 is involved in mitochondrial GABA transport, we isolated mitochondria from SFXN1 knockout cells and determined whether GABA-induced swelling was affected. Compared to WT mitochondria, a stark reduction in GABA swelling was observed with loss of SFXN1 (Fig4. A). Importantly, while we did observe a slight decrease in membrane potential in the absence of SFXN1 (Extended Data Fig4. A), GABA swelling was not altered by FCCP treatment (Extended Data Fig4. B-C), consistent with earlier studies demonstrating the mitochondrial transport of most neutral amino acids is insensitive to membrane potential[40,63–65].

To examine the effects of loss of SFXN1 on GABA metabolism, we overexpressed ABAT in HEK293T cells (Extended Data Fig.4 D), treated them with $^{13}C_4$-GABA and looked for downstream TCA cycle labeling through the GABA shunt (Fig4. B), a well-conserved pathway in both eukaryotic and prokaryotic cells[66]. ABAT overexpression significantly increased M+4 malate and M+4 aspartate in HEK293T cells after adding $^{13}C_4$-GABA (Extended Data Fig.4 E), which was sensitive to the ABAT-specific inhibitor Vigabatrin[67] (Fig.4 C). Knockout of SFXN1 significantly inhibited ABAT-dependent $^{13}C_4$-GABA labeling, which was increased by over-expression of SFXN5, and perhaps SFXN2 (Fig4. D-E), indicating these paralogs may also influence mitochondrial GABA transport. In support of this, over-expression of SFXN2 and SFXN5 also increased GABA swelling in SFXN1 knockout mitochondria, while SFXN3 and SFXN4 had no effect (Fig4. F).

Figure4

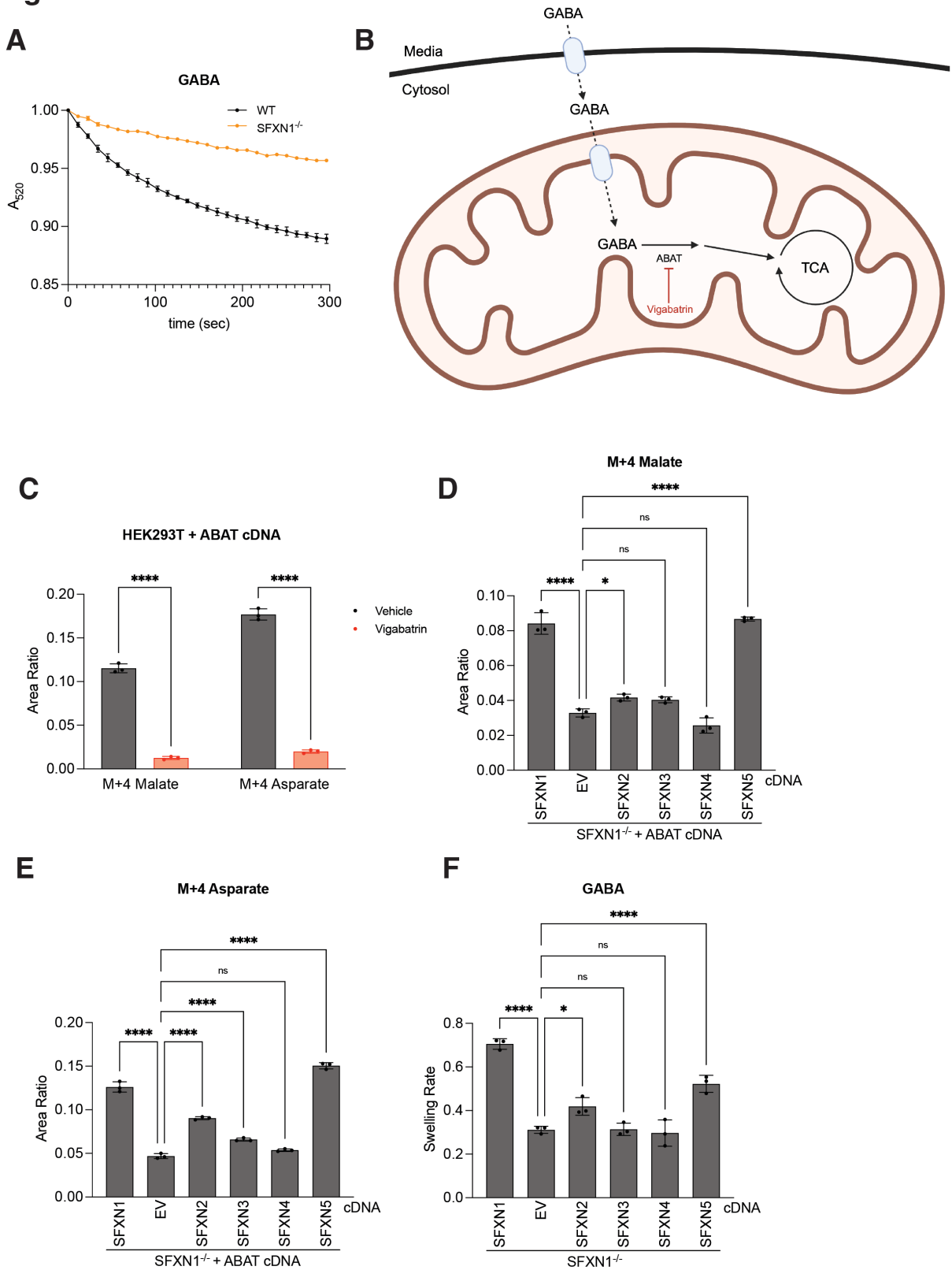
A
GABA
WT
SFXN1-/-
A520
time (sec)
B
GABA
Media
Cytosol
GABA
GABA
ABAT
TCA
Vigabatrin
C
HEK293T + ABAT cDNA
Area Ratio
Vehicle
Vigabatrin
M+4 Malate
M+4 Asparate
D
M+4 Malate
Area Ratio
SFXN1
EV
SFXN2
SFXN3
SFXN4
SFXN5
cDNA
SFXN1-/- + ABAT cDNA
E
M+4 Asparate
Area Ratio
SFXN1-/- + ABAT cDNA
F
GABA
Swelling Rate
SFXN1-/-

Fig. 4. SFXN1 regulates mitochondrial GABA permeability. (A) Swelling curves of HEK239T mitochondria treated with GABA; n=3 ± SD. **(B)** Schematic of GABA tracing. **(C)** Relative whole cell M+4 malate and M+4 aspartate levels of HEK239T cells expressing ABAT cDNA cultured in $^{13}C_4$-GABA for 30 minutes. Cells were pre-treated with either vehicle (DMSO) or 1mM Vigabatrin for 24 hours before media was refreshed with the same conditions plus tracer; n=3 ± SD, two-way ANOVA followed by Šídák's multiple comparisons test ****p < 0.0001. **(D-E)** Relative whole cell M+4 malate and M+4 aspartate levels of HEK239T cells cultured in $^{13}C_4$-GABA for 30 minutes. Area ratios were normalized to ABAT levels determined by western blot densitometry; n=3 ± SD, one-way ANOVA followed by Dunnett's multiple comparisons test ***p = 0.001, ****p < 0.0001, ns is not significant. **(F)** Swelling rates of HEK293T mitochondria treated with GABA; one-way ANOVA followed by Dunnett's multiple comparisons test *p <0.05, ****p < 0.0001, ns is not significant.

Extended Data Figure 4

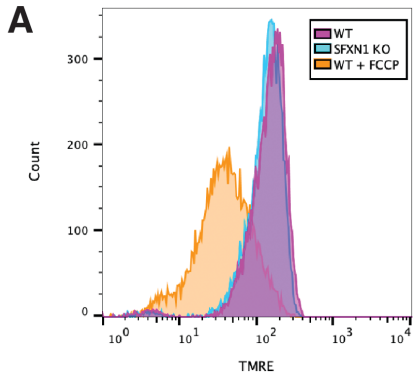

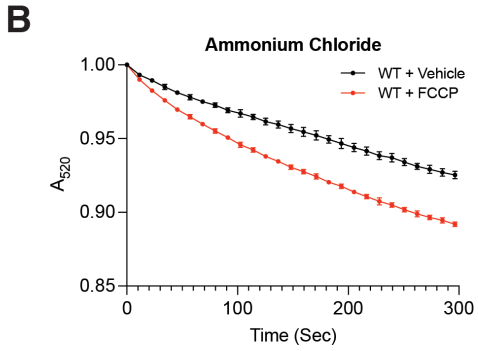

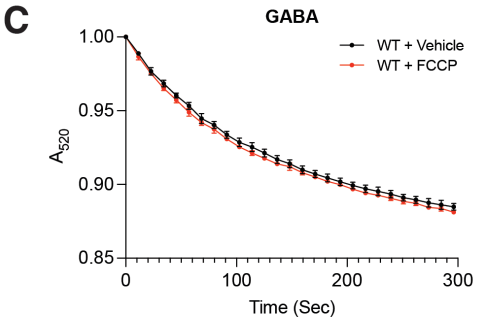

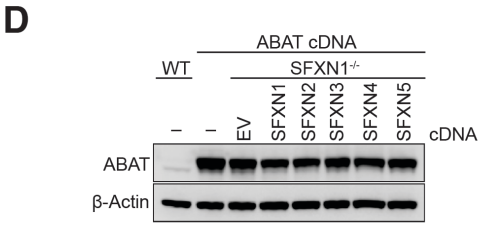

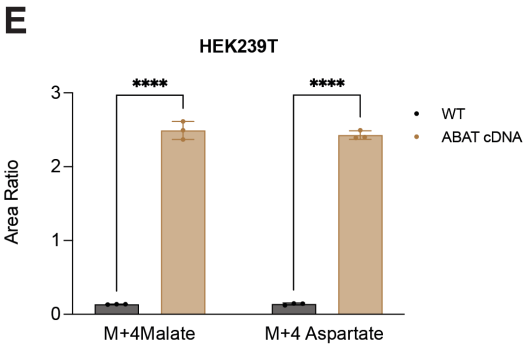

Extended Data Fig. 4. (A) Relative fluorescence intensity histograms of HEK293T cells treated with TMRE. WT cells were co-treated with FCCP as a control; *n*=3. **(B-C)** Swelling curves of HEK239T mitochondria treated with either ammonium chloride or GABA. Cells were pre-treated with either vehicle (DMSO) or 20 nM FCCP for 30 minutes before swelling; *n*=3 ± SD. **(D)** Immunoblot of HEK293T cells. β-Actin was used as a loading control. **(E)** Relative whole cell M+4 malate and M+4 aspartate levels of HEK239T cells cultured in $^{13}C_4$-GABA for 2 hours; *n*=3 ± SD.

Materials and Methods

Reagents

Antibodies for SFXN1 (HPA019543), and SFXN2 (HPA026834) were obtained from Atlas Antibodies, FLAG (F1804) from Sigma-Aldrich, β-Tubulin (2146), β-Actin (D6A9), Vinculin (E1E9V), and Citrate Synthase (CS) (D7V8B) from Cell Signaling Technology, PYCR3 (OTI1B12) from Novus Biologicals, PYCR1 (13108-1-AP), and PYCR2 (17146) from Proteintech, SFXN4 (PA5-35980) from Invitrogen, and Cytochrome C (Cyt C) (ab13575) and SLC25A38 (ab133614) from Abcam. Horseradish peroxidase–coupled anti-mouse and rabbit secondary antibody were obtained from Cell Signaling Technologies. For cell culture, DMEM (10-017-CV), RPMI (15-040-CV), and penicillin/streptomycin (30-002-CI) were obtained from Corning, FreeStyle 293 Expression Medium (12338018) was obtained from Gibco, and DMEM without glucose, glutamine, serine, glycine, sodium pyruvate (D9802-01) was obtained from United States Biological. Pierce Anti-HA Magnetic Beads (88837) were obtained from Thermo Scientific. $^{13}C_5$-L-Glutamine and $^{13}C_4$-GABA were obtained from Cambridge Isotope laboratories and all other amino acids, ammonium chloride, FCCP, rotenone, TMRE, potassium EDTA, polybrene, Tris, Sucrose, magnesium chloride, and potassium chloride were obtained from Sigma-Aldrich. Vigabatrin was obtained from Cayman Chemical Company. (Rac)-SHIN2 was obtained from MedChem Express. For transfection, X-tremeGENE 9 was obtained from Roche, Lipofectamine 3000 obtained from Invitrogen, and TransIT-Lenti Transfection Reagent was obtained from Mirus Bio. For LC-MS, HPLC grade water was obtained from Sigma-Aldrich, and HPLC ultra gradient acetonitrile was obtained from Avantor. For cloning, NEB stable competent cells, T4 DNA ligase, BbsI, Esp3I, T4 Polynucleotide Kinase, T4 Ligation Buffer,

CutSmart Buffer, and Shrimp Alkaline Phosphatase were obtained from New England Biolabs.

Cell lines and plasmids

HEK293T and K562 cells were obtained from ATCC. HEK293T cells were used for virus production and all studies unless otherwise stated. ABAT Lentiviral Vector (Human) (CMV) (pLenti-GIII-CMV) (110070610195) was obtained from abm. The plasmids lentiCRISPRv2-Opti (#163126), pSpCas9(BB)-2A-GFP (PX458) (#48138), pU6-(BbsI)_CBh-Cas9-T2A-BFP (#64323), pMXs_FLAG-SFXN1 (#110634), pMXs_FLAG-SFXN2 (#110636), pMXs_FLAG-SFXN3 (#110637), pMXs_FLAG-SFXN4 (#110638), pMXs_FLAG-SFXN5 (#110639), pCMV-VSV-G (#8454), pCL-Eco (#12371), pLV hU6-sgRNA hUbC-dCas9-KRAB-T2a-Puro (#71236), pMDLg/pRRE (#12251), pRSV-Rev (#12253), and pMD2.G (#12259) were obtained from Addgene.

Cell culture

For passaging, lentiviral production, and mitochondrial immunopurification experiments, HEK293T cells were grown in DMEM (10-017-CV) supplemented with 10% fetal bovine serum (FBS) and penicillin/streptomycin. K562 cells were passaged in RPMI (15-040-CV) supplemented with 10% FBS, 2 mM glutamine and penicillin/streptomycin. For isolating mitochondria for swelling assays, HEK293T cells were grown in suspension in FreeStyle 293 Expression Medium (12338018) supplemented with 1% FBS and penicillin/streptomycin, and K562 cells were grown in suspension in RPMI (15-040-CV) supplemented with 5% FBS, 2mM glutamine, 0.1% Pluronic and penicillin/streptomycin.

Virus production and transduction

For lentivirus production, HEK293T cells at 80% confluency were transfected with pMDLg/pRRE, pRSV-Rev, pMD2.G, and one of the following: ABAT Lentiviral Vector (Human) (CMV) (pLenti-GIII-CMV), lentiCRISPRv2-Opti, or pLV hU6-sgRNA hUbC-dCas9-KRAB-T2a-Puro with TransIT-Lenti Transfection Reagent. After 48 hours, the virus-containing media was passed through a 0.45 μm filter and stored at −80 °C. For lentiviral transduction, 200,000 HEK293T cells were seeded in 2 mL of culture medium per well in 6-well plates, and after 24 hours the medium was replaced with 1 mL of virus-containing medium. After 24 hours, virus-containing medium was removed and cells expanded into 10 cm plates. 24 hours later, cells were selected with puromycin. Retroviral production and transduction with pMXs plasmids was performed as previously described[68]. Briefly, HEK293T cells were spinfected with retrovirus at 1,200 x g for 45 min at 37 °C. After 18 hours, virus was removed and cells were expanded. Selection medium was added 48 hours post-transduction.

The following oligonucleotides were cloned into lentiCRISPRv2-Opti to generate the cell lines used in the mitochondrial swelling screen:

sgSLC25A16 (1): 5'-CACCGCGGACCCTAACCATGTCAAG-3'

sgSLC25A16 (2): 5'-AAACCTTGACATGGTTAGGGTCCGC-3'

sgSLC25A30 (1): 5'-CACCGTGCCTGGCGTAACATCGCGG-3'

sgSLC25A30 (2): 5'-AAACCCGCGATGTTACGCCAGGCAC-3'

sgSLC25A35 (1): 5'-CACCGGAGGAACCGACGATAACTCG-3'

sgSLC25A35 (2): 5’-AAACCGAGTTATCGTCGGTTCCTCC-3’

sgSLC25A38 (1): 5’-CACCGGAGGAGCATCTATCACAGTG-3’

sgSLC25A38 (2): 5’-AAACCACTGTGATAGATGCTCCTCC-3’

sgSLC25A53 (1): 5’-CACCGTAAAGTTGGAAACGGCCCCA-3’

sgSLC25A53 (2): 5’-AAACTGGGGCCGTTTCCAACTTTAC-3’

sgSFXN1 (1): 5’-CACCGGTTCCCATTCTCATCCGTGA-3’

sgSFXN1 (2): 5’-AAACTCACGGATGAGAATGGGAACC-3’

sgSFXN2 (1): 5’-CACCGCAGATACAAAGACAGTGCGG-3’

sgSFXN2 (2): 5’-AAACCCGCACTGTCTTTGTATCTGC-3’

sgSFXN3 (1): 5’-CACCGGGGCACAAATCTGCCGACCA-3’

sgSFXN3 (2): 5’-AAACTGGTCGGCAGATTTGTGCCCC-3’

sgSFXN4 (1): 5’-CACCGACGGACTTGATCCCTTTCAG-3’

sgSFXN4 (2): 5’-AAACCTGAAAGGGATCAAGTCCGTC-3’

sgSFXN5 (1): 5’-CACCGCAGTGACAAAGAGTGTGCGA-3’

sgSFXN5 (2): 5’-AAACTCGCACACTCTTTGTCACTGC-3’

sgNTC (1): 5’-CACCGTAACCGATACTCCCCACATT-3’

sgNTC (2): 5’-AAACAATGTGGGGAGTATCGGTTAC-3’

The following oligonucleotides were also used to target SLC25A21 for the mitochondrial swelling assay with proline

sgSLC25A21 (1): 5’- CACCGAATATACATACCCTTCCATT-3’

sgSLC25A21 (2): 5’- AAACAATGGAAGGGTATGTATATTC-3’

The following oligonucleotides were cloned into pLV hU6-sgRNA hUbC-dCas9-KRAB-T2a-Puro to generate -PYCR3 cell lines

sgPYCR3 (1): CACCGCGGCGTCCGAGGCAACAAGA

sgPYCR3 (1): AAACTCTTGTTGCCTCGGACGCCGC

Generation of CRISPR knockout cell lines

Knockout lines were generated using a previously described protocol[69]. Briefly, HEK293T or K562 cells were transfected with pSpCas9(BB)-2A-GFP (PX458) or pU6-(BbsI)_CBh-Cas9-T2A-BFP containing guides of interest. 48 hours later, BFP/GFP positive cells were single cell sorted into 96 well plates and split up to establish clonal lines. Knockout of genes of interest were confirmed by western blot. The following oligonucleotides were cloned into either pSpCas9(BB)-2A-GFP (PX458) or pU6-(BbsI)_CBh-Cas9-T2A-BFP to generate clonal knockout lines:

sgSFXN1 (1): 5'-CACCGTCTTCACTGTAACTGACCCC-3'

sgSFXN1 (2): 5'-AAACGGGGTCAGTTACAGTGAAGAC-3'

sgSFXN4 (1): 5'-CACCGGCGCACGTTGGGCTCAATGA-3'

sgSFXN4 (2): 5'-AAACTCATTGAGCCCAACGTGCGCC-3'

sgPYCR1 (1A): 5'-CACCGAGAGCCGGTGCCATCTGTGG-3'

sgPYCR1 (2A): 5'-AAACCCACAGATGGCACCGGCTCTC-3'

sgPYCR1 (1B): 5'-CACCGCTGCTGTGAAGCCCTTGGCC-3'

sgPYCR1 (2B): 5'-AAACGGCCAAGGGCTTCACAGCAGC-3'

sgPYCR2 (1A): 5'-CACCGGATGGTGACACCAGCCGCAC-3'

sgPYCR2 (2A): 5'-AAACGTGCGGCTGGTGTCACCATCC-3'

sgPYCR2 (1B): 5'-CACCGGAACCTGACACGCAGCAACA-3'

sgPYCR2 (2B): 5'-AAACTGTTGCTGCGTGTCAGGTTCC-3'

sgPYCR3 (1A): 5'-CACCGTGGATGGGCGGTGAGCGCAG-3'

sgPYCR3 (2A): 5'-AAACCTGCGCTCACCGCCCATCCAC-3'

sgPYCR3 (1B): 5'-CACCGCCCACGAAGCCCACGCGCCG-3'

sgPYCR3 (2B): 5'-AAACCGGCGCGTGGGCTTCGTGGGC-3'

PYCR1/2, PYCR3, and PYCR 1/2/3 knockout lines were generated using 2 guides per gene

Immunoblotting

Western blots were performed as previously described[70]. Briefly, cells were washed 1 x in PBS and lysed in RIPA buffer containing protease inhibitors. Proteins were resolved using SDS-PAGE and transferred to nitrocellulose membranes for immunoblotting using the iBlot2 Dry Blotting System (Thermo Fisher, IB21001, IB23001). Antibodies were used in TBST with 5% (w/v) non-fat dry milk. Primary antibodies were used at 1:1000 dilution, and HRP-linked secondary antibodies were used at 1:5000 dilution.

Mitochondrial isolation and swelling assay

Isolation of mitochondria and the swelling assay were carried out using a previously described protocol[68]. Briefly, 1x 10^9 HEK293T cells grown in FreeStyle 293 Expression Medium (12338018) supplemented with 1% FBS and penicillin/streptomycin were washed with cold PBS and resuspended in cold isolation buffer (250 mM sucrose, 10 mM Tris pH 7.5, 10 mM KCl, 1.5 mM $MgCl_2$, 1 mM potassium EDTA). Cells were lysed on ice using 30 strokes with a dounce homogenizer and tight fit pestle, and mitochondria were isolated by differential centrifugation. Mitochondria were diluted to 2 mg/mL in room temperature swelling buffer (20 mM Tris pH 7.5, 0.5 mM potassium EDTA, 10 μM rotenone) and incubated at room temperature for 30 minutes before swelling was initiated by adding an equal volume of room temperature swelling buffer containing 500 mM substrate (250 mM final concentration). Swelling was monitored by measuring absorbance at 520 nm using a microplate reader, and swelling rates were determined as the absolute value of the change in absorbance at 520 nm from 0 to 90 seconds. Swelling rates were normalized to simultaneously swollen WT mitochondria unless otherwise stated.

$^{13}C_5$-L-glutamine and $^{13}C_3$-L-serine tracing

For media measurements 200,000 HEK293T cells were seeded per well in Poly-D-Lysine coated 6-well plates in 2 mL of DMEM (17-207-CV) supplemented with 4.5 g/L glucose, 2mM L-glutamine, 10% dialyzed FBS, and penicillin/streptomycin. For whole cells 400,000 cells were used. 16 hours later the media was removed and cells were washed 1x with PBS and incubated in fresh media with 2mM L-glutamine substituted

with 2mM $^{13}C_5$-L-glutamine. For media, 24 hours later 15 uL of media was collected and briefly vortexed with 150 μL of extraction buffer (HPLC grade 80% methanol 20% water containing isotopically labeled amino acid standards). For whole cell metabolite quantification, cells were washed 1x with cold blood bank saline at the indicated time points and lysed with 400 μL of cold extraction buffer and vortexed at 4°C for 10 minutes. Both media and whole cell samples were then centrifuged at 20,000 x g for 10 minutes to remove insoluble material. The supernatant was then filtered through a 10 kDa PES filter and metabolites were quantified by LC-MS. Peak areas were normalized to isotopically labeled internal standards to yield area ratios, and these ratios were normalized to cell counts performed using a Cellometer Auto T4 Plus Cell Counter (Nexcelcom Bioscience) on separately plated cells that were treated with matching experimental conditions. $^{13}C_3$-L-serine tracing was performed using the same protocol, except cells were cultured in DMEM (D9802-01) supplemented with 4.5 g/L glucose, 2mM L-glutamine, 400 μM L-serine, 10% dialyzed FBS, and penicillin/streptomycin. For tracing media, 400 μM L-Serine was substituted with 400 μM $^{13}C_3$-L-Serine

Proline proliferation experiments

HEK293T cells were seeded per well in Poly-D-Lysine coated 6-well plates in 2 mL of DMEM (10-017-CV) supplemented with 10% dialyzed FBS and penicillin/streptomycin. 16 hours later the media was removed and cells were washed 1x with PBS and incubated in fresh media supplemented with either vehicle or 1 mM proline. Separately plated cells were also counted at this time using a Cellometer Auto T4 Plus Cell Counter (Nexcelcom Bioscience). 48 hours later, cells were counted again and doublings were determined as $\log_2$ fold change between the counts.

$^{13}C_4$-GABA tracing

400,000 HEK293T cells were seeded per well in Poly-D-Lysine coated 6-well plates in 2 mL of DMEM (10-017-CV) supplemented with 10% dialyzed FBS and penicillin/streptomycin. 16 hours later the media was removed and cells were washed 1x with PBS, and cells were incubated in fresh media supplemented with 1mM GABA. 24 hours later, the cells were washed 1x with PBS and fresh media was added with 1mM GABA substituted with 1mM $^{13}C_4$-GABA. Cells were washed 1x with cold blood bank saline at the indicated time points and lysed with 400 µL of cold extraction buffer and vortexed at 4°C for 10 minutes. Samples were then centrifuged at 20,000 x g for 10 minutes to remove insoluble material. The supernatant was then filtered through a 10 kDa PES filter and metabolites were quantified by LC-MS. Peak areas were normalized to isotopically labeled internal standards to yield area ratios, and these ratios were normalized to cell counts using separately plated cells that were treated with matching experimental conditions.

Immunopurification of mitochondria for metabolomics

Mitochondria were immunopurified for metabolomics using a protocol adapted from previous studies[51,68,71]. 10x 10^6 HEK293T cells were seeded in 150 mm plates in 20 mL of DMEM (10-017-CV) supplemented with 10% FBS and penicillin/streptomycin. 16 hours later the plates were placed on ice, media was removed and cells were scraped into 5 mL of cold KPBS and centrifuged at 250 x g for 3 mintues. All following steps were performed at 4°C. Cell pellets were resuspended in 1 mL of KPBS and lysed with 10 strokes using a syringe attached to a 26G needle and centrifuged at 1100 x g for 2

mintues. 5 µl of supernatant was taken for input immunoblotting, and the rest was rotated with 100 µl of KPBS-equilibrated pierce anti-HA- magnetic beads for 5 minutes. The beads were then bound to a magnet and washed 3x with 1 mL KPBS. Before the third wash was removed, 5 µl was taken for IP immunoblotting. 100 µl of extraction buffer was then added and the beads were vortexed for 10 minutes. The beads were then magnet removed, and excess beads and insoluble material were removed by centrifugation at 20,000 x g for 10 minutes. The supernatant was collected and analyzed by LC-MS. Peak areas were normalized to the summed peak areas of all internal isotopic amino acid standards, which was then normalized to Cytochrome C levels determined by immunoblot densitometry. Statistical analysis for untargeted metabolomics was performed using MetaboAnalyst 6.0 operating on one factor default settings[72].

Polar metabolite LC–MS.

Polar metabolite profiling was performed using a previously described protocol[73]. Briefly, LC–MS was carried out using a QExactive orbitrap mass spectrometer equipped with a Dionex Ultimate 3000 UPLC system (Thermofisher). All samples were injected onto a SeQuant ZIC-pHILIC 2.1 mm × 150 mm (5 µm particle size) column (Millipore Sigma), and chromatography was performed starting with 20% buffer A (20 mM ammonium carbonate, 0.1% ammonium hydroxide), and 80% acetonitrile. A chromatographic gradient of linearly decreasing acetonitrile concentration was used with the mass spectrometer operating in full scan, polarity-switching mode. Metabolite identification was determined by referencing a library of chemical standards which was

constructed using external standard pools[74], and relative quantification of metabolites was carried out using XCalibur 2.2 software (Thermo Fisher Scientific).

Quantitative proteomics

Mitochondria in isolation buffer or whole cells washed 3x with cold PBS were flash frozen in liquid nitrogen and stored at -80°C. Tandem mass tag MS was carried out by the Thermo Fisher Scientific Center for Multiplexed Proteomics at Harvard Medical School (https://tcmp.hms.harvard.edu)

Sample Preparation for Mass Spectrometry

Samples for protein analysis were prepared essentially as previously described[75,76]. Proteomes (from whole cells or isolated mitochondria) were extracted using a buffer containing 200 mM EPPS pH 8.5, 8M urea, 0.1% SDS and protease inhibitors. Following lysis, ~150 µg of each sample was reduced with 5 mM TCEP. Cysteine residues were alkylated using 10 mM iodoacetimide for 20 minutes at RT in the dark. Excess iodoacetimide was quenched with 10 mM DTT. A buffer exchange was carried out using a modified SP3 protocol[77]. Briefly, ~1500 µg of Cytiva SpeedBead Magnetic Carboxylate Modified Particles (65152105050250 and 4515210505250), mixed at a 1:1 ratio, were added to each sample. 100% ethanol was added to each sample to achieve a final ethanol concentration of at least 50%. Samples were incubated with gentle shaking for 15 mins. Samples were washed three times with 80% ethanol. Protein was eluted from SP3 beads using 200 mM EPPS pH 8.5 containing Lys-C (1:50: Wako, 129-02541) and incubated overnight at room temperature. Samples were further digested with

trypsin (1:50; ThermoFisher Scientific, 90305R20) at 37°C with vigorous shaking. Acetonitrile was added to each sample to achieve a final concentration of ~33%. Each sample was labelled, in the presence of SP3 beads, with ~360 μg of TMTPro 16-plex reagents (ThermoFisher Scientific). Following confirmation of satisfactory labelling (>97%), excess TMT was quenched by addition of hydroxylamine to a final concentration of 0.3%. The full volume from each sample was pooled and acetonitrile was removed by vacuum centrifugation for 1 hour. The pooled sample was acidified using formic acid and peptides were de-salted using a Sep-Pak 50mg tC18 cartridge (Waters). Peptides were eluted in 70% acetonitrile, 1% formic acid and dried by vacuum centrifugation.

Basic pH reversed-phase separation (BPRP)

TMT labeled peptides were solubilized in 5% ACN/10 mM ammonium bicarbonate, pH 8.0 and ~300 μg of TMT labeled peptides were separated by an Agilent 300 Extend C18 column (3.5 μm particles, 4.6 mm ID and 250 mm in length). An Agilent 1260 binary pump coupled with a photodiode array (PDA) detector (Thermo Scientific) was used to separate the peptides. A 45 minute linear gradient from 10% to 40% acetonitrile in 10 mM ammonium bicarbonate pH 8.0 (flow rate of 0.6 mL/min) separated the peptide mixtures into a total of 96 fractions (36 seconds). A total of 96 Fractions were consolidated into 24 samples in a checkerboard fashion and vacuum dried to completion. Each sample was desalted via Stage Tips and re-dissolved in 5% FA/ 5% ACN for LC-MS3 analysis.

Liquid chromatography separation and tandem mass spectrometry (LC-MS3)

Proteome data were collected on an Orbitrap Fusion Lumos mass spectrometer (ThermoFisher Scientific) coupled to a Proxeon EASY-nLC 1000 LC pump (ThermoFisher Scientific). Fractionated peptides were separated using a 120 min gradient at 550 nL/min on a 35 cm column (i.d. 100 μm, Accucore, 2.6 μm, 150 Å) packed in-house. MS1 data were collected in the Orbitrap (120,000 resolution; maximum injection time 50 ms; AGC 6×10^5). Charge states between 2 and 6 were required for MS2 analysis, and a 120 s dynamic exclusion window was used. Top 10 MS2 scans were performed in the ion trap with CID fragmentation (isolation window 0.5 Da; Rapid; NCE 35%; maximum injection time 50 ms; AGC 1.5×10^4). An on-line real-time search algorithm (Orbiter) was used to trigger MS3 scans for quantification[78]. MS3 scans were collected in the Orbitrap using a resolution of 50,000, NCE of 55%, maximum injection time of 200 ms, and AGC of 3.0×10^5. The close out was set at two peptides per protein per fraction.[78]

Data analysis

Raw files were converted to mzXML, and monoisotopic peaks were re-assigned using Monocle[79]. Searches were performed using the Comet search algorithm against a human database downloaded from Uniprot in May 2021. A 50 ppm precursor ion tolerance, 1.0005 fragment ion tolerance, and 0.4 fragment bin offset for MS2 scans collected in the ion trap. TMTpro on lysine residues and peptide N-termini (+304.2071 Da) and carbamidomethylation of cysteine residues (+57.0215 Da) were set as static modifications, while oxidation of methionine residues (+15.9949 Da) was set as a variable modification.

Each run was filtered separately to 1% False Discovery Rate (FDR) on the peptide-spectrum match (PSM) level. Then proteins were filtered to the target 1% FDR level across the entire combined data set. For reporter ion quantification, a 0.003 Da window around the theoretical m/z of each reporter ion was scanned, and the most intense m/z was used. Reporter ion intensities were adjusted to correct for isotopic impurities of the different TMTpro reagents according to manufacturer specifications. Peptides were filtered to include only those with a summed signal-to-noise (SN) ≥ 160 across all TMT channels. The signal-to-noise (S/N) measurements of peptides assigned to each protein were summed (for a given protein). These values were normalized so that the sum of the signal for all proteins in each channel was equivalent thereby accounting for equal protein loading. For volcano plots only proteins with ≥ 3 peptides were reported.

Generation of SCON SFXN1-floxed mice

The SCON SFXN1-floxed mice were generated via microinjection at the 1-cell stage[80] For microinjection, 25 µl of CRISPR injection mix was prepared in nuclease-free buffer (10 mM TRIS-HCl, pH 7.4 and 0.25 mM EDTA), consisting of spCas9 mRNA (100 ng/µl), spCas9 protein (50 ng/µl), sgRNA (50 ng/µl), and ssODN (20 ng/µl, GenScript). The mixture was centrifuged at 13,000 × g at 4 °C for 15–20 min to prevent the clogging of the injection needles.

Intestinal organoid culture and $^{13}C_5$-L-glutamine tracing

Intestinal organoids were isolated and cultured as previously described[81]. For $^{13}C_5$-L-glutamine tracing, intestinal crypts samples were isolated and cultured in crypt culture

medium for 48 hours, and then placed into fresh media containing 0.2 mM $^{13}C_5$-L-glutamine. After 24 hours 15µl of media was added to 150 µl of extraction buffer which was briefly vortexed and centrifuged at 20,000 x g for 10 minutes. The supernatant was then filtered through a 10 kDa PES filter and metabolites were quantified by LC-MS. Peak areas were normalized to isotopically labeled internal standards to yield area ratios, and these ratios were normalized to total organoid protein determined by BCA.

TMRE staining and fluorescence

Cell staining with TMRE and fluorescence measurements were performed using a previously described protocol[82]. Briefly, HEK293T cells were incubated in DMEM (10-017-CV) supplemented with 10% dialyzed FBS, penicillin/streptomycin, and 150 nM TMRE for 5 minutes at room temperature. Fluorescence was measured by flow cytometry using a 561 nm laser.

CRISPR-Cas9 proliferation screen

CRISPR-Cas9 proliferation screens were performed using an adapted previously described protocol[83]. Briefly, HEK293T cells were grown in DMEM (10-017-CV) supplemented with 10% fetal bovine serum (FBS) and penicillin/streptomycin and transduced with a CRISPR lentivirus library targeting mitochondrial transporters. After selection with puromycin, DNA was isolated, and the remaining cells were grown in DMEM (10-017-CV) supplemented with 10% dialyzed FBS and penicillin/streptomycin. After approximately 14 population doublings, DNA was isolated again, and sgRNA was amplified by PCR and submitted for high throughput sequencing. Data analysis was performed using the MAGeCKFlute pipeline[84].

Schematics

All schematics were created with BioRender.com

Statistical analysis

Two tailed t-tests were used for comparing differences between two groups, and Analysis of Variance (ANOVA) followed by either Šídák's or Dunnett's multiple comparison tests was used for comparing differences between more than two groups. $p < 0.05$ was considered statistically significant, and most analyses and plots were generated using GraphPad PRISM 9.

Acknowledgements

Thank you to all members of the Vander Heiden lab for thoughtful discussions and feedback. Thank you to Jonathan Van Vranken and the Thermo Fisher Scientific Center for Multiplexed Proteomics at Harvard Medical School for performing quantitative proteomics and analysis. Thank you to Charles H. Adelmann for providing the mitochondrial transporter CRISPR library. Thank you to Izabella Pena for providing the Mito-tag plasmid.

Author Contributions

S.B. and F.C. performed experiments. P.C.R provided experimental design. K.L.A. and A.M.D provided critical supplies. Ö.H.Y, M.H., and N.K. provided critical feedback. S.B. and M.G.V.H designed the study and wrote the chapter with input from all authors.

References

(1) Kunji, E. R. S.; King, M. S.; Ruprecht, J. J.; Thangaratnarajah, C. The SLC25 Carrier Family: Important Transport Proteins in Mitochondrial Physiology and Pathology. *Physiology* **2020**, *35* (5), 302–327. https://doi.org/10.1152/physiol.00009.2020.

(2) Ruprecht, J. J.; Kunji, E. R. S. The SLC25 Mitochondrial Carrier Family: Structure and Mechanism. *Trends Biochem. Sci.* **2020**, *45* (3), 244–258. https://doi.org/10.1016/j.tibs.2019.11.001.

(3) Fleming, M. D.; Campagna, D. R.; Haslett, J. N.; Trenor, C. C.; Andrews, N. C. A Mutation in a Mitochondrial Transmembrane Protein Is Responsible for the Pleiotropic Hematological and Skeletal Phenotype of Flexed-Tail (f/f) Mice. *Genes Dev.* **2001**, *15* (6), 652–657. https://doi.org/10.1101/gad.873001.

(4) Kory, N.; Wyant, G. A.; Prakash, G.; uit de Bos, J.; Bottanelli, F.; Pacold, M. E.; Chan, S. H.; Lewis, C. A.; Wang, T.; Keys, H. R.; Guo, Y. E.; Sabatini, D. M. SFXN1 Is a Mitochondrial Serine Transporter Required for One-Carbon Metabolism. *Science* **2018**, *362* (6416), eaat9528. https://doi.org/10.1126/science.aat9528.

(5) Herzig, S.; Raemy, E.; Montessuit, S.; Veuthey, J.-L.; Zamboni, N.; Westermann, B.; Kunji, E. R. S.; Martinou, J.-C. Identification and Functional Expression of the Mitochondrial Pyruvate Carrier. *Science* **2012**, *337* (6090), 93–96. https://doi.org/10.1126/science.1218530.

(6) Bricker, D. K.; Taylor, E. B.; Schell, J. C.; Orsak, T.; Boutron, A.; Chen, Y.-C.; Cox, J. E.; Cardon, C. M.; Van Vranken, J. G.; Dephoure, N.; Redin, C.; Boudina, S.; Gygi,

S. P.; Brivet, M.; Thummel, C. S.; Rutter, J. A Mitochondrial Pyruvate Carrier Required for Pyruvate Uptake in Yeast, Drosophila, and Humans. *Science* **2012**, *337* (6090), 96–100. https://doi.org/10.1126/science.1218099.

(7) Nagampalli, R. S. K.; Quesñay, J. E. N.; Adamoski, D.; Islam, Z.; Birch, J.; Sebinelli, H. G.; Girard, R. M. B. M.; Ascenção, C. F. R.; Fala, A. M.; Pauletti, B. A.; Consonni, S. R.; de Oliveira, J. F.; Silva, A. C. T.; Franchini, K. G.; Leme, A. F. P.; Silber, A. M.; Ciancaglini, P.; Moraes, I.; Dias, S. M. G.; Ambrosio, A. L. B. Human Mitochondrial Pyruvate Carrier 2 as an Autonomous Membrane Transporter. *Sci. Rep.* **2018**, *8* (1), 3510. https://doi.org/10.1038/s41598-018-21740-z.

(8) De Stefani, D.; Raffaello, A.; Teardo, E.; Szabò, I.; Rizzuto, R. A Forty-Kilodalton Protein of the Inner Membrane Is the Mitochondrial Calcium Uniporter. *Nature* **2011**, *476* (7360), 336–340. https://doi.org/10.1038/nature10230.

(9) Baughman, J. M.; Perocchi, F.; Girgis, H. S.; Plovanich, M.; Belcher-Timme, C. A.; Sancak, Y.; Bao, X. R.; Strittmatter, L.; Goldberger, O.; Bogorad, R. L.; Koteliansky, V.; Mootha, V. K. Integrative Genomics Identifies MCU as an Essential Component of the Mitochondrial Calcium Uniporter. *Nature* **2011**, *476* (7360), 341–345. https://doi.org/10.1038/nature10234.

(10) 20,000 Picometers under the OMM: Diving into the Vastness of Mitochondrial Metabolite Transport. *EMBO Rep.* **2020**, *21* (5), e50071. https://doi.org/10.15252/embr.202050071.

(11) Rath, S.; Sharma, R.; Gupta, R.; Ast, T.; Chan, C.; Durham, T. J.; Goodman, R. P.; Grabarek, Z.; Haas, M. E.; Hung, W. H. W.; Joshi, P. R.; Jourdain, A. A.; Kim, S. H.; Kotrys, A. V.; Lam, S. S.; McCoy, J. G.; Meisel, J. D.; Miranda, M.; Panda, A.; Patgiri, A.; Rogers, R.; Sadre, S.; Shah, H.; Skinner, O. S.; To, T.-L.; Walker, M. A.;

Wang, H.; Ward, P. S.; Wengrod, J.; Yuan, C.-C.; Calvo, S. E.; Mootha, V. K. MitoCarta3.0: An Updated Mitochondrial Proteome Now with Sub-Organelle Localization and Pathway Annotations. *Nucleic Acids Res.* **2021**, *49* (D1), D1541–D1547. https://doi.org/10.1093/nar/gkaa1011.

(12) Morgenstern, M.; Peikert, C. D.; Lübbert, P.; Suppanz, I.; Klemm, C.; Alka, O.; Steiert, C.; Naumenko, N.; Schendzielorz, A.; Melchionda, L.; Mühlhäuser, W. W. D.; Knapp, B.; Busch, J. D.; Stiller, S. B.; Dannenmaier, S.; Lindau, C.; Licheva, M.; Eickhorst, C.; Galbusera, R.; Zerbes, R. M.; Ryan, M. T.; Kraft, C.; Kozjak-Pavlovic, V.; Drepper, F.; Dennerlein, S.; Oeljeklaus, S.; Pfanner, N.; Wiedemann, N.; Warscheid, B. Quantitative High-Confidence Human Mitochondrial Proteome and Its Dynamics in Cellular Context. *Cell Metab.* **2021**, *33* (12), 2464-2483.e18. https://doi.org/10.1016/j.cmet.2021.11.001.

(13) Indiveri, C.; Krämer, R.; Palmieri, F. Reconstitution of the Malate/Aspartate Shuttle from Mitochondria. *J. Biol. Chem.* **1987**, *262* (33), 15979–15983. https://doi.org/10.1016/S0021-9258(18)47685-5.

(14) Palmieri, L.; Pardo, B.; Lasorsa, F. M.; del Arco, A.; Kobayashi, K.; Iijima, M.; Runswick, M. J.; Walker, J. E.; Saheki, T.; Satrústegui, J.; Palmieri, F. Citrin and Aralar1 Are Ca2+-Stimulated Aspartate/Glutamate Transporters in Mitochondria. *EMBO J.* **2001**, *20* (18), 5060–5069. https://doi.org/10.1093/emboj/20.18.5060.

(15) Monné, M.; Vozza, A.; Lasorsa, F. M.; Porcelli, V.; Palmieri, F. Mitochondrial Carriers for Aspartate, Glutamate and Other Amino Acids: A Review. *Int. J. Mol. Sci.* **2019**, *20* (18), 4456. https://doi.org/10.3390/ijms20184456.

(16) Vozza, A.; Parisi, G.; De Leonardis, F.; Lasorsa, F. M.; Castegna, A.; Amorese, D.; Marmo, R.; Calcagnile, V. M.; Palmieri, L.; Ricquier, D.; Paradies, E.; Scarcia, P.;

Palmieri, F.; Bouillaud, F.; Fiermonte, G. UCP2 Transports C4 Metabolites out of Mitochondria, Regulating Glucose and Glutamine Oxidation. *Proc. Natl. Acad. Sci.* **2014**, *111* (3), 960–965. https://doi.org/10.1073/pnas.1317400111.

(17) Fiermonte, G.; Palmieri, L.; Todisco, S.; Agrimi, G.; Palmieri, F.; Walker, J. E. Identification of the Mitochondrial Glutamate Transporter: BACTERIAL EXPRESSION, RECONSTITUTION, FUNCTIONAL CHARACTERIZATION, AND TISSUE DISTRIBUTION OF TWO HUMAN ISOFORMS*. *J. Biol. Chem.* **2002**, *277* (22), 19289–19294. https://doi.org/10.1074/jbc.M201572200.

(18) Casimir, M.; Lasorsa, F. M.; Rubi, B.; Caille, D.; Palmieri, F.; Meda, P.; Maechler, P. Mitochondrial Glutamate Carrier GC1 as a Newly Identified Player in the Control of Glucose-Stimulated Insulin Secretion*. *J. Biol. Chem.* **2009**, *284* (37), 25004–25014. https://doi.org/10.1074/jbc.M109.015495.

(19) Indiveri, C.; Tonazzi, A.; Palmieri, F. Identification and Purification of the Ornithine/Citrulline Carrier from Rat Liver Mitochondira. *Eur. J. Biochem.* **1992**, *207* (2), 449–454. https://doi.org/10.1111/j.1432-1033.1992.tb17070.x.

(20) Fiermonte, G.; Dolce, V.; David, L.; Santorelli, F. M.; Dionisi-Vici, C.; Palmieri, F.; Walker, J. E. The Mitochondrial Ornithine Transporter: BACTERIAL EXPRESSION, RECONSTITUTION, FUNCTIONAL CHARACTERIZATION, AND TISSUE DISTRIBUTION OF TWO HUMAN ISOFORMS*. *J. Biol. Chem.* **2003**, *278* (35), 32778–32783. https://doi.org/10.1074/jbc.M302317200.

(21) Porcelli, V.; Fiermonte, G.; Longo, A.; Palmieri, F. The Human Gene SLC25A29, of Solute Carrier Family 25, Encodes a Mitochondrial Transporter of Basic Amino Acids. *J. Biol. Chem.* **2014**, *289* (19), 13374–13384. https://doi.org/10.1074/jbc.M114.547448.

(22) Blemings, K. P.; Crenshaw, T. D.; Swick, R. W.; Benevenga, N. J. Lysine-α-Ketoglutarate Reductase and Saccharopine Dehydrogenase Are Located Only in the Mitochondrial Matrix in Rat Liver1. *J. Nutr.* **1994**, *124* (8), 1215–1221. https://doi.org/10.1093/jn/124.8.1215.

(23) Lunetti, P.; Damiano, F.; De Benedetto, G.; Siculella, L.; Pennetta, A.; Muto, L.; Paradies, E.; Marobbio, C. M. T.; Dolce, V.; Capobianco, L. Characterization of Human and Yeast Mitochondrial Glycine Carriers with Implications for Heme Biosynthesis and Anemia. *J. Biol. Chem.* **2016**, *291* (38), 19746–19759. https://doi.org/10.1074/jbc.M116.736876.

(24) Guernsey, D. L.; Jiang, H.; Campagna, D. R.; Evans, S. C.; Ferguson, M.; Kellogg, M. D.; Lachance, M.; Matsuoka, M.; Nightingale, M.; Rideout, A.; Saint-Amant, L.; Schmidt, P. J.; Orr, A.; Bottomley, S. S.; Fleming, M. D.; Ludman, M.; Dyack, S.; Fernandez, C. V.; Samuels, M. E. Mutations in Mitochondrial Carrier Family Gene SLC25A38 Cause Nonsyndromic Autosomal Recessive Congenital Sideroblastic Anemia. *Nat. Genet.* **2009**, *41* (6), 651–653. https://doi.org/10.1038/ng.359.

(25) Yoneshiro, T.; Wang, Q.; Tajima, K.; Matsushita, M.; Maki, H.; Igarashi, K.; Dai, Z.; White, P. J.; McGarrah, R. W.; Ilkayeva, O. R.; Deleye, Y.; Oguri, Y.; Kuroda, M.; Ikeda, K.; Li, H.; Ueno, A.; Ohishi, M.; Ishikawa, T.; Kim, K.; Chen, Y.; Sponton, C. H.; Pradhan, R. N.; Majd, H.; Greiner, V. J.; Yoneshiro, M.; Brown, Z.; Chondronikola, M.; Takahashi, H.; Goto, T.; Kawada, T.; Sidossis, L.; Szoka, F. C.; McManus, M. T.; Saito, M.; Soga, T.; Kajimura, S. BCAA Catabolism in Brown Fat Controls Energy Homeostasis through SLC25A44. *Nature* **2019**, *572* (7771), 614–619. https://doi.org/10.1038/s41586-019-1503-x.

(26) Yoneshiro, T.; Kataoka, N.; Walejko, J. M.; Ikeda, K.; Brown, Z.; Yoneshiro, M.; Crown, S. B.; Osawa, T.; Sakai, J.; McGarrah, R. W.; White, P. J.; Nakamura, K.; Kajimura, S. Metabolic Flexibility via Mitochondrial BCAA Carrier SLC25A44 Is Required for Optimal Fever. *eLife* **2021**, *10*, e66865. https://doi.org/10.7554/eLife.66865.

(27) Pan, S.; Fan, M.; Liu, Z.; Li, X.; Wang, H. Serine, Glycine and One-Carbon Metabolism in Cancer (Review). *Int. J. Oncol.* **2020**, *58* (2), 158–170. https://doi.org/10.3892/ijo.2020.5158.

(28) Yoo, H. C.; Park, S. J.; Nam, M.; Kang, J.; Kim, K.; Yeo, J. H.; Kim, J.-K.; Heo, Y.; Lee, H. S.; Lee, M. Y.; Lee, C. W.; Kang, J. S.; Kim, Y.-H.; Lee, J.; Choi, J.; Hwang, G.-S.; Bang, S.; Han, J. M. A Variant of SLC1A5 Is a Mitochondrial Glutamine Transporter for Metabolic Reprogramming in Cancer Cells. *Cell Metab.* **2020**, *31* (2), 267-283.e12. https://doi.org/10.1016/j.cmet.2019.11.020.

(29) Papalazarou, V.; Newman, A. C.; Huerta-Uribe, A.; Legrave, N. M.; Falcone, M.; Zhang, T.; McGarry, L.; Athineos, D.; Shanks, E.; Blyth, K.; Vousden, K. H.; Maddocks, O. D. K. Phenotypic Profiling of Solute Carriers Characterizes Serine Transport in Cancer. *Nat. Metab.* **2023**, *5* (12), 2148–2168. https://doi.org/10.1038/s42255-023-00936-2.

(30) Pious, D. A.; Hawley, P. Effect of Antibiotics on Respiration in Human Cells. *Pediatr. Res.* **1972**, *6* (8), 687–692. https://doi.org/10.1203/00006450-197208000-00007.

(31) Kay, E. J.; Paterson, K.; Riera-Domingo, C.; Sumpton, D.; Däbritz, J. H. M.; Tardito, S.; Boldrini, C.; Hernandez-Fernaud, J. R.; Athineos, D.; Dhayade, S.; Stepanova, E.; Gjerga, E.; Neilson, L. J.; Lilla, S.; Hedley, A.; Koulouras, G.;

McGregor, G.; Jamieson, C.; Johnson, R. M.; Park, M.; Kirschner, K.; Miller, C.; Kamphorst, J. J.; Loayza-Puch, F.; Saez-Rodriguez, J.; Mazzone, M.; Blyth, K.; Zagnoni, M.; Zanivan, S. Cancer-Associated Fibroblasts Require Proline Synthesis by PYCR1 for the Deposition of pro-Tumorigenic Extracellular Matrix. *Nat. Metab.* **2022**, *4* (6), 693–710. https://doi.org/10.1038/s42255-022-00582-0.

(32) Crabtree, G. W.; Park, A. J.; Gordon, J. A.; Gogos, J. A. Cytosolic Accumulation of L-Proline Disrupts GABA-Ergic Transmission through GAD Blockade. *Cell Rep.* **2016**, *17* (2), 570–582. https://doi.org/10.1016/j.celrep.2016.09.029.

(33) Yao, Y.; Han, W. Proline Metabolism in Neurological and Psychiatric Disorders. *Mol. Cells* **2022**, *45* (11), 781–788. https://doi.org/10.14348/molcells.2022.0115.

(34) Andersen, J. V.; Schousboe, A. Milestone Review: Metabolic Dynamics of Glutamate and GABA Mediated Neurotransmission — The Essential Roles of Astrocytes. *J. Neurochem.* **2023**, *166* (2), 109–137. https://doi.org/10.1111/jnc.15811.

(35) Meyer, J. Proline Transport in Rat Liver Mitochondria. *Arch. Biochem. Biophys.* **1977**, *178* (2), 387–395. https://doi.org/10.1016/0003-9861(77)90208-9.

(36) Di Martino, C.; Pizzuto, R.; Pallotta, M. L.; De Santis, A.; Passarella, S. Mitochondrial Transport in Proline Catabolism in Plants: The Existence of Two Separate Translocators in Mitochondria Isolated from Durum Wheat Seedlings. *Planta* **2006**, *223* (6), 1123–1133. https://doi.org/10.1007/s00425-005-0166-z.

(37) Pallotta, M. L. L-Proline Uptake in Saccharomyces Cerevisiae Mitochondria Can Contribute to Bioenergetics during Nutrient Stress as Alternative Mitochondrial Fuel. *World J. Microbiol. Biotechnol.* **2014**, *30* (1), 19–31. https://doi.org/10.1007/s11274-013-1415-0.

(38) Atlante, A.; Passarella, S.; Pierro, P.; Quagliariello, E. Proline Transport in Rat Kidney Mitochondria. *Arch. Biochem. Biophys.* **1994**, *309* (1), 139–148. https://doi.org/10.1006/abbi.1994.1096.

(39) Chappell, J. B. SYSTEMS USED FOR THE TRANSPORT OF SUBSTRATES INTO MITOCHONDRIA. *Br. Med. Bull.* **1968**, *24* (2), 150–157. https://doi.org/10.1093/oxfordjournals.bmb.a070618.

(40) LaNoue, K. F.; Schoolwerth, A. C. Metabolite Transport in Mitochondria. *Annu. Rev. Biochem.* **1979**, *48* (1), 871–922. https://doi.org/10.1146/annurev.bi.48.070179.004255.

(41) Garlid, K. D.; Beavis, A. D. Swelling and Contraction of the Mitochondrial Matrix. II. Quantitative Application of the Light Scattering Technique to Solute Transport across the Inner Membrane. *J. Biol. Chem.* **1985**, *260* (25), 13434–13441. https://doi.org/10.1016/S0021-9258(17)38739-2.

(42) Beavis, A. D.; Brannan, R. D.; Garlid, K. D. Swelling and Contraction of the Mitochondrial Matrix. I. A Structural Interpretation of the Relationship between Light Scattering and Matrix Volume. *J. Biol. Chem.* **1985**, *260* (25), 13424–13433. https://doi.org/10.1016/S0021-9258(17)38738-0.

(43) Sanjana, N. E.; Shalem, O.; Zhang, F. Improved Vectors and Genome-Wide Libraries for CRISPR Screening. *Nat. Methods* **2014**, *11* (8), 783–784. https://doi.org/10.1038/nmeth.3047.

(44) Halling, P. J.; Brand, M. D.; Chappell, J. B. Permeability of Mitochondria to Neutral Amino Acids. *FEBS Lett.* **1973**, *34* (2), 169–171. https://doi.org/10.1016/0014-5793(73)80785-9.

(45) Ingeniis, J. D.; Ratnikov, B.; Richardson, A. D.; Scott, D. A.; Aza-Blanc, P.; De, S. K.; Kazanov, M.; Pellecchia, M.; Ronai, Z.; Osterman, A. L.; Smith, J. W. Functional Specialization in Proline Biosynthesis of Melanoma. *PLOS ONE* **2012**, *7* (9), e45190. https://doi.org/10.1371/journal.pone.0045190.

(46) Westbrook, R. L.; Bridges, E.; Roberts, J.; Escribano-Gonzalez, C.; Eales, K. L.; Vettore, L. A.; Walker, P. D.; Vera-Siguenza, E.; Rana, H.; Cuozzo, F.; Eskla, K.-L.; Vellama, H.; Shaaban, A.; Nixon, C.; Luuk, H.; Lavery, G. G.; Hodson, D. J.; Harris, A. L.; Tennant, D. A. Proline Synthesis through PYCR1 Is Required to Support Cancer Cell Proliferation and Survival in Oxygen-Limiting Conditions. *Cell Rep.* **2022**, *38* (5), 110320. https://doi.org/10.1016/j.celrep.2022.110320.

(47) Acoba, M. G.; Alpergin, E. S. S.; Renuse, S.; Fernández-del-Río, L.; Lu, Y.-W.; Khalimonchuk, O.; Clarke, C. F.; Pandey, A.; Wolfgang, M. J.; Claypool, S. M. The Mitochondrial Carrier SFXN1 Is Critical for Complex III Integrity and Cellular Metabolism. *Cell Rep.* **2021**, *34* (11), 108869. https://doi.org/10.1016/j.celrep.2021.108869.

(48) Jackson, T. D.; Crameri, J. J.; Muellner-Wong, L.; Frazier, A. E.; Palmer, C. S.; Formosa, L. E.; Hock, D. H.; Fujihara, K. M.; Stait, T.; Sharpe, A. J.; Thorburn, D. R.; Ryan, M. T.; Stroud, D. A.; Stojanovski, D. Sideroflexin 4 Is a Complex I Assembly Factor That Interacts with the MCIA Complex and Is Required for the Assembly of the ND2 Module. *Proc. Natl. Acad. Sci.* **2022**, *119* (13), e2115566119. https://doi.org/10.1073/pnas.2115566119.

(49) Curthoys, N. P.; Watford, M. Regulation of Glutaminase Activity and Glutamine Metabolism. *Annu. Rev. Nutr.* **1995**, *15*, 133–159. https://doi.org/10.1146/annurev.nu.15.070195.001025.

(50) Watford, M. Glutamine Metabolism and Function in Relation to Proline Synthesis and the Safety of Glutamine and Proline Supplementation123. *J. Nutr.* **2008**, *138* (10), 2003S-2007S. https://doi.org/10.1093/jn/138.10.2003S.

(51) Chen, W. W.; Freinkman, E.; Wang, T.; Birsoy, K.; Sabatini, D. M. Absolute Quantification of Matrix Metabolites Reveals the Dynamics of Mitochondrial Metabolism. *Cell* **2016**, *166* (5), 1324-1337.e11. https://doi.org/10.1016/j.cell.2016.07.040.

(52) Soula, M.; Weber, R. A.; Zilka, O.; Alwaseem, H.; La, K.; Yen, F.; Molina, H.; Garcia-Bermudez, J.; Pratt, D. A.; Birsoy, K. Metabolic Determinants of Cancer Cell Sensitivity to Canonical Ferroptosis Inducers. *Nat. Chem. Biol.* **2020**, *16* (12), 1351–1360. https://doi.org/10.1038/s41589-020-0613-y.

(53) Lewis, C. A.; Parker, S. J.; Fiske, B. P.; McCloskey, D.; Gui, D. Y.; Green, C. R.; Vokes, N. I.; Feist, A. M.; Vander Heiden, M. G.; Metallo, C. M. Tracing Compartmentalized NADPH Metabolism in the Cytosol and Mitochondria of Mammalian Cells. *Mol. Cell* **2014**, *55* (2), 253–263. https://doi.org/10.1016/j.molcel.2014.05.008.

(54) Stoner, G. D.; Merchant, D. J. Amino Acid Utilization by L-M Strain Mouse Cells in a Chemically Defined Medium. *In Vitro* **1972**, *7* (6), 330–343. https://doi.org/10.1007/BF02618888.

(55) Newman, A. C.; Maddocks, O. D. K. One-Carbon Metabolism in Cancer. *Br. J. Cancer* **2017**, *116* (12), 1499–1504. https://doi.org/10.1038/bjc.2017.118.

(56) García-Cañaveras, J. C.; Lancho, O.; Ducker, G. S.; Ghergurovich, J. M.; Xu, X.; da Silva-Diz, V.; Minuzzo, S.; Indraccolo, S.; Kim, H.; Herranz, D.; Rabinowitz, J. D. SHMT Inhibition Is Effective and Synergizes with Methotrexate in T-Cell Acute

Lymphoblastic Leukemia. *Leukemia* **2021**, *35* (2), 377–388. https://doi.org/10.1038/s41375-020-0845-6.

(57) Kandasamy, P.; Gyimesi, G.; Kanai, Y.; Hediger, M. A. Amino Acid Transporters Revisited: New Views in Health and Disease. *Trends Biochem. Sci.* **2018**, *43* (10), 752–789. https://doi.org/10.1016/j.tibs.2018.05.003.

(58) Bröer, S.; Gether, U. The Solute Carrier 6 Family of Transporters. *Br. J. Pharmacol.* **2012**, *167* (2), 256–278. https://doi.org/10.1111/j.1476-5381.2012.01975.x.

(59) Sims, K. L.; Davis, G. A.; Bloom, F. E. Activities of 3,4-Dihydroxy-L-Phenylalanine and 5-Hydroxy-L-Tryptophan Decarboxylases in Rat Brain: Assay Characteristics and Distribution. *J. Neurochem.* **1973**, *20* (2), 449–464. https://doi.org/10.1111/j.1471-4159.1973.tb12144.x.

(60) Schnaitman, C.; Erwin, V. G.; Greenawalt, J. W. The Submitochondrial Localization of Monoamine Oxidase. An Enzymatic Marker for the Outer Membrane of Rat Liver Mitochondria. *J. Cell Biol.* **1967**, *32* (3), 719–735. https://doi.org/10.1083/jcb.32.3.719.

(61) Schousboe, I.; Bro, B.; Schousboe, A. Intramitochondrial Localization of the 4-Aminobutyrate-2-Oxoglutarate Transaminase from Ox Brain. *Biochem. J.* **1977**, *162* (2), 303–307.

(62) Passarella, S.; Atlante, A.; Barile, M.; Quagliariello, E. Carrier Mediated GABA Translocation into Rat Brain Mitochondria. *Biochem. Biophys. Res. Commun.* **1984**, *121* (3), 770–778. https://doi.org/10.1016/0006-291X(84)90745-9.

(63) Benavides, J.; Garcia, M. L.; Lopez-Lahoya, J.; Ugarte, M.; Valdivieso, F. Glycine Transport in Rat Brain and Liver Mitochondria. *Biochim. Biophys. Acta BBA -*

Biomembr. **1980**, *598* (3), 588–594. https://doi.org/10.1016/0005-2736(80)90038-3.

(64) Brand, M. D.; Chappell, J. B. Permeability of Mitochondria from Rat Brain and Rat Liver to Gaba. *J. Neurochem.* **1974**, *22* (1), 47–51. https://doi.org/10.1111/j.1471-4159.1974.tb12177.x.

(65) Cybulski, R. L.; Fisher, R. R. Mitochondrial Neutral Amino Acid Transport: Evidence for a Carrier Mediated Mechanism. *Biochemistry* **1977**, *16* (23), 5116–5120. https://doi.org/10.1021/bi00642a026.

(66) Bouché, N.; Lacombe, B.; Fromm, H. GABA Signaling: A Conserved and Ubiquitous Mechanism. *Trends Cell Biol.* **2003**, *13* (12), 607–610. https://doi.org/10.1016/j.tcb.2003.10.001.

(67) Jung, M. J.; Lippert, B.; Metcalf, B. W.; Böhlen, P.; Schechter, P. J. Gamma-Vinyl GABA (4-Amino-Hex-5-Enoic Acid), a New Selective Irreversible Inhibitor of GABA-T: Effects on Brain GABA Metabolism in Mice. *J. Neurochem.* **1977**, *29* (5), 797–802. https://doi.org/10.1111/j.1471-4159.1977.tb10721.x.

(68) Pena, I. A.; Shi, J. S.; Chang, S. M.; Yang, J.; Block, S.; Adelmann, C. H.; Keys, H. R.; Ge, P.; Bathla, S.; Withan, I.; Sienski, G.; Nairn, A.; Sabatini, D. M.; Lewis, C. A.; Kory, N.; Vander Heiden, M. G.; Heiman, M. SLC25A38 Is Required for Mitochondrial Pyridoxal 5'-Phosphate (PLP) Accumulation. *[Manuscript under revision]*

(69) Darnell, A. M.; Subramaniam, A. R.; O'Shea, E. K. Translational Control through Differential Ribosome Pausing during Amino Acid Limitation in Mammalian Cells. *Mol. Cell* **2018**, *71* (2), 229-243.e11. https://doi.org/10.1016/j.molcel.2018.06.041.

(70) Luengo, A.; Li, Z.; Gui, D. Y.; Sullivan, L. B.; Zagorulya, M.; Do, B. T.; Ferreira, R.; Naamati, A.; Ali, A.; Lewis, C. A.; Thomas, C. J.; Spranger, S.; Matheson, N. J.; Vander Heiden, M. G. Increased Demand for NAD+ Relative to ATP Drives Aerobic Glycolysis. *Mol. Cell* **2021**, *81* (4), 691-707.e6. https://doi.org/10.1016/j.molcel.2020.12.012.

(71) Chen, W. W.; Freinkman, E.; Sabatini, D. M. Rapid Immunopurification of Mitochondria for Metabolite Profiling and Absolute Quantification of Matrix Metabolites. *Nat. Protoc.* **2017**, *12* (10), 2215–2231. https://doi.org/10.1038/nprot.2017.104.

(72) Pang, Z.; Lu, Y.; Zhou, G.; Hui, F.; Xu, L.; Viau, C.; Spigelman, A. F.; MacDonald, P. E.; Wishart, D. S.; Li, S.; Xia, J. MetaboAnalyst 6.0: Towards a Unified Platform for Metabolomics Data Processing, Analysis and Interpretation. *Nucleic Acids Res.* **2024**, *52* (W1), W398–W406. https://doi.org/10.1093/nar/gkae253.

(73) Chidley, C.; Darnell, A. M.; Gaudio, B. L.; Lien, E. C.; Barbeau, A. M.; Vander Heiden, M. G.; Sorger, P. K. A CRISPRi/a Screening Platform to Study Cellular Nutrient Transport in Diverse Microenvironments. *Nat. Cell Biol.* **2024**, *26* (5), 825–838. https://doi.org/10.1038/s41556-024-01402-1.

(74) Sullivan, M. R.; Danai, L. V.; Lewis, C. A.; Chan, S. H.; Gui, D. Y.; Kunchok, T.; Dennstedt, E. A.; Vander Heiden, M. G.; Muir, A. Quantification of Microenvironmental Metabolites in Murine Cancers Reveals Determinants of Tumor Nutrient Availability. *eLife* **2019**, *8*, e44235. https://doi.org/10.7554/eLife.44235.

(75) Navarrete-Perea, J.; Yu, Q.; Gygi, S. P.; Paulo, J. A. Streamlined Tandem Mass Tag (SL-TMT) Protocol: An Efficient Strategy for Quantitative (Phospho)Proteome

Profiling Using Tandem Mass Tag-Synchronous Precursor Selection-MS3. *J. Proteome Res.* **2018**, *17* (6), 2226–2236. https://doi.org/10.1021/acs.jproteome.8b00217.

(76) Li, J.; Cai, Z.; Bomgarden, R. D.; Pike, I.; Kuhn, K.; Rogers, J. C.; Roberts, T. M.; Gygi, S. P.; Paulo, J. A. TMTpro-18plex: The Expanded and Complete Set of TMTpro Reagents for Sample Multiplexing. *J. Proteome Res.* **2021**, *20* (5), 2964–2972. https://doi.org/10.1021/acs.jproteome.1c00168.

(77) Hughes, C. S.; Moggridge, S.; Müller, T.; Sorensen, P. H.; Morin, G. B.; Krijgsveld, J. Single-Pot, Solid-Phase-Enhanced Sample Preparation for Proteomics Experiments. *Nat. Protoc.* **2019**, *14* (1), 68–85. https://doi.org/10.1038/s41596-018-0082-x.

(78) Schweppe, D. K.; Eng, J. K.; Yu, Q.; Bailey, D.; Rad, R.; Navarrete-Perea, J.; Huttlin, E. L.; Erickson, B. K.; Paulo, J. A.; Gygi, S. P. Full-Featured, Real-Time Database Searching Platform Enables Fast and Accurate Multiplexed Quantitative Proteomics. *J. Proteome Res.* **2020**, *19* (5), 2026–2034. https://doi.org/10.1021/acs.jproteome.9b00860.

(79) Rad, R.; Li, J.; Mintseris, J.; O'Connell, J.; Gygi, S. P.; Schweppe, D. K. Improved Monoisotopic Mass Estimation for Deeper Proteome Coverage. *J. Proteome Res.* **2021**, *20* (1), 591–598. https://doi.org/10.1021/acs.jproteome.0c00563.

(80) Wu, S.-H. S.; Lee, H.; Szép-Bakonyi, R.; Colozza, G.; Boese, A.; Gert, K. R.; Hallay, N.; Lee, J.-H.; Kim, J.; Zhu, Y.; Linssen, M. M.; Pilat-Carotta, S.; Hohenstein, P.; Theussl, H.-C.; Pauli, A.; Koo, B.-K. SCON—a Short Conditional intrON for Conditional Knockout with One-Step Zygote Injection. *Exp. Mol. Med.* **2022**, *54* (12), 2188–2199. https://doi.org/10.1038/s12276-022-00891-0.

(81) Mana, M. D.; Hussey, A. M.; Tzouanas, C. N.; Imada, S.; Millan, Y. B.; Bahceci, D.; Saiz, D. R.; Webb, A. T.; Lewis, C. A.; Carmeliet, P.; Mihaylova, M. M.; Shalek, A. K.; Yilmaz, Ö. H. High-Fat Diet-Activated Fatty Acid Oxidation Mediates Intestinal Stemness and Tumorigenicity. *Cell Rep.* **2021**, *35* (10). https://doi.org/10.1016/j.celrep.2021.109212.

(82) Crowley, L. C.; Christensen, M. E.; Waterhouse, N. J. Measuring Mitochondrial Transmembrane Potential by TMRE Staining. *Cold Spring Harb. Protoc.* **2016**, *2016* (12), pdb.prot087361. https://doi.org/10.1101/pdb.prot087361.

(83) Adelmann, C. H.; Wang, T.; Sabatini, D. M.; Lander, E. S. Genome-Wide CRISPR/Cas9 Screening for Identification of Cancer Genes in Cell Lines. In *Cancer Driver Genes*; Starr, T. K., Ed.; Methods in Molecular Biology; Springer New York: New York, NY, 2019; Vol. 1907, pp 125–136. https://doi.org/10.1007/978-1-4939-8967-6_10.

(84) Wang, B.; Wang, M.; Zhang, W.; Xiao, T.; Chen, C.-H.; Wu, A.; Wu, F.; Traugh, N.; Wang, X.; Li, Z.; Mei, S.; Cui, Y.; Shi, S.; Lipp, J. J.; Hinterndorfer, M.; Zuber, J.; Brown, M.; Li, W.; Liu, X. S. Integrative Analysis of Pooled CRISPR Genetic Screens Using MAGeCKFlute. *Nat. Protoc.* **2019**, *14* (3), 756–780. https://doi.org/10.1038/s41596-018-0113-7.

Chapter 3: New insights and future directions

Authors: Samuel Block[1,2], Matthew G. Vander Heiden[1,2,3]

Author Affiliation:

[1]Koch Institute for Integrative Cancer Research, Massachusetts Institute of Technology, Cambridge, MA 02139, USA
[2]Department of Biology, Massachusetts Institute of Technology, Cambridge, MA 02139, USA
[3]Dana-Farber Cancer Institute, Boston, MA 02115, USA

Discussion

A variety of enzymatic reactions are compartmentalized in mitochondria in eukaryotes. Consequently, metabolites must be transported across the inner mitochondrial membrane to coordinate metabolism in the mitochondria with reactions in the cytosol. Despite data generated nearly 50 years ago suggesting the existence of a mitochondrial carrier with broad specificity for polar neutral amino acids[1,2], no such carrier has been reported in humans. Using mitochondrial swelling and metabolic profiling, we identify the sideroflexins as enablers of mitochondrial transport of several polar neutral amino acids, including proline, glycine, serine, threonine, beta-alanine, hypotaurine, taurine, and GABA. While our data suggest that sideroflexins are required for these amino acids to efficiently cross the mitochondrial inner membrane, we do not provide evidence that they are direct carriers, although this has been reported for serine[3]. Reconstitution of sideroflexins into proteoliposomes is needed to determine if these proteins are bona fide transporters for these substrates; however, it is unlikely that SFXN1 is acting as a chaperone for another carrier since levels of mitochondrial transporters were unaffected by loss of SFXN1. Interestingly, SFXN4, which has a reported role as a chaperone for complex I mitochondrial proteins[4], did not rescue any transport defect induced by loss of SFXN1, consistent with its evolutionary divergence from the other sideroflexins[3].

We found that loss of SFXN1 reduces mitochondrial proline permeability and inhibits proline synthesis in multiple systems. Interestingly, we also found that loss of mitochondrial proline synthesis did not reduce cell growth in the absence of exogenous proline, indicating that proliferation-based screens would be ineffective at revealing

mitochondrial proline transporters. Mitochondrial proline synthesis has been shown to support cancer cell proliferation by acting as an alternative electron acceptor[5], and also supports collagen synthesis[6] and desmoplasia from cancer-associated fibroblasts[7], which can limit delivery of therapeutics[8]. In addition, some cancers may be sensitive to dietary proline restriction[9]. Upregulation of SFXN1 has been found in breast[10] and lung[11] cancer, and this is associated with poor prognosis[11,12]. These findings may be due, in part, to SFXN1s role in proline synthesis, although a role in other mitochondrial metabolic pathways might also contribute to this phenotype. For instance, loss of SFXN1 also inhibits mitochondrial transport of both serine and glycine, which impairs one-carbon metabolism and nucleotide synthesis[3]. Furthermore, we have demonstrated that loss of SFXN1 lowers mitochondrial GABA permeability and inhibits GABA catabolism, and Low GABA levels are also predictive of poor prognosis in breast cancer[13], while the growth of cells isolated from breast cancer-brain metastases are sensitive to Vigabatrin[14].

Loss of SFXN1 predicts a poor outcome in hepatocellular carcinoma and inhibits toxicity induced by a high-fat diet[15]. This may be due to an inhibitory effect on reactive oxygen species generation[15], since loss of SFXN1 also protects cells from ferroptosis inducers leading to mitochondrial accumulation of taurine and hypotaurine[16], which could prevent ferroptosis by acting as antioxidants[16–19]. Interestingly, apoptosis due to ROS generation by complex I in taurine deficient mice can be rescued with mitotempo[20], a mitochondrial specific antioxidant. Our data suggest that hypotaurine and taurine might accumulate in SFXN1 knockout mitochondria due to decreased export, providing a potential mechanistic link between SFXN1 loss and ferroptosis resistance, which like

apoptosis can be inhibited by mitochondrial ROS quenching[21]. However, evidence of human mitochondrial taurine or hypotaurine synthesis is lacking, although mitochondria isolated from rat liver have demonstrated L-cysteinesuflinate decarboxylase activity[22]. Since this produces hypotaurine which can undergo hydrogen peroxide mediated oxidation to taurine[23], its possible mitochondria are capable of synthesizing these metabolites.

We found that loss of SFXN1 inhibited M+2 glycine media secretion from cells cultured in $^{13}C_3$-L-serine, in line with previous studies[3]. However, we also found that loss of SFXN1 inhibited mitochondrial glycine permeability, which could be rescued by SFXN2 and SFXN3, indicating these proteins regulate mitochondrial glycine transport. Since SFXN1 was reported as synthetic lethal with loss of cytosolic SHMT1 in media lacking serine[3], it's possible this phenotype arose from reductions in both mitochondrial serine export and glycine import, since both processes are needed for providing cytosolic serine through mitochondrial SHMT2. Furthermore, loss of function mutations in SFXN1 result in anemia[24], likely due to impaired heme biosynthesis[25,26]. Since mitochondrial glycine is required for heme biosynthesis through ALAS[27], our data indicate that these mutations likely impair heme synthesis due to impaired mitochondrial glycine or serine availability.

Only one mitochondrial GABA transporter has been characterized in plants[28], and while a mutation in aralar was identified that led to an increase in the cytoplasmic/mitochondrial GABA ratio in flies[29], there was no evidence that mitochondrial GABA transport was altered. Our study shows that loss of SFXN1 results

in a mitochondrial GABA transport defect that impairs GABA degradation, which can be rescued by SFXN5, and partially by SFXN2. SFXN2 is expressed predominantly in the kidney, while SFXN1 and SFXN5 are expressed throughout the brain[3]. Interestingly, SFXN5 expression is largely restricted to astrocytes[30,31]. Since astrocytes regulate synaptic GABA levels through mitochondrial recycling[32], drugs targeting SFXN5 could be effective in the treatment of disorders associated with dysregulated GABAergic transmission, such as epilepsy which is currently treated with the plasma membrane GABA transporter 1 (GAT1) inhibitor Tigabine[33] and the ABAT inhibitor Vigabatrin[34], although neurons may also contribute to GABA recycling[32].

Lower levels of SFXN1 were found in the brains of Alzheimer's patients[35] as well as rats that had undergone ovariectamy[36], and a P-element insertion in the fly sideroflexin orthologue enhanced Tau-mediated toxicity[35]. Since Alzheimer's and ovariectomy are associated with dysregulated GABAergic neurotransmission[37,38], decreased SFXN1 could contribute to this by disrupting GABA-level homeostasis. However, SFXN1 could influence these conditions through regulation of other amino acids. Glycine and beta-alanine are also neurotransmitters, and taurine, proline, and serine have known neuromodulating properties[39]. Since these amino acids are found throughout the body, including GABA[40], future studies are needed to determine how mitochondrial metabolism influences the levels of these amino acids in different tissues and to what extent the sideroflexins are involved.

References

(1) Meyer, J. Proline Transport in Rat Liver Mitochondria. *Arch. Biochem. Biophys.* **1977**, *178* (2), 387–395. https://doi.org/10.1016/0003-9861(77)90208-9.

(2) Cybulski, R. L.; Fisher, R. R. Mitochondrial Neutral Amino Acid Transport: Evidence for a Carrier Mediated Mechanism. *Biochemistry* **1977**, *16* (23), 5116–5120. https://doi.org/10.1021/bi00642a026.

(3) Kory, N.; Wyant, G. A.; Prakash, G.; uit de Bos, J.; Bottanelli, F.; Pacold, M. E.; Chan, S. H.; Lewis, C. A.; Wang, T.; Keys, H. R.; Guo, Y. E.; Sabatini, D. M. SFXN1 Is a Mitochondrial Serine Transporter Required for One-Carbon Metabolism. *Science* **2018**, *362* (6416), eaat9528. https://doi.org/10.1126/science.aat9528.

(4) Jackson, T. D.; Crameri, J. J.; Muellner-Wong, L.; Frazier, A. E.; Palmer, C. S.; Formosa, L. E.; Hock, D. H.; Fujihara, K. M.; Stait, T.; Sharpe, A. J.; Thorburn, D. R.; Ryan, M. T.; Stroud, D. A.; Stojanovski, D. Sideroflexin 4 Is a Complex I Assembly Factor That Interacts with the MCIA Complex and Is Required for the Assembly of the ND2 Module. *Proc. Natl. Acad. Sci.* **2022**, *119* (13), e2115566119. https://doi.org/10.1073/pnas.2115566119.

(5) Westbrook, R. L.; Bridges, E.; Roberts, J.; Escribano-Gonzalez, C.; Eales, K. L.; Vettore, L. A.; Walker, P. D.; Vera-Siguenza, E.; Rana, H.; Cuozzo, F.; Eskla, K.-L.; Vellama, H.; Shaaban, A.; Nixon, C.; Luuk, H.; Lavery, G. G.; Hodson, D. J.; Harris, A. L.; Tennant, D. A. Proline Synthesis through PYCR1 Is Required to Support Cancer Cell Proliferation and Survival in Oxygen-Limiting Conditions. *Cell Rep.* **2022**, *38* (5), 110320. https://doi.org/10.1016/j.celrep.2022.110320.

(6) Schwörer, S.; Berisa, M.; Violante, S.; Qin, W.; Zhu, J.; Hendrickson, R. C.; Cross, J. R.; Thompson, C. B. Proline Biosynthesis Is a Vent for TGFβ-Induced Mitochondrial Redox Stress. *EMBO J.* **2020**, *39* (8), e103334. https://doi.org/10.15252/embj.2019103334.

(7) Kay, E. J.; Paterson, K.; Riera-Domingo, C.; Sumpton, D.; Däbritz, J. H. M.; Tardito, S.; Boldrini, C.; Hernandez-Fernaud, J. R.; Athineos, D.; Dhayade, S.; Stepanova, E.; Gjerga, E.; Neilson, L. J.; Lilla, S.; Hedley, A.; Koulouras, G.; McGregor, G.; Jamieson, C.; Johnson, R. M.; Park, M.; Kirschner, K.; Miller, C.; Kamphorst, J. J.; Loayza-Puch, F.; Saez-Rodriguez, J.; Mazzone, M.; Blyth, K.; Zagnoni, M.; Zanivan, S. Cancer-Associated Fibroblasts Require Proline Synthesis by PYCR1 for the Deposition of pro-Tumorigenic Extracellular Matrix. *Nat. Metab.* **2022**, *4* (6), 693–710. https://doi.org/10.1038/s42255-022-00582-0.

(8) Ebelt, N. D.; Zamloot, V.; Manuel, E. R. Targeting Desmoplasia in Pancreatic Cancer as an Essential First Step to Effective Therapy. *Oncotarget* **2020**, *11* (38), 3486–3488. https://doi.org/10.18632/oncotarget.27745.

(9) Sahu, N.; Dela Cruz, D.; Gao, M.; Sandoval, W.; Haverty, P. M.; Liu, J.; Stephan, J.-P.; Haley, B.; Classon, M.; Hatzivassiliou, G.; Settleman, J. Proline Starvation Induces Unresolved ER Stress and Hinders mTORC1-Dependent Tumorigenesis. *Cell Metab.* **2016**, *24* (5), 753–761. https://doi.org/10.1016/j.cmet.2016.08.008.

(10) Andriani, L.; Ling, Y.-X.; Yang, S.-Y.; Zhao, Q.; Ma, X.-Y.; Huang, M.-Y.; Zhang, Y.-L.; Zhang, F.-L.; Li, D.-Q.; Shao, Z.-M. Sideroflexin-1 Promotes Progression and Sensitivity to Lapatinib in Triple-Negative Breast Cancer by Inhibiting TOLLIP-Mediated Autophagic Degradation of CIP2A. *Cancer Lett.* **2024**, *597*, 217008. https://doi.org/10.1016/j.canlet.2024.217008.

(11) Chen, L.; Kang, Y.; Jiang, Y.; You, J.; Huang, C.; Xu, X.; Chen, F. Overexpression of SFXN1 Indicates Poor Prognosis and Promotes Tumor Progression in Lung Adenocarcinoma. *Pathol. Res. Pract.* **2022**, *237*, 154031. https://doi.org/10.1016/j.prp.2022.154031.

(12) Yuan, D.; Liu, J.; Sang, W.; Li, Q. Comprehensive Analysis of the Role of SFXN Family in Breast Cancer. *Open Med. Wars. Pol.* **2023**, *18* (1), 20230685. https://doi.org/10.1515/med-2023-0685.

(13) Brzozowska, A.; Burdan, F.; Duma, D.; Solski, J.; Mazurkiewicz, M. γ-Amino Butyric Acid (GABA) Level as an Overall Survival Risk Factor in Breast Cancer. *Ann. Agric. Environ. Med. AAEM* **2017**, *24* (3), 435–439. https://doi.org/10.26444/aaem/75891.

(14) Neman, J.; Termini, J.; Wilczynski, S.; Vaidehi, N.; Choy, C.; Kowolik, C. M.; Li, H.; Hambrecht, A. C.; Roberts, E.; Jandial, R. Human Breast Cancer Metastases to the Brain Display GABAergic Properties in the Neural Niche. *Proc. Natl. Acad. Sci.* **2014**, *111* (3), 984–989. https://doi.org/10.1073/pnas.1322098111.

(15) Yagi, K.; Shimada, S.; Akiyama, Y.; Hatano, M.; Asano, D.; Ishikawa, Y.; Ueda, H.; Watanabe, S.; Akahoshi, K.; Ono, H.; Tanabe, M.; Tanaka, S. Loss of SFXN1 Mitigates Lipotoxicity and Predicts Poor Outcome in Non-Viral Hepatocellular Carcinoma. *Sci. Rep.* **2023**, *13* (1), 9449. https://doi.org/10.1038/s41598-023-36660-w.

(16) Soula, M.; Weber, R. A.; Zilka, O.; Alwaseem, H.; La, K.; Yen, F.; Molina, H.; Garcia-Bermudez, J.; Pratt, D. A.; Birsoy, K. Metabolic Determinants of Cancer Cell Sensitivity to Canonical Ferroptosis Inducers. *Nat. Chem. Biol.* **2020**, *16* (12), 1351–1360. https://doi.org/10.1038/s41589-020-0613-y.

(17) Aruoma, O. I.; Halliwell, B.; Hoey, B. M.; Butler, J. The Antioxidant Action of Taurine, Hypotaurine and Their Metabolic Precursors. *Biochem. J.* **1988**, *256* (1), 251–255. https://doi.org/10.1042/bj2560251.

(18) Xiao, H.; Du, X.; Tao, Z.; Jing, N.; Bao, S.; Gao, W.; Dong, B.; Fang, Y. Taurine Inhibits Ferroptosis Mediated by the Crosstalk between Tumor Cells and Tumor-Associated Macrophages in Prostate Cancer. *Adv. Sci.* **2023**, *11* (3), 2303894. https://doi.org/10.1002/advs.202303894.

(19) Tadolini, B.; Pintus, G.; Pinna, G. G.; Bennardini, F.; Franconi, F. Effects of Taurine and Hypotaurine on Lipid Peroxidation. *Biochem. Biophys. Res. Commun.* **1995**, *213* (3), 820–826. https://doi.org/10.1006/bbrc.1995.2203.

(20) Jong, C. J.; Ito, T.; Prentice, H.; Wu, J.-Y.; Schaffer, S. W. Role of Mitochondria and Endoplasmic Reticulum in Taurine-Deficiency-Mediated Apoptosis. *Nutrients* **2017**, *9* (8), 795. https://doi.org/10.3390/nu9080795.

(21) Oh, S.-J.; Ikeda, M.; Ide, T.; Hur, K. Y.; Lee, M.-S. Mitochondrial Event as an Ultimate Step in Ferroptosis. *Cell Death Discov.* **2022**, *8* (1), 1–13. https://doi.org/10.1038/s41420-022-01199-8.

(22) Ubuka, T.; Okada, A.; Nakamura, H. Production of Hypotaurine from L-Cysteinesulfinate by Rat Liver Mitochondria. *Amino Acids* **2008**, *35* (1), 53–58. https://doi.org/10.1007/s00726-007-0633-x.

(23) Grove, R. Q.; Karpowicz, S. J. Reaction of Hypotaurine or Taurine with Superoxide Produces the Organic Peroxysulfonic Acid Peroxytaurine. *Free Radic. Biol. Med.* **2017**, *108*, 575–584. https://doi.org/10.1016/j.freeradbiomed.2017.04.342.

(24) Fleming, M. D.; Campagna, D. R.; Haslett, J. N.; Trenor, C. C.; Andrews, N. C. A Mutation in a Mitochondrial Transmembrane Protein Is Responsible for the Pleiotropic Hematological and Skeletal Phenotype of Flexed-Tail (f/f) Mice. *Genes Dev.* **2001**, *15* (6), 652–657. https://doi.org/10.1101/gad.873001.

(25) Acoba, M. G.; Alpergin, E. S. S.; Renuse, S.; Fernández-del-Río, L.; Lu, Y.-W.; Khalimonchuk, O.; Clarke, C. F.; Pandey, A.; Wolfgang, M. J.; Claypool, S. M. The Mitochondrial Carrier SFXN1 Is Critical for Complex III Integrity and Cellular Metabolism. *Cell Rep.* **2021**, *34* (11), 108869. https://doi.org/10.1016/j.celrep.2021.108869.

(26) Bao, B.; An, W.; Lu, Q.; Wang, Y.; Lu, Z.; Tu, J.; Zhang, H.; Duan, Y.; Yuan, W.; Zhu, X.; Jia, H. Sfxn1 Is Essential for Erythrocyte Maturation via Facilitating Hemoglobin Production in Zebrafish. *Biochim. Biophys. Acta Mol. Basis Dis.* **2021**, *1867* (5), 166096. https://doi.org/10.1016/j.bbadis.2021.166096.

(27) Gibson, K. D.; Laver, W. G.; Neuberger, A. Initial Stages in the Biosynthesis of Porphyrins. 2. The Formation of δ-Aminolaevulic Acid from Glycine and Succinyl-Coenzyme A by Particles from Chicken Erythrocytes. *Biochem. J.* **1958**, *70* (1), 71–81.

(28) Michaeli, S.; Fait, A.; Lagor, K.; Nunes-Nesi, A.; Grillich, N.; Yellin, A.; Bar, D.; Khan, M.; Fernie, A. R.; Turano, F. J.; Fromm, H. A Mitochondrial GABA Permease Connects the GABA Shunt and the TCA Cycle, and Is Essential for Normal Carbon Metabolism. *Plant J.* **2011**, *67* (3), 485–498. https://doi.org/10.1111/j.1365-313X.2011.04612.x.

(29) Kanellopoulos, A. K.; Mariano, V.; Spinazzi, M.; Woo, Y. J.; McLean, C.; Pech, U.; Li, K. W.; Armstrong, J. D.; Giangrande, A.; Callaerts, P.; Smit, A. B.; Abrahams,

B. S.; Fiala, A.; Achsel, T.; Bagni, C. Aralar Sequesters GABA into Hyperactive Mitochondria, Causing Social Behavior Deficits. *Cell* **2020**, *180* (6), 1178-1197.e20. https://doi.org/10.1016/j.cell.2020.02.044.

(30) Fecher, C.; Trovò, L.; Müller, S. A.; Snaidero, N.; Wettmarshausen, J.; Heink, S.; Ortiz, O.; Wagner, I.; Kühn, R.; Hartmann, J.; Karl, R. M.; Konnerth, A.; Korn, T.; Wurst, W.; Merkler, D.; Lichtenthaler, S. F.; Perocchi, F.; Misgeld, T. Cell-Type-Specific Profiling of Brain Mitochondria Reveals Functional and Molecular Diversity. *Nat. Neurosci.* **2019**, *22* (10), 1731–1742. https://doi.org/10.1038/s41593-019-0479-z.

(31) Stokum, J. A.; Shim, B.; Huang, W.; Kane, M.; Smith, J. A.; Gerzanich, V.; Simard, J. M. A Large Portion of the Astrocyte Proteome Is Dedicated to Perivascular Endfeet, Including Critical Components of the Electron Transport Chain. *J. Cereb. Blood Flow Metab.* **2021**, *41* (10), 2546–2560. https://doi.org/10.1177/0271678X211004182.

(32) Andersen, J. V.; Schousboe, A. Milestone Review: Metabolic Dynamics of Glutamate and GABA Mediated Neurotransmission — The Essential Roles of Astrocytes. *J. Neurochem.* **2023**, *166* (2), 109–137. https://doi.org/10.1111/jnc.15811.

(33) Schousboe, A.; Wellendorph, P.; Frølund, B.; Clausen, R. P.; Krogsgaard-Larsen, P. Astrocytic GABA Transporters: Pharmacological Properties and Targets for Antiepileptic Drugs. *Adv. Neurobiol.* **2017**, *16*, 283–296. https://doi.org/10.1007/978-3-319-55769-4_14.

(34) Ben-Menachem, E. Mechanism of Action of Vigabatrin: Correcting Misperceptions. *Acta Neurol. Scand.* **2011**, *124* (s192), 5–15. https://doi.org/10.1111/j.1600-0404.2011.01596.x.

(35) Minjarez, B.; Calderón-González, K. G.; Rustarazo, Ma. L. V.; Herrera-Aguirre, M. E.; Labra-Barrios, M. L.; Rincon-Limas, D. E.; del Pino, M. M. S.; Mena, R.; Luna-Arias, J. P. Identification of Proteins That Are Differentially Expressed in Brains with Alzheimer's Disease Using iTRAQ Labeling and Tandem Mass Spectrometry. *J. Proteomics* **2016**, *139*, 103–121. https://doi.org/10.1016/j.jprot.2016.03.022.

(36) Fang, Y.-Y.; Zeng, P.; Qu, N.; Ning, L.-N.; Chu, J.; Zhang, T.; Zhou, X.-W.; Tian, Q. Evidence of Altered Depression and Dementia-Related Proteins in the Brains of Young Rats after Ovariectomy. *J. Neurochem.* **2018**, *146* (6), 703–721. https://doi.org/10.1111/jnc.14537.

(37) Jiménez-Balado, J.; Eich, T. S. GABAergic Dysfunction, Neural Network Hyperactivity and Memory Impairments in Human Aging and Alzheimer's Disease. *Semin. Cell Dev. Biol.* **2021**, *116*, 146–159. https://doi.org/10.1016/j.semcdb.2021.01.005.

(38) Jüptner, M.; Jussofie, A.; Hiemke, C. Effects of Ovariectomy and Steroid Replacement on GABAA Receptor Binding in Female Rat Brain. *J. Steroid Biochem. Mol. Biol.* **1991**, *38* (2), 141–147. https://doi.org/10.1016/0960-0760(91)90119-p.

(39) Dalangin, R.; Kim, A.; Campbell, R. E. The Role of Amino Acids in Neurotransmission and Fluorescent Tools for Their Detection. *Int. J. Mol. Sci.* **2020**, *21* (17), 6197. https://doi.org/10.3390/ijms21176197.

(40) Erdö, S. L.; Wolff, J. R. Gamma-Aminobutyric Acid Outside the Mammalian Brain. *J. Neurochem.* **1990**, *54* (2), 363–372. https://doi.org/10.1111/j.1471-4159.1990.tb01882.x.